Åbo Akademi University

Vinay Kumar

Roll-to-Roll Processing of Nanocellulose into Coatings

Laboratory of Paper Coating and Converting
Centre for Functional Materials at Biological Interfaces
Faculty of Science and Engineering

Vinay Kumar

Born 1987 in Imlota, India

Received his B.Tech. degree from Indian Institute of Technology Roorkee in 2010.

Recevied his M.Sc. (Tech.) degree from the department of Chemical Engineering at Åbo Akademi University in 2012.

Joined the Laboratory of Paper Coating and Converting in 2010.

Roll-to-Roll Processing of Nanocellulose into Coatings

Vinay Kumar

Academic Dissertation

Laboratory of Paper Coating and Converting
Center for Functional Materials at Biological Interfaces
Faculty of Science and Engineering
Åbo Akademi University
Åbo/Turku, Finland
2018

Supervisor

Professor Martti Toivakka
Laboratory of Paper Coating and Converting
Faculty of Science and Engineering
Åbo Akademi University
FI-20500 Turku, Finland

Examiners

Associate Professor Julien Bras
Laboratory of Pulp and Paper Sciences (LGP2)
Grenoble Institute of Technology (INP)
F-38000 Grenoble, France

Professor Kaj Backfolk
School of Energy Systems
Lappeenranta University of Technology
FI-53851 Lappeenranta, Finland

ISBN 978-952-12-3672-3
ISBN 978-952-12-3673-0 (pdf)
Painosalama Oy – Turku, Finland 2018

To *my parents*

Preface and Acknowledgements

This work was carried out at the Laboratory of Paper Coating and Converting (Paf), and the Center for Functional Materials at Biological Interfaces (FunMat) from January 2013 to December 2017. There were no industrial partners involved in this project. However, there were collaborations with others laboratories for acquiring materials, equipment, etc. The graduate school for doctoral studies at Åbo Akademi University is gratefully acknowledged for financing this work. Sincere appreciations for the financial support also go to FunMat and JPÅA, the Rector of Åbo Akademi University, and Kautesäätiö.

I am immensely grateful to my supervisor Prof. Martti Toivakka for providing me with the wonderful opportunity to carry out this doctoral work and grow under his able guidance. Your support, patience, trust, and encouragement throughout my doctoral studies have been commendable. The sense of responsibility and the freedom of thought you instill in your students are unparalleled. You have contributed so much to my professional and personal development that I will be indebted to you forever.

I sincerely appreciate Prof. Douglas Bousfield at the University of Maine for providing us with the material used in this work and for his unwavering support and guidance throughout. This work is a result of several fruitful collaborations, and I express my deep gratitude to all the contributors.

One of the most important part of my life in Finland has been the Paf family. All the members, past and present, of this family have helped me grow in one way or another. I want to thank Mari Nurmi for her caring attitude, willingness to help, and ensuring the well-being of students from abroad. You have been very kind, and I will always be grateful to you. Sincere thanks to ÄV, Jani, Pauliina, and Peter for ensuring that all the equipment in the laboratory worked without hiccups. I admire your attitude to problem solving. Jarkko, I would like to thank you for the support and enthusiasm you have provided through great discussions on several occasions. Your energy and passion is commendable. I am deeply grateful to my work roommate and friend Dimitar, who is always ready to help. You have taught me many things, including the guitar playing (you are a great teacher!), and I am thankful for your patience and kind-heartedness all along. I sincerely appreciate the company of Kofi, Joel, Diosa, Ruut, Mahdi, Mukunda, Yiran, Linda and Vishu during work hours and outside. We have shared great moments together, and I hope to keep this friendship going for the times to come. Some of you (Pav, Hanna, Roger, Milena, Sergey, Farid, Mika, Mengxiao, David, Axel, and Shaoxia) no longer work at Paf, but I still remember your wonderful contributions to my life at Paf.

I also express my sincere gratitude to Marika Ginman and Agneta Hermansson for taking care of all the practical matters, so I could focus on research.

I owe an enormous debt of gratitude to Björn 'ÄV' Friberg and family. The list of things you have done for me is endless. You introduced me to the culture of sailing, and our sailing trip to Stockholm on S/y Söötä Öödi[2] will remain unforgettable to me. Thank you for inviting me to your Christmas and other celebrations. I will cherish forever this relation and the wonderful moments we have spent together.

I would also like to acknowledge my friends without whom the stay in Finland would not be as wonderful. Rajesh (Koppu), you of course deserve to be the first in this list, but words will never be enough to describe our friendship. Your journey from a learner to an inspirer makes me proud. Special thanks to Aayush for being a great support on and off work, you add value to everyone's life you come across. I also express my sincere gratitude to the super caring friend, Ankitha. Thank you, Sonu and Alexandra, for your wonderful company all along. I appreciate Tamoghna, Pallavi, Debanga, Susmita, Shishir, Hasan, Mohit, Ayush, Rishabh, Megha, Toqeer, Jasir, Bhanu, Neeraj, Paulo, Jasmina, Vaida and Katja for the countless number of pleasant memories. There are many others (you know who you are!), who have been with me through this journey, and I sincerely appreciate you all.

Finally, last but by no means least, I am sincerely thankful to my beloved ones for their never-ending support and encouragement. I am deeply grateful to my wife, Deepika. You joined me in Finland at a time when I was extremely occupied at work. You offered your unconditional love and support to help me sail through the phase. I cherish your understanding and care.

Åbo, January 2018

Vinay Kumar

Abstract

Paper and paperboard consumption is growing worldwide. However, the demand for traditional graphic paper grades is dwindling in mature markets, e.g. Europe, due to an increasing influence of the electronic media. For a sustainable growth, it is essential for the paper industry to expand its product portfolio to aim for novel value-added applications that can utilize the paper industry raw material, e.g. pulp, in unconventional ways. Nanocellulose, a product of the wood biomass itself, shows a considerable promise in this context. Paper, modified with barrier and functional coatings, is attracting interest as a potential sustainable solution to the environmental concerns associated with petroleum-derived plastics commonly used in various packaging applications. Excellent oil and gas barrier properties along with functionalization possibility of nanocellulose films and coatings seem valuable in proliferating the use of such paper. It is vital to produce nanocellulose films and coatings on a large scale to reap these benefits. However, nanocellulose suspensions cannot be coated or formed into films easily using the traditional coating and metering constructions. This is due to either clogging caused by the aggregation of nanocellulose fibers or the excessively high viscosity of nanocellulose suspensions, resulting in coating and film defects, poor coating/film quality, and poor process runnability. Besides, these suspensions contain large amounts of water, usually more than 95 wt%, which is challenging to dry in a continuous process.

In this work, coating of nanocellulose suspensions is enabled by utilizing their apparent shear thinning behavior, which extends to high shear rates in pressure-driven flow through a slot-die. The resulting low effective process viscosity of the suspensions allows forming a wet film and coating application onto paper. The slot-die is used in an unconventional manner, where it acts as both a shearing and a metering element. A conventional slot-die operation does not involve post metering, i.e. all the material coming out from the slot is transferred to the substrate. The process developed in this work successfully demonstrates continuous roll-to-roll coating of nanocellulose onto paper-based substrates. The resulting coatings improved barrier (air, grease, mineral oil and heptane) properties significantly, along with enhancing strength properties.

The utility of the developed process was also demonstrated for coating of nanographite suspensions, with similar characteristics as nanocellulose suspensions, onto paper-based substrate. The novel coating technique allowed depositing thick conductive coating layers, which was otherwise challenging using the conventional coating techniques.

There are still challenges that need to be addressed to speed up the potential upscaling of this coating technique. For example, the pumping requirements to feed the slot-die limit the maximum solids content of the suspension to be coated. Furthermore, it is rather difficult to manufacture, with precision, wide slot-dies required for industrial scale. Nevertheless, this process shows some promise in enabling the use of nanocellulose at the industrial scale, which may help improve the forest-based industry profitability, and contribute to curbing the menace of climate change and achieving a sustainable planet.

Keywords
Nanocellulose, Microfibrillated cellulose (MFC), Nanofibrillated cellulose (NFC), Nanographite, Low and high shear rate rheology, Water retention, Slot-die, Roll-to-roll coating, Strength and barrier properties, Conductive coating

Svensk Sammanfattning

Förbrukningen av papper och kartong ökar i hela världen. Efterfrågan på traditionella tryckpapperskvaliteter på mogna marknader, t.ex. i Europa, minskar dock på grund av elektronisk medias ökade närvaro. En hållbar tillväxt kräver att pappersindustrin expanderar sin produktportfölj med nya applikationer som ger ett ökat mervärde. Dessa bör vara baserade på vedbaserade naturfibrer, det råmaterial som idag används av pappersindustrin, och som nu bör utnyttjas på okonventionella sätt. Nanocellulosa, en produkt som härstammar från träbiomassa, uppvisar mycket lovande egenskaper i detta sammanhang. Ur miljösynpunkt väcker modifierat papper, som försetts med ett barriärskikt och funktionella bestrykningsskikt, stort intresse som ett potentiellt hållbart alternativ till olika konventionella, oljebaserade plastprodukter. Utmärkta olje- och gasbarriäregenskaper, tillsammans med möjligheterna till funktionalisering av nanocellulosafilmer och – bestrykningar verkar vara värdefulla faktorer som kan leda till en ökad pappersanvändning. För att man skall kunna dra full nytta av de ovan nämnda fördelarna, bör nanocellulosafilmer och -bestrykningar produceras i stor skala. Nanocellulosasuspensioner kan emellertid inte bestrykas eller formas med hjälp av traditionell bestrykning- och doseringsutrustning, eftersom traditionell utrustning sätts igen av aggregerade nanocellulosafibrer eller av allt för högviskösa nanocellulosasuspensioner. Aggregeringen förorsakar defekter hos bestrykningsskikt och -filmer, dålig bestrykning-/filmkvalitet, och dålig körbarhet hos processen. Dessutom består suspensionerna vanligen av mer än 95 viktprocent vatten, vilket ställer stora krav på kontinuerliga torkningsprocesser.

I detta arbete utnyttjades de skjuvtunnande egenskaperna hos nanocellulosususpensioner för att skapa en ny bestrykningsmetod för dem. Dessa egenskaper sträcker sig upp till höga skjuvhastigheter i tryckdrivna flöden i smala gap. Den resulterande, låga effektiva processviskositeten hos suspensionerna möjliggör bildning av en våtfilm och, därmed, bestrykning på papper med en sk. slot-die geometri. Slot-die används här okonventionellt, både för att introducera skjuvning hos materialet, och för att dosera det. I det konventionella operationssättet för slot-die-bestrykning används ingen avschabring utan all bestrykningsmaterial från munstycket överförs på substratet. Processen som utvecklades demonstrerade framgångsrikt en kontinuerlig bestrykning av nanocellulosa på pappersbaserade substrat. De resulterande bestrykningarna uppvisar signifikant förbättrade barriäregenskaper (luft, fett, mineralolja, och heptan), samt förbättrade hållfasthetsegenskaper.

Användbarheten hos den nyutvecklade processen demonstrerades även genom bestrykning av nanografitsuspensioner på pappersbaserat substrat. Dessa suspensioners egenskaper motsvarar i hög grad egenskaperna hos nanocellulosasuspensioner. Dessutom tillåter den nya bestrykningstekniken bestrykning av tjocka, ledande bestrykningsskikt, vilket är problematiskt att utföra med hjälp av konventionella bestrykningstekniker.

Många utmaningar bör ännu lösas för att en eventuell uppskalning av den här bestrykningsprocessen skall kunna påskyndas. En utmaning är t.ex. att pumpningskapaciteten vid matningen av slot-die begränsar torrhalten hos bestrykningssuspensionen. Utöver detta är det ganska svårt att precisionstillverka breda slot-die för industriellt bruk. Denna process är dock ganska lovande när det gäller att möjliggöra en ökad användning av nanocellulosa i industriell skala, vilket kan bidra till en ökad lönsamhet hos skogsbaserade industrier, till en minskad klimatförändring, och till uppnåendet av en hållbar användning av vår planet.

Keywords
Nanocellulosa, mikrofibrillerad cellulosa (MFC), nanofibrillerad cellulosa (NFC), nanografit, låg och höga skjuvhastighet reologi, vattenretention, slot-die, kontinuerlig bestrykning, hållfasthets och barriäregenskaper, ledande bestrykning

List of Original Publications

Publication I. V. Kumar, R. Bollström, A. Yang, Q. Chen, G. Chen, P. Salminen, D. Bousfield, and M. Toivakka, "Comparison of nano- and microfibrillated cellulose films", *Cellulose* **21**, 3443–3456 (2014).

Publication II. V. Kumar, B. Nazari, D. Bousfield, and M. Toivakka, "Rheology of microfibrillated cellulose suspensions in pressure-driven flow", *Applied Rheology* **26**, 43534 (2016).

Publication III. V. Kumar, A. Elfving, H. Koivula, D. Bousfield, and M. Toivakka, "Roll-to-roll processed cellulose nanofiber coatings", *Industrial and Engineering Chemistry Research* **55**, 3603–3613 (2016).

Publication IV. V. Kumar, V. R. Koppolu, D. Bousfield, and M. Toivakka, "Substrate role in coating of microfibrillated cellulose suspensions", *Cellulose* **24**, 1247–1260 (2017).

Publication V. V. Kumar, S. Forsberg, A. Engström, M. Nurmi, B. Andres, C. Dahlström, and M. Toivakka, "Conductive nanographite-nanocellulose coatings on paper", *Flexible and Printed Electronics* **2**, 035002 (2017).

Author's Contribution

Publication I: Comparison of nano- and microfibrillated cellulose films.

The author participated in planning of the work. MFC and NFC suspensions were produced at the University of Maine and South China University of Technology, respectively. The author was responsible for film preparation and characterization. Sanna Auvinen at Tampere University of Technology measured the oxygen barrier, and Jun Liu at Åbo Akademi University determined the carboxylate content. Camila Honorato and Linus Silvander at Åbo Akademi University acquired the TEM and SEM images, respectively. The author analyzed the data and wrote the manuscript.

Publication II: Rheology of microfibrillated cellulose suspensions in pressure-driven flow.

The author planned the work together with Martti Toivakka. The author prepared the experimental setup for slot rheology measurements, conducted the experiments, and analyzed the results. The author finalized the manuscript.

Publication III: Roll-to-roll processed cellulose nanofiber coatings.

The author planned the work together with Martti Toivakka. The author modified the coating apparatus and performed the coating experiments. Hanna Koivula at the University of Helsinki conducted the mineral oil barrier tests. Ruut Kummala and Linus Silvander at Åbo Akademi University acquired the TEM and SEM images, respectively. The author conducted all other tests, analyzed the results, and wrote the manuscript.

Publication IV: Substrate role in coating of microfibrillated cellulose.

The author planned the work. The author, with help from Rajesh Koppolu, did all the coatings and characterization tests, except SEM and TEM imaging, which were done by Ruut Kummala and Linus Silvander, respectively. The author analyzed the results and wrote the manuscript.

Publication V: Conductive nanographite-nanocellulose coatings on paper.

The author planed the work together with the co-authors. The suspensions were prepared at the Mid Sweden University. The author did the rheology measurements and coating experiments. Christina Dahlström acquired the SEM images. The author was responsible for finalizing the manuscript.

List of Supporting Publications

Articles in Peer-reviewed International Journals and Conferences

1. V. Kumar, V. Ottesen, Ø. W. Gregersen, K. Syverud, and M. Toivakka, "Coatability of cellulose nanofibril suspensions – role of rheology and water retention", *Bioresources* **12**, 7656–7679 (2017).
2. V. Ottesen, V. Kumar, M. Toivakka, G. Chinga-Carrasco, K. Syverud, and Ø. W. Gregersen, "Viability and properties of roll-to-roll coating of highly fibrillated cellulose nanofibrils on a challenging surface", *Nordic Pulp and Paper Research Journal* **32**, 179–188 (2017).
3. V. Kumar, D. Bousfield, and M. Toivakka, "Slot die coating of nanocellulose on paperboard", *TAPPI Journal* **(in press)**.
4. B. Nazari, V. Kumar, D. Bousfield, and M. Toivakka, "Rheology of cellulose nanofibers suspensions: boundary driven flow", *Journal of Rheology* **60,** 1151–1159 (2016).
5. V. Kumar, E. Lazarus, P. Salminen, D. Bousfield, and M. Toivakka, "Influence of nanolatex addition on cellulose nanofiber film properties", *Nordic Pulp and Paper Research Journal* **31**, 333–340 (2016).
6. C. Honorato, V. Kumar, J. Liu, H. Koivula, C. Xu, and M. Toivakka, "Transparent nanocellulose-pigment composite films", *Journal of Materials Science* **50**, 7343–7352 (2015).
7. K. Torvinen, F. Pettersson, P. Lahtinen, K. Arstila, V. Kumar, R. Österbacka, M. Toivakka, and J.J. Saarinen, "Nanoporous kaolin – cellulose nanofibril composites for printed electronics", *Flexible and Printed Electronics* **2**, 024004 (2017).
8. D. Valtakari, J. Liu, V. Kumar, C. Xu, M. Toivakka, and J.J. Saarinen, "Conductivity of PEDOT:PSS on spin-coated and drop cast nanofibrillar cellulose thin films", *Nanoscale Research Letters* **10**, 386 (2015).
9. P. Alam, P. Fagerlund, P. Hägerstrand, J. Töyrylä, S. Amini, M. Tadayon, A. Miserez, V. Kumar, M. Pahlevan, and M. Toivakka, "l-Lysine templated CaCO3 precipitated to flax develops flowery crystal structures that improve the mechanical properties of natural fibre reinforced composites", *Composites Part A: Applied Science and Manufacturing* **75**, 84–88 (2015).
10. V. Kumar (presenter), S. Forsberg, A. Engström, M. Nurmi, C. Dahlström, and M. Toivakka, "Conductive carbon-nanocellulose coatings on paper", Proceedings of TAPPI Papercon, Minneapolis, MN, USA (2017). Oral presentation.
11. M. Toivakka (presenter), V. Kumar, and D. Bousfield, "Slot coating of nanocellulose for barrier applications", Proceedings of TAPPI Papercon, Minneapolis, MN, USA (2017). Oral presentation.

12. V. Kumar, E. Lazarus (presenter), P. Salminen, D. Bousfield, and M. Toivakka, "The effect of latex characteristics and addition level on the properties of cellulose nanofiber films", Proceedings of TAPPI Papercon, Minneapolis, MN, USA (2017). Oral presentation.
13. V. Kumar (presenter), A. Elfving, D. Bousfield, and M. Toivakka, "Nanocellulose coatability on paper in a roll-to-roll process", Proceedings of 14th TAPPI Advanced Coating Symposium, Stockholm, Sweden (2016). Oral presentation.
14. M. Toivakka (presenter), V. Kumar, A. Elfving, B. Nazari, and D. Bousfield, "Roll-to-roll coating of cellulose nanofiber suspensions", Proceedings of 18th International Coating Science and Technology Symposium, Pittsburgh, PA, USA (2016). Oral presentation.
15. S. Forsberg (presenter), V. Kumar, A. Engström, M. Nurmi, C. Dahlström, and M. Toivakka, "Effect of calendering and coating formulations on conductivity in paper-based electrodes", Proceedings of 14th TAPPI Advanced Coating Symposium, Stockholm, Sweden (2016). Oral presentation.
16. E. Lazarus, V. Kumar, P. Salminen (presenter), D. Bousfield, and M. Toivakka, "The effect of latex characteristics and addition level on the properties of cellulose nanofiber films", Proceedings of 5th ISETPP & 3rd IPEC, Guangzhou, China (2016). Oral presentation.
17. M. Toivakka (presenter), V. Kumar, A. Elfving, B. Nazari, and D. Bousfield, "Roll-to-roll coating of cellulose nanofiber suspensions", Proceedings of 5th ISETPP & 3rd IPEC, Guangzhou, China (2016). Oral presentation.
18. V. Kumar (presenter), D. Bousfield, and M. Toivakka, "Microfibrillated cellulose suspensions in slot flow", Annual Transactions of the Nordic Rheology Society, Nordic Rheology conference, Karlstad, Sweden (2015). Oral presentation.
19. T. Syrovy (presenter), V. Kumar, M. Toivakka, C. Xu, L. Syrova, J. Reboun, and D. Bousfield, "Fully printed biodegradable nanocellulose-based humidity sensor for SMART LABEL applications", Proceedings of the International Research Conference of IARIGAI, Helsinki, Finland (2015). Oral presentation.
20. S. Renvall (presenter), V. Kumar, M. Toivakka, and P. Salminen, "Short time water absorption into multilayer curtain coated linerboard", Proceedings of TAPPI PaperCon, Atlanta, GA, USA (2013). Oral presentation.

Non-reviewed Conference Publications

1. V. Kumar (presenter), V. R. Koppolu, D. Bousfield, and M. Toivakka, "Substrate requirements for roll-to-roll processed nanocellulose coatings", TAPPI International conference on nanotechnology for renewable materials, Montreal, Canada (2017). Oral presentation.

2. V. Kumar (presenter), and M. Toivakka, “Roll-to-roll processing of nanocellulose into coatings for barrier and functional applications”, The 11th Biennial Johan Gullichsen Colloquium: Sustainability driven innovations, Helsinki, Finland (2017). Oral presentation.
3. V. Kumar (presenter), “Roll-to-roll processing of nanocellulose into coatings for barrier and functional applications”, The Marcus Wallenberg Symposium, Stockholm, Sweden (2017). Poster presentation.
4. V. Kumar (presenter), A. Elfving, H. Koivula, D. Bousfield, and M. Toivakka, “Roll-to-roll processed nanocellulose coatings for barriers applications”, TAPPI International conference on nanotechnology for renewable materials, Grenoble, France (2016). Oral presentation.
5. M. Toivakka (presenter), and V. Kumar, “Roll-to-roll coating of nanocellulosic barriers on paper”, TAPPI PLACE Conference, Fort Worth, Texas, USA (2016). Oral presentation.
6. V. Kumar (presenter), E. Lazarus, P. Salminen, D. Bousfield, and M. Toivakka, “High toughness and high haze nanolatex-cellulose nanofiber films”, International Paper and Coating Chemistry Symposium & International Paper Physics Conference, Tokyo, Japan (2015). Oral presentation.
7. V. Kumar (presenter), “CNF suspensions in slot flow”, Cellulose Materials Doctoral Students Summer Conference, Autrans, France (2015). Oral presentation.
8. V. Kumar (presenter), “MFC vs NFC Films”, Cellulose Materials Doctoral Students Summer Conference, Bad Munster am Stein, Germany (2014). Oral presentation.
9. V. Kumar (presenter), R. Bollström, A. Yang, Q. Chen, G. Chen, P. Salminen, D. Bousfield, and M. Toivakka, “Transparent NFC films for sensing applications”, TAPPI International conference on nanotechnology for renewable materials, Vancouver, BC, Canada (2014). Poster presentation.

Nomenclature and Abbreviations

AFM	Atomic force microscopy
AKD	Alkylketene dimer
ANFC	ARBOCEL nanofibrillated cellulose
ASTM	American Society for Testing and Materials
ATR-FTIR	Attenuated total reflectance - Fourier transform infrared spectroscopy
BC	Bacterial cellulose
BNC	Bacterial nanocellulose
CEPI	Confederation of European Paper Industries
CFD	Computational fluid dynamics
CHX	Chlorhexidine digluconate
CLC	Cylindrical laboratory coater
CMC	Carboxymethyl cellulose
CNC	Cellulose nanocrystals
CNF	Cellulose nanofibers
CNW	Cellulose nanowhiskers
DP	Degree of polymerization
DS	Degree of substitution
FUNMAT	Center for functional materials
gsm	Grams per square meter
GWR	Gravimetric water retention
HC	Hydrocarb
HVTR	Heptane vapor transmission rate
IGT	Institut für Graphische Technik
KIT	Grease barrier test method

L&W	Lorentzen & Wettre
MCR	Modular compact rheometer
MFC	Microfibrillated cellulose
MNFC	Micronanofibrillated cellulose
NA	Numerical aperture
NCC	Nanocrystalline cellulose
NFC	Nanofibrillated cellulose
OM	Optical microscopy
OMFC	Omya microfibrillated cellulose
OTR	Oxygen transmission rate
PAF	Pappersförädling
pph	parts per hundred
PPS	Parker Print Surf
PVOH	Polyvinyl alcohol
RH	Relative humidity
RISI	Resource Information Systems Inc
RK	Rotary Koater
SEM	Scanning electron microscopy
SWG	Slot-web gap
TAPPI	Technical Association of the Pulp & Paper Industry
TEA	Tensile energy absorption
TEM	Transmission electron microscopy
TEMPO	2,2,6,6,-tetramethylpiperidine-1-oxyl
TS	Tensile strength
WLT	Water layer thickness
WVTR	Water vapor transmission rate

Contents

1. Introduction

1.1 Background and motivation

Paper and paperboard products are ubiquitous in our daily lives. There is a multitude of paper grades consumed worldwide for various purposes such as packaging, writing and printing, and household sanitation. The current global consumption of paper and board has already surpassed 400 million tons per annum (**Figure 1a**), and a recent global paper market study by Pöyry forecasts it to 482 million tons per annum in 2030 [1]. The ratio of worldwide consumption of different paper and board grades keeps changing according to the technological and socioeconomic evolution and developments [2]. For instance, the increasing influence of electronic media has led to a stagnation or even decline in the demand of graphic paper grades, especially in mature markets such as Europe (**Figure 1b**). However, packaging paper grades are enjoying growth as petroleum-derived plastics are becoming more and more disfavored due to environmental concerns.

In order to sustain a profitable growth, it is essential for the paper industry to improve the existing paper products along with expanding the product portfolio to aim for novel value-added applications. This could include mechanical and barrier performance improvements in existing packaging grades, improvement of printing properties in graphic paper grades, and introduction of new paper grades with added functionality for high-end applications such as biomedicine and electronics. Furthermore, novel product streams could be developed that can utilize the paper industry raw material, i.e. pulp, in unconventional ways. A material that shows a considerable promise in achieving these goals for the pulp and paper industry is nanocellulose — a product of the wood biomass itself.

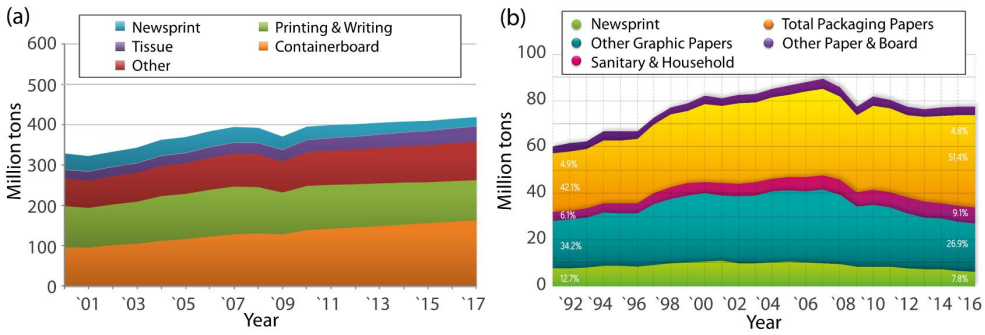

Figure 1. Paper and board consumption by grade. (a) World (Source: RISI [3]), and (b) Europe (Source: CEPI Statistics [4]).

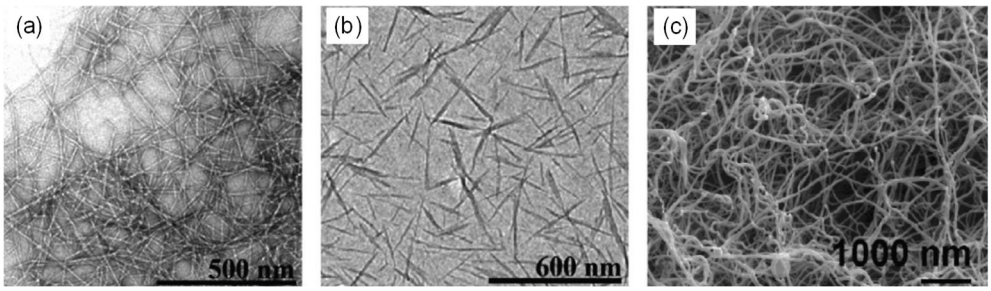

Figure 2. Representative transmission electron micrographs of: (a) CNFs, (b) CNCs, and (c) scanning electron micrograph of BNC. (Source: [5]).

Nanocellulose refers to numerous kinds of cellulosic materials which have at least one dimension on the nano-scale [5]. They are classified into three broad categories: (I) cellulose nanocrystals (CNCs), also referred to as nanocrystalline cellulose (NCC) and cellulose nanowhiskers (CNWs); (II) cellulose nanofibers (CNFs), also referred to as nanofibrillated cellulose (NFC) and microfibrillated cellulose (MFC); and (III) bacterial nanocellulose (BNC), or simply bacterial cellulose (BC). Different approaches are used to extract these nanoparticles from cellulose sources, resulting in particles with varied morphology (**Figure 2**) and functionality [6, 7]. It is noted that a fourth type of nanocellulose produced using e-spinning has also been reported recently [8].

CNCs and CNFs are manufactured via a top-down approach: breaking down wood or plant cellulose fibers using enzymatic and/or chemical/physical methodologies [9]. Contrarily, BNC is obtained via a bottom-up procedure: biotechnological assembly of cellulose from low-molecular weight carbon sources, such as D-glucose, using certain bacteria [5]. CNCs are extracted from wood or plant cellulose fibers using acid hydrolysis, with first production dating back to the late 1940s [10, 11]. The acid hydrolysis dissolves amorphous cellulose regions, resulting in crystalline rod-shaped CNC particles that measure 5–20 nm in diameter and 100–500 nm in length. CNFs are produced from cellulose fibers using various mechanical treatments, such as homogenization, microfluidization, refining, grinding, and ball milling. In the early 1980s, Turbak and Herrick et al. [12, 13] at ITT Rayonier published the first studies on the production of MFC from wood cellulose fibers using repeated high-pressure homogenization treatment. In recent years, various enzymatic [14] and/or chemical [15-17] pre-treatments have been utilized to reduce the energy consumption and improve the efficiency of the mechanical treatment process. With a diameter below 100 nm and a length reaching several micrometers, CNFs are high aspect ratio fibers containing both amorphous and crystalline cellulose domains. Classically, CNFs are comparable to “spaghetti”-like structures, whereas CNCs are “rice”-like [18]. BNC is synthesized extracellularly by several species of ubiquitous fermentation bacteria, most importantly

Gluconacetobacter xylinus [19]. With an average diameter of 20–100 nm and a length of several micrometers, BNC fibers form stable entangled network structures.

In the past decade, both academia and industry have shown a prominent interest in nanocellulose, which is evident from the exponential growth (**Figure 3**) in the number of patents and publications on the subject. This widespread appeal of nanocellulose is attributable to its salient features, such as biodegradability, renewability, mechanical robustness, flexibility, large specific surface area, high aspect ratio, non-toxicity and biocompatibility, low density, and surface-accessible hydroxyl groups that can be modified chemically to provide additional functionalities [20, 21]. Nanocellulose films are particularly exciting due to their excellent barrier performance against oils and oxygen [22, 23], combined with interesting optical properties [23-25] and low coefficient of thermal expansion [25, 26]. These remarkable properties make nanocellulose a high-performance natural material attractive for several current or potential applications, including, but not limited to, composites [5, 27-32], films [33], aerogels and hydrogels [34], electronics [35], biomedicine [36-38], rheology modification [12, 39, 40], packaging [41-43], and paper manufacturing [9, 18, 31, 33, 44-47].

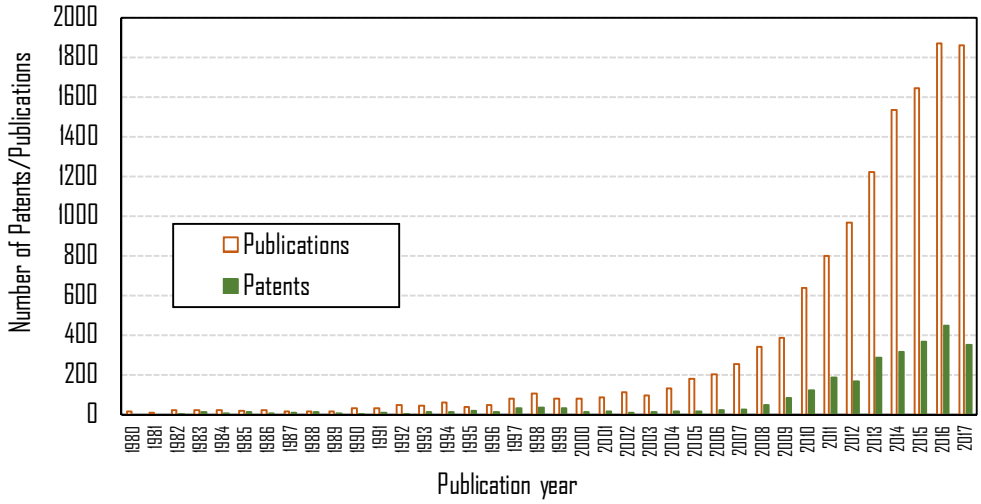

Figure 3. Annual number of patents and scientific publications on nanocellulose[1].

[1]SciFinder combined answer set (21.09.2017): (microfibrillated cellulose, microfibrillar cellulose, cellulose microfibrils, nanocellulose, nanosized cellulose, nanofibrillated cellulose, nanofibrillar cellulose, cellulose nanofibrils, cellulose nanofibers, cellulose nanoparticles, nanoparticle cellulose, cellulose nanofillers, cellulose crystallites, cellulose microcrystals, cellulose nanocrystallites, cellulose nanocrystals, nanocrystalline cellulose, cellulose nanowhiskers, bacterial cellulose, bacterial nanocellulose). Patents document type: Patent; Publications document type: Journal, Book, Conference, Dissertation, Editorial, Letter, Report, and Review.

Currently, the greatest volume potential for the use of nanocellulose is projected to be in the paper industry [31, 48-50]. Surprisingly, the literature on the usage of nanocellulose in paper industry is relatively new and scarce, as is evident from a recent book chapter by Bardet and Bras [18] and reviews by Brodin et al. [51], Lindström et al. [9, 31, 47], Osong et al. [44], Boufi et al. [52], Samyn et al. [45] and Hubbe et al. [33]. The studies reported so far have explored bulk and/or surface applications of nanocellulose in paper to improve mechanical, barrier, printing and/or functional properties. Furthermore, surface coating of paper with nanocellulose has been suggested to offer greater potential for barrier, printing and functional applications, provided large-scale production can be achieved [18]. Most of the previous reports on nanocellulose coatings on paper or other substrates have been on small-scale batch processes, except the work by Kinnunen-Raudaskoski et al. [53]. This is due to several challenges in continuous coating of nanocellulose suspensions, relating to their complex rheological behavior [54, 55] and low solids content, usually below 5%.

The complexity of the rheological properties of nanocellulose suspensions can be attributed to their highly anisotropic nature, i.e. aspect ratio above 100, of the constituent nanofibrils. Interestingly, they display highly shear thinning and thixotropic behavior, which can be advantageous in coating applications [9]. However, these suspensions, even at low solids content, are extremely viscous and have significant yield stress making their pumping to the coating unit and subsequent film formation difficult. Rheology of nanocellulose suspensions in low shear rate regime, i.e. up to 1 000 s^{-1}, under boundary-driven flow conditions has been frequently reported and reviewed [9, 47, 55-58]. However, high shear rheology under pressure-driven flow conditions has received little to no attention, excepting the work by Iotti et al. [59]. This is important because the shear rates in high-speed coating operations in paper manufacturing can easily be 10^4 – 10^6 s^{-1} [60]. Therefore, research effort on exploring high shear rheology is much needed, which could be helpful in overcoming the rheological challenges in processing these suspensions into coatings. In addition, water retention characteristics of nanocellulose suspensions are equally important to understand and control for a successful coating operation, because paper-based substrates may not withstand large amounts of water in these suspensions, leading to runnability problems such as web breaks. Furthermore, the role of additives such as carboxymethyl cellulose (CMC) on the rheological and water retention behavior is worth exploring. An understanding of all these parameters is essential when developing novel processes to coat nanocellulose suspensions on paper or other substrates in a continuous manner for various barrier and functional applications.

1.2 Research Objectives and Thesis Structure

The main objective of this work was to develop and demonstrate a novel surface engineering technique that can help overcome the challenges associated with roll-to-roll processing of nanocellulose suspensions into coatings. This creates opportunities for the production of fully biodegradable packaging as a replacement for petroleum-derived materials. The continuous processing also helps accelerating the development of novel products based on functional coatings containing nanocellulose. The main objective was divided into four sub tasks:

(i) The first task was to understand nanocellulose characteristics such as fibril morphology, dimensions, charge content etc., that likely affect the suspension behavior.

(ii) The second task was to determine nanocellulose suspension rheology and water retention properties, which might play critical roles in their coatability. In this regard, understanding high shear rheology was of importance.

(iii) The third task was to devise a technique to coat nanocellulose suspensions in a continuous roll-to-roll manner. A further goal was to optimize coating process and suspension parameters along with substrate characteristics to improve coatability and final coating properties.

(iv) The fourth and final task was to demonstrate the utility of the developed process for coating of functional materials with similar suspension properties as pure nanocellulose.

This thesis summarizes the work of five publications addressing the tasks mentioned above. Chapter 2 provides a brief overview of the literature on nanocellulose with attention to rheology of nanocellulose suspensions and their coating applications. Chapter 3 describes various materials, characterization techniques and coating methods used in this study. Chapter 4 summarizes the main results, followed by concluding remarks in Chapter 5. For more details, the reader may consult the attached publications. Some closely related publications (Supporting Publications: 1–6) have been intentionally excluded in order to focus the thesis on MFC coating.

2. Literature Review

This chapter provides a brief overview of the research published so far on nanocellulose. Instead of trying to review the vast amount of literature (**Figure 3**), this chapter will focus only on the topics essential to discuss the results in this thesis. Where appropriate, recent reviews are cited for further information on each topic.

2.1 Cellulose and Nanocellulose

Cellulose is the most abundant biopolymer on the planet, with annual growth estimated to be approximately 1.5×10^{12} tons [61]. There has been a long-standing scientific interest in cellulose due to its inherent renewable and biodegradable properties. Cellulose can be found throughout nature in plants, animals, algae, fungi, and minerals [62]. However, the major source of cellulose is plant fiber. Plant cell walls comprise 40–50 wt% cellulose, serving as a reinforcement and structuring element, accompanied by hemicelluloses and lignin.

Cellulose consists of β-D-glucopyranose ring units in $^4C_1$-chair conformation [62]. These units are linked by (1→4)-glucosidic bonds forming a 1.3 nm long "Cellobiose unit", which is considered the repeating unit of cellulose (**Figure 4**). Cellulose molecules are completely linear with an average degree of polymerization (DP) in the range of 1 000–30 000, corresponding to chain lengths of 500–15 000 nm [62]. These molecules have a strong tendency to form intermolecular and intramolecular hydrogen bonds, which significantly influence their properties, such as solubility, chemical reactivity, and crystallinity.

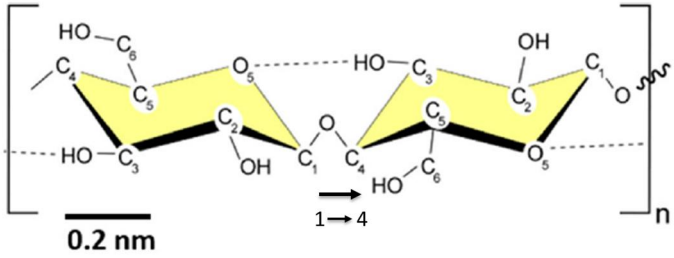

Figure 4. Schematic representation of a Cellobiose repeat unit, showing the directionality of the 1-4 linkage and intra-chain hydrogen bonding (dotted line). (Modified from [21]).

Nanocellulose is an exciting new renewable material produced either by downsizing of macroscopic cellulose fibers via various chemical and/or mechanical means or by fermentation of glucose using certain bacteria. As mentioned in Chapter 1, there are three classes of nanocellulose: (I) CNCs, (II) CNFs, and (III) BNC. All three exhibit several unique properties dictating their efficacy and functionality in various applications [7]. However, the focus of this thesis is the CNF material. The advantage of CNF (to BNC and CNC) is that it can be produced at a relatively large scale, with a variety of functional groups, and by a multitude of industrially attractive processes [47]. CNFs have been described using diversified terms in literature [63]. Recently, Technical Association of the Pulp & Paper Industry (TAPPI: WI 3021) and International Organization for Standardization (ISO/TS 20477:2017) have proposed standard terms and their definitions for cellulose nanomaterial, based on the size of the constituting units. Both these standards follow the terminology CNF and CNC for cellulose nanofibrils/nanofibers and cellulose nanocrystals, respectively. Some researchers, including Turbak et al. [12] and Herrick et al. [13], have used the nomenclature Microfibrillated Cellulose (MFC) and Nanofibrillated Cellulose (NFC) to designate CNF. This thesis also follows the nomenclature MFC and NFC, simply due to the previous use of this nomenclature in the included publications, except **Publication III**, where the same material was referred to as CNF. Furthermore, this thesis differentiates the nanocellulose materials as MFC and NFC based on their production method. For example, the material produced using a pure mechanical treatment, with an optional preliminary enzymatic treatment, is designated MFC, and the material produced using any chemical pre-treatments followed by the mechanical treatment is designated NFC.

2.2 Production of MFC and NFC

Cellulose, along with hemicellulose and lignin, is the building block of plant cell walls, as shown in **Figure 5**. The first step in the production of MFC and NFC is the process of liberation of cellulose fibers from plant cell walls by removing lignin and hemicelluloses. Pulp and paper industries have been using lignin removal processes, referred to as pulping and bleaching, for long. The obtained cellulose fibers are subsequently treated using disk refiners or other mechanical treatments in stock preparation processes to control the final paper properties. The purpose of such treatments, also referred to as fibrillation, is to delaminate fiber cell wall to expose cellulose microfibrils. This increases the specific surface area and volume of fibers, which improves the inter-fiber bonding during papermaking. However, numerous hydrogen bonds present between microfibrils in cellulose fibers impede the level of fibrillation achieved with these mechanical treatments. The production of highly fibrillated cellulose or individual microfibrils using such treatments requires excessive amounts of energy and, therefore, is not considered viable for papermaking purposes.

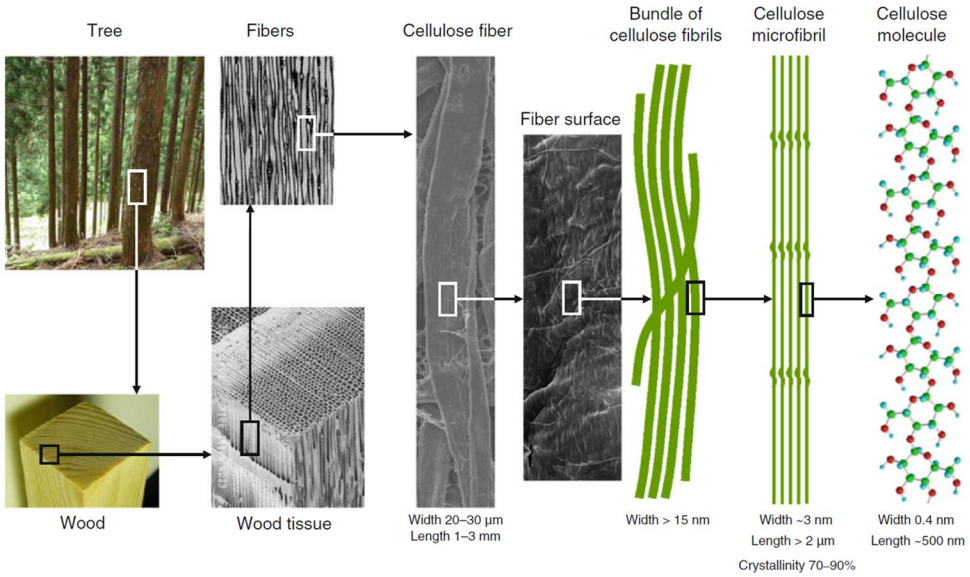

Figure 5. Hierarchical structure of wood cellulose. (Source: [20]).

There are plenty of cellulose raw material sources for MFC/NFC production. Typical sources include woods (softwood and hardwood) and non-woods (cotton, coir, jute, flax, hemp, ramie, kenaf, reed, bagasse, bamboo, straw etc.). Hardwoods and softwoods differ in their anatomy, with the structure of hardwood being more complex and heterogeneous than that of softwood. For achieving the same level of fibrillation, mechanical treatment required for the softwood cellulose fibers is more lenient compared to the hardwood cellulose fibers [64]. Non-woods are also attracting attention for MFC and NFC production due to their lignin amounts being inherently low, resulting in easier extraction of cellulose fibers and lower energy consumption for subsequent fibrillation. The raw material source affects the physical and chemical properties of MFC/NFC obtained. For example, a recent study found bamboo pulp NFC to outperform the NFC obtained from softwood and hardwood pulps in terms of film strength and oxygen barrier properties [65].

The credit for the first production of MFC goes to Turbak et al. [12] and Herrick et al. [13], who developed a new method in the 1980s to obtain highly fibrillated cellulose directly from wood cellulose fibers. MFC was obtained by passing a 2 wt% wood pulp suspension multiple times through a homogenizer at a pressure of approximately 550 bars and a controlled temperature of 70–80 °C. This mechanical treatment delaminated the cellulose fibers and liberated microfibrils with diameters less than 100 nm. However, the process was deemed unviable due to a very high energy consumption, amounting to over 30 000 kWh/ton, and extensive clogging of the homogenizer [9]. According to

Lindström [47], the energy consumption during disintegration is due to the cohesion of the fiber cell wall, and the clogging is due to the aggregation of fibers.

Since the early 2000s, several different routes have been explored to reduce the energy consumption, to mitigate the clogging tendency, and to improve the degree of fibrillation in MFC and NFC manufacturing. These approaches have involved pre-treatment of the cellulose fibers using various physical, chemical and/or enzymatic methods prior to the mechanical treatment. Targeted at facilitating the cellulose fiber wall delamination process and diminishing fiber flocculation, these approaches can be classified into two broad categories [9, 31, 66]: (i) introduction of surface charges and (ii) mild enzymatic hydrolysis. In addition, various mechanical treatments have been explored over the past decade. The following sub-sections briefly discuss the two categories of pre-treatments and the different mechanical treatments used for MFC and NFC production, which has been the subject of numerous reviews [5, 20, 44, 66-70].

2.2.1 Introduction of Surface Charges

In the first category of pre-treatments, swelling of fibers, is induced by electrostatic repulsion between charged groups on fiber surface. These charged groups can be introduced onto the fiber surface either by pulping or bleaching procedures or through oxidative treatments. According to Lindström [47], the charged groups, both those naturally occurring in the wood fibers and those created during pulping and bleaching operations result in a charge content of 20–300 μeq/g on fibers, depending on pulp type and extent of bleaching. However, this charge content is usually not sufficient to ease the fiber delamination process significantly. Therefore, a number of oxidation/modification procedures are employed to increase the charge content on fiber surface. 2,2,6,6,-tetramethylpiperidine-1-oxyl radical (TEMPO)-mediated oxidation [16] and carboxymethylation [17] are the most commonly investigated procedures among others, such as carboxylation via periodate chlorite oxidation [71], sulphonation [72, 73], and cationization [74].

TEMPO-mediated Oxidation

TEMPO-mediated oxidation is a promising method for introducing surface charges on cellulose fibers, to facilitate the cell wall delamination [75]. TEMPO is a water-soluble radical that can be used for selective oxidation of the primary C-6 hydroxyl groups of cellulose [76, 77]. The most widely used procedure is the TEMPO/NaBr/NaClO system under mild alkaline conditions, which first converts the primary alcohol groups of cellulose into aldehydes and subsequently into carboxylic groups [16, 78]. The oxidation results in negatively charged fibers repelling each other, thus easing fibrillation. However, the aldehyde intermediates can undergo beta-elimination reactions, degrading the DP of

cellulose [47]. This can be avoided by using the TEMPO/NaClO/$NaClO_2$ system under neutral or slightly acidic conditions [79, 80].

Carboxymethylation

Wågberg et al. [17] recently reported the production of NFC using carboxymethylation pre-treatment. Cellulosic fibers behave as polyelectrolytic gels in the presence of abundant carboxymethyl groups on the cell wall [66]. In the presence of monovalent counter ions, the fibers swell and reduce the cohesion of the cell wall. The advantage of the carboxymethylation process in the refining of pulp has already been known for many years [81], but the underlying mechanism became known much later [82]. It is worth noting that the commercial production of CMC, which utilizes the carboxymethylation process, dates back to the early 1920s in Germany [83].

The charge content after the oxidative treatments usually ranges from 300 to 2000 μeq/g, and it has been shown that higher charge content results in lower energy consumption [71]. Furthermore, the high charge content significantly mitigates the clogging of homogenizers due to reduced friction between nanofibrils via electrostatic repulsion [9, 84]. Hydrophilic polymers such as cellulose derivatives and gums also facilitate the mechanical delamination process due to reduced flocculation of fibers, as observed by Turbak et al. [12] and Herrick et al. [13].

2.2.2 Mild Enzymatic Hydrolysis

In the second category, a mild enzymatic hydrolysis of cellulose fibers is used to reduce the energy consumption for mechanical treatment. It is interesting to note that the use of cellulase enzyme as catalyst for hydrolysis of cellulose to improve fibrillation for papermaking purposes was suggested already in 1962 [85]. Recently, Pääkkö et al. [14] and Henriksson et al. [86] demonstrated enzymatic hydrolysis of pulp to produce MFC with significantly reduced energy consumption. Endoglucanase, a type of cellulase, used by the authors, hydrolyses the amorphous regions of the cellulose chain. Therefore, it is important to activate the fiber cell wall using pre-refining before the enzymatic treatment to improve its accessibility to the enzyme. The enzymatic pre-treatment is usually followed by a post-refining treatment to reduce the fiber length in order to minimize the flocculation and clogging tendency during homogenization, which is the last step. The enzymatic approach has been suggested to be suitable for large-scale manufacturing of MFC at reasonable costs [9].

2.2.3 Mechanical Treatments

An array of methodologies exists for the mechanical treatment step in the production of MFC and NFC (**Figure 6**). Homogenization, grinding, and refining are the most frequently employed procedures among others, such as extrusion, blending, ultrasonication, cryocrushing, steam explosion, ball milling, aqueous counter collision etc. Homogenization, grinding and refining are discussed briefly in the following sub-sections.

Homogenization

The concept of homogenization has been used extensively in food, cosmetics and pharmaceutical industries for long. Two common equipments employed for homogenization are homogenizers and microfluidizers.

Homogenizers utilize a positive-displacement piston pump and a spring-loaded valve assembly to subject cellulose fibers to extremely high-impact shearing forces. Dilute slurries of cellulose fibers, pumped at high pressure, pass through a tiny gap between the impact ring and the valve (**Figure 6**), which opens and closes in rapid succession. These reciprocating mechanical forces promote a high degree of fibrillation of the cellulose fibers, resulting in production of MFC and/or NFC.

Microfluidizers utilize Z- or Y-shaped (**Figure 6**) pressure-treatment constrictions to achieve fibrillation. Cellulose suspension is accelerated through these narrow, 100–400 μm in width, orifices at high pressure. This promotes intense particle collision and strong shear forces, which split the fibers off into fibrils. A smaller constriction requires higher pressure, resulting in a higher degree of fibrillation.

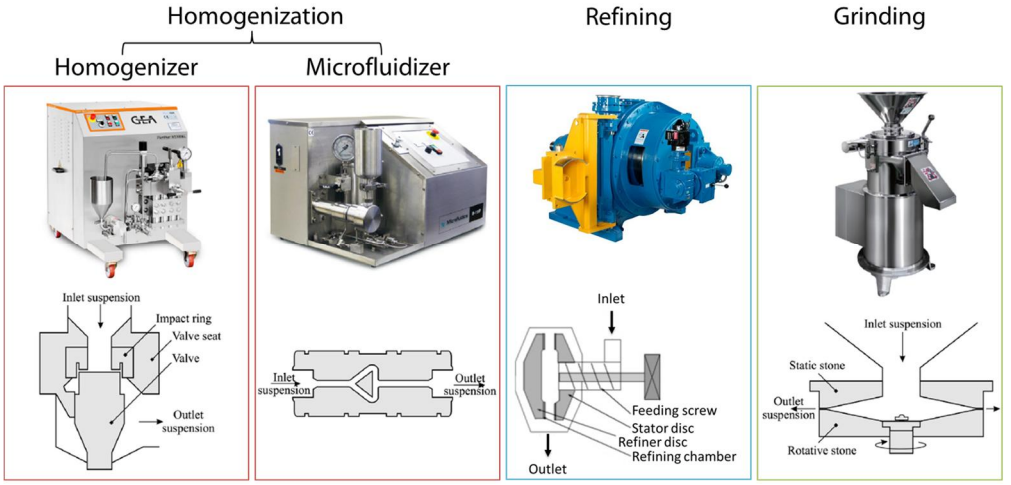

Figure 6. Mechanical treatment methods for MFC/NFC production. (Modified from [69]).

Refining

Refining is another mechanical approach that can be used to fibrillate cellulose fibers. It has already been used in paper industry for long as an essential step in developing the quality level of pulp fibers [87]. A refiner utilizes the gap between two metal discs, usually one rotating and one stationary (**Figure 6**), with grooved surfaces to apply high shear forces on the fiber suspension in aqueous medium. This process is known to swell and peel the fiber's cell wall leading to increased specific surface and volume [88]. However, it degrades the DP of cellulose through a variety of simultaneous changes such as fiber shortening or cutting, and fines formation [57]. Nevertheless, specialized refiners with careful gap control seem to be scalable options for MFC and NFC production. This is attributable to the clog-free operation and the potential to use higher concentration fiber suspensions in the refiner compared to the homogenization equipment.

Grinding

Grinding is another common MFC and NFC manufacturing process similar to refining, except that the rotor and the stator of the grinder are ceramic, and the gap-clearance is narrower. Supermasscolloider grinder (MasukoSangyo Co. Ltd., Japan), or simply Masuko grinder, is a good example of this treatment process. In this process, the fiber suspension is passed through the narrow gap between static and rotating grinding stones, resulting in disintegration of fibers through frictional forces and the high impact of the grinding action. The possibility of gap adjustment controls the level of fibrillation achieved and helps avoid the problem of clogging. The merits of the grinding method, i.e. simplicity and robustness, make it ideal for large-scale MFC production.

Another mechanical treatment method worth mentioning is co-grinding of cellulose fibers with minerals such as kaolin and calcium carbonate, where the grinding media transfer high shear forces to fibers, resulting in fibrillation. The outcome is a composite of MFC and mineral. This method has been patented [89, 90] and industrialized [91] under the name FiberLean MFC by the filler suppliers Omya Development AG and Imerys SA.

The different production techniques lead to MFC and NFC with varied morphology and properties. For example, the MFC produced using mechanical treatments alone or with enzymatic pre-treatment display a wider size distribution, as compared to NFC produced employing chemical pre-treatments. It is generally difficult to compare different delamination methods and to quantify the MFC/NFC quality vs. energy consumption.

2.3 Characterization of MFC/NFC

There is a wide variation in the kinds of MFC and NFC obtained using different raw materials and production routes, which makes it difficult to compare their properties reported in literature. Furthermore, the understanding of properties of MFC/NFC is still growing, and a lack of universally accepted protocols for sample preparation and characterization of these systems hinders the effective comparison of different findings in literature [56]. Proper characterization of these materials is of the utmost importance for safety and facilitating their usage in potential applications, as suggested in the recent reviews by Naderi et al. [56] and Kangas et al. [92].

2.3.1 Morphology and Surface Charge

Microscopic imaging has been the primary method of assessing fibrillated cellulose for morphology, structure and particle size distribution, although it is time consuming and based on subjective characterization of small portions of a large sample [44]. Optical microscopy (OM), scanning electron microscopy (SEM), transmission electron microscopy (TEM) and atomic force microscopy (AFM) have been the most commonly employed imaging techniques. The diameter of nanofibrils can be estimated with precision using high magnification, but it is rather difficult to accurately determine their length due to the high aspect ratio. A lower magnification may be used to capture the whole length, but the nanofibrils become undetectable due to their nanoscale diameter. Based on the data from several reports, Chirayil et al. [93] have confirmed that MFC and NFC are long and flexible spaghetti-like structures with 1–100 nm diameter and several microns length, and they consist of alternating crystalline and amorphous regions. Furthermore, it is well established that MFCs produced using mechanical treatment alone or enzymatic pre-treatment differ considerably, in terms of morphology and size distribution, from NFCs produced employing chemical pre-treatments [69]. Generally, MFCs prepared using the former methods have a slightly larger diameter and wider size distribution compared to NFCs produced using the latter methods. Moreover, MFCs possess flocculated structures [94-96]. These differences arise from the low level of fibrillation achieved in MFCs, resulting in some portion of non-fibrillated macroscopic fibers or fiber fragments [69].

A well-dispersed MFC/NFC suspension is key to fully exploiting the micro/nano-scale properties of fibrils. It is important to not confuse dispersion with fibrillation. Fibrillation indicates the degree of delamination of fiber during mechanical treatment. On the other hand, dispersion is an indication of how separated the individual MFC/NFC fibrils are in the suspension. The state of MFC/NFC dispersion is dependent on the charge density of fibrils and presence of additives. It is essential to estimate the surface charge of MFCs and NFCs for

predicting their behavior in suspensions. The surface chemical properties of MFCs are very similar to that of native cellulose, whereas chemical pre-treatments used for NFC production naturally change the cellulose chemistry, creating the need for surface chemical analysis [92]. Zeta potential measurements have been found useful in determining the charge levels on cellulose surface [97-99]. In addition, different conductometric and potentiometric titration methods have been utilized for determination of surface charge and content of functional groups on the surface of cellulose nanofibrils [15, 100, 101]. In most reports, the charge content of NFCs is usually higher compared to MFCs due to the chemical pre-treatments utilized in their production, resulting in more stable suspensions. Zeta potential can also be used to evaluate the dispersion and stability of MFC/NFC suspensions and the adsorption of additives on fibrils. A high magnitude of zeta potential indicates a well-dispersed colloidal system because of high repulsive forces between the constituents.

2.3.2 Water Retention

Water retention is the term used for ability of a material to resist dewatering. Many studies have evaluated the water retention of pulp suspensions [102-104] and MFC/NFC suspensions [12, 13, 78, 102, 104, 105]. Some [104] have even used the water retention value to evaluate the degree of fibrillation of MFC/NFC. Water retention values of MFC/NFC suspensions are generally an order of magnitude higher compared to the pulp suspensions [105]. This is attributable to the high specific surface area, high aspect ratio and volume of fibrils in MFC/NFC imparting high water holding capability [13]. Furthermore, higher carboxylate content results in a higher water retention value of NFC [78]. The high water retaining capability of MFC/NFC is undesirable for papermaking due to the slow dewatering rates. However, some studies have utilized this capability for tuning the dewatering rates of pigment coating suspensions [57, 58, 106-108].

For paper coating process, water drainage of coating suspension is a critical parameter influencing coatability. Dewatering rates of a coating slurry affect the coating rheology and processing conditions. A too quick or too slow water drainage may have negative impact on the coating process and the final coating properties. The dewatering rates of pure MFC/NFC suspensions are usually an order of magnitude higher than the conventional pigment coating suspensions due to very low solids content of the former. No study has evaluated the influence of dewatering rate of pure MFC suspensions on their coatability. The large amount of water in MFC suspensions makes it essential to understand and control the dewatering rate for successful coating on paper-based substrates. For example, a quick release of large amounts of water from MFC suspensions into

paper during coating can cause fiber swelling and de-bonding leading to runnability problems, such as web breaks.

2.3.3 Rheology

Understanding rheology of MFC/NFC suspensions is not only of theoretical importance, but it is also critical for their successful processing, which involves several operations, such as mixing, pumping, extrusion and coating. Even at low solids content, MFC/NFC suspensions exhibit a gel-like behavior and complex rheological properties, as is evident from several recent reviews [47, 54-58, 66, 109, 110].

The rheological response of MFC/NFC suspensions depends on shape, dimensions, crystalline structure, and surface properties of constituent fibrils, and it changes with solids content [14, 111-113], ionic strength [111, 114-119], temperature [13, 59, 120], and presence of additives [94, 121-123]. Production process and cellulose raw material source strongly influence the physical and chemical properties of MFC/NFC, which in turn affects the rheology [59, 111, 120, 124-127]. For example, MFCs usually possess flocculated structures in water [95, 96], whereas NFCs are colloidally stable due to presence of high charge on the surface [120, 128]. MFCs demonstrate lower network strength compared to NFCs at equivalent solids content due to higher surface area and degree of entanglement in the latter [55, 120, 129]. However, both types of suspensions display shear thinning and thixotropic behavior. In context of the work herein, the reports on rheology of MFC suspensions are discussed in detail.

A variety of techniques involving rotational rheometers [14, 111, 120, 129, 130] and pipe [131, 132] or capillary [59] rheometers are generally employed to measure the flow properties and viscoelasticity of MFC suspensions. Furthermore, different geometries, e.g. parallel-plate-type, cone-plate-type, Couette-type, vane-type etc., and gap sizes are utilized in rotational rheometers. However, the multi-length-scale heterogeneity of MFC suspensions requires stringent protocols for sample handling and analysis of the rheological data [56]. For example, a Couette-type geometry with a gap size of at least 1 mm was suggested more advantageous compared to others, when studying rheology of MFC suspensions that are prone to flocculation and phase separation [133]. Naderi and Lindström [54] highlighted the importance of pre-shearing of MFC suspensions for achieving reliable results. Mohtaschemi et al. [130] stressed the importance of using vane rheometer to avoid wall slip, while Nechyporchuk et al. [129] and Naderi and Lindström [120] suggested using serrated geometries, instead of smooth geometries, to diminish the slip effects. It is important to note that wall slip/depletion may dramatically affect the viscosity values obtained using the standard geometries. Nevertheless, this effective viscosity data can be useful for designing/processing purposes. A combination of rheological

measurements and a visualization device has been recommended for a precise determination of the rheological response of these suspensions [55, 56].

MFC suspensions demonstrate gel-like behavior even at solids content as low as 0.125% [14]. The gel-like microstructure leads to a considerable yield-stress for MFC suspensions [57]. The strong and flocculated gel network is due to the physical entanglements between fibrils, which grow with increasing solids content. The linear viscoelastic behavior of the MFC gel structure can be determined using oscillatory shear measurements. The strain domains where storage (G′) and loss (G″) moduli are strain independent, i.e. the linear viscoelastic regions, are first determined with oscillatory strain sweeps. Subsequently, the oscillatory frequency measurements are performed at a strain within the linear viscoelastic region [55]. For MFC suspensions, G′ has been reported higher than G″, indicating the solid-like behavior dominance, and both the dynamic moduli (G′ and G″) have been reported to increase with solids content [111, 113, 129, 134, 135]. Furthermore, beyond the critical network forming concentration for MFC suspensions, G′ in linear viscoelastic region increases exponentially as a function of the solids content. The exponent values for MFC suspensions reported in literature range from 2.25–3.7 [14, 111, 135, 136]. These values are slightly higher than the theoretically proposed values (2–2.5) for entangled fibrous gels and semi-flexible polymer systems [137, 138], but they are in agreement with the values summarized for pulp suspensions, i.e. 1.7–3 and 2–3, in recent reviews by Kerekes et al. [139] and Derakhshandeh et al. [140], respectively. Some authors have also utilized the storage modulus value as an indicator of the fibrillation level achieved [54, 133, 136].

Similar to viscoelastic measurements, shear viscosity measurements have also been utilized to assess the fibrillation level of MFC by some researchers [13, 141, 142]. The viscosity increases with increasing degree of fibrillation, and flow curves with reduced fluctuations are obtained. It is well known that MFC suspensions possess shear thinning and thixotropic properties due to the prevailing fibril organization being broken down by shearing and the time it takes to reach an equilibrium at any given shear rate [14, 57, 96, 111]. The flow of MFC suspensions disrupts the network structure and may also involve the deformation and rupture of individual flocs [57]. Interestingly, Saarikoski et al. [96] and Karppinen et al. [95] have reported a flocculated fibril structure in 2% MFC suspension even when subjected to shear rates up to 1 000 s^{-1}, though the size of flocs decreased with increasing shear rate. Furthermore, some studies have reported a Newtonian plateau or “kink” in the viscosity curve [14, 95], and a hysteresis loop when increasing-decreasing (or vice versa) the shear rate [59]. These phenomena are associated with formation and breakdown of shear-induced structures in MFC suspensions.

Some authors [95, 96, 143] combined rheological measurements and image-analysis to study the structural changes related to the origin of the Newtonian plateau. It was reported that flocs in MFC suspensions form a sintered structure, and the structure change with increasing shear rates happens in three stages. First, the large flocs break into floc rolls elongated along the Couette height, forming chain-like structures. As the shear rates increase further, the floc rolls start to disintegrate and form small individual spherical flocs. Finally, at high shear rates, the flocs are detached, and their size is inversely proportional to the shear rate. Furthermore, this transition in floc structure was reversible upon decreasing the shear rate. However, the measured shear stress during back ramp, typically at low shear rates, was lower; hypothesized to be due to some irreversible aggregation of the MFC network caused by the high shear rates. Shear rates beyond 1 000 s^{-1} were not explored to ascertain any further changes in floc structure, and the conclusion is based on the study of the macro-sized constituents of the investigated MFC [56].

The shear thinning of MFC suspensions can be attributed to breakdown of fibril flocs and consequent alignment of the individual fibrils in the direction of flow. However, a low power law index, typically below 0.2, suggests presence of fiber-depleted water-rich lubrication layer between the bulk material and the geometry wall, in which most of the shearing happens. According to Buscall [144] and Barnes [145], the wall depletion occurs in flow of dispersions in rheometer because of the displacement of the dispersed phase away from solid boundaries due to various forces (steric, hydrodynamic, viscoelastic and chemical), forming a lower-viscosity, particle-depleted liquid boundary layer on micron scale. The creation of such a low-viscosity boundary layer at the wall provides a lubricating (slip) effect, resulting in low flow resistance [145]. This wall depletion phenomenon has been known to occur for a long time [146, 147]. Furthermore, Phillips et al. [148], Joseph [149], and Pan et al. [150] have also confirmed the flow/shear-induced particle migration away from the wall. There are recent works demonstrating the existence of a few microns thick fiber-depleted layer near boundary walls in flow of MFC suspensions [131, 132, 151]. This behavior resembles that of pulp suspensions [140, 152, 153].

From the above review of literature on rheology of MFC suspensions, it is clear that producing reliable information on their rheology using conventional rheometers is rather challenging due to the high aspect ratio of fibrils, strong interfibrillar forces, wide size distribution of fibrils, and their flocculating and phase-separating tendencies. The physical entanglement of fibrils, the growth or breakdown of flocs with shear brings in further complexity. Furthermore, there is a lack of work on high shear rheology, especially in pressure-driven flow, of these suspensions. In the author's knowledge, Iotti's [59] is the only study that

has only briefly presented the high shear rate (beyond 200 000 s^{-1}) rheology results of MFC suspensions (1% solids), and they found a dilatant behavior. It is important to characterize the rheology at high shear rates using pressure-driven flow to predict process behavior, e.g. in extrusion or coating operation. Such understanding may help in designing a suitable process for conversion of nanocellulose into products. Furthermore, the pressure-driven flow may help overcome the challenges associated with boundary-driven flow, e.g. only measurements at low solids content are possible, in rheological determination of MFC suspensions. A combination of zeta potential, charge density, water retention, and rheology measurements can potentially be utilized to improve the MFC processability.

2.4 MFC and NFC Films

It is well known from papermaking that cellulose fibers stick together through hydrogen bonding to form paper upon evaporation of excess water from pulp suspension. In a similar fashion, MFC/NFC fibrils tend to form strong and transparent films with excellent oil and gas barrier performance. Strong hydrogen bonding between fibrils arising from their high surface area and nanoscale size are responsible for the superior mechanical performance of the films compared to the conventional paper [154]. The high crystalline content of MFC/NFC is believed to account for the film's denser character and attractive barrier properties [22, 155, 156]. In addition, much smaller diameters of MFC/NFC fibrils compared to the wavelength of visible light allows them to either suppress the light scattering [25] or cause it in the forward direction [157], resulting in transparent films. The past decade has witnessed extensive research effort on MFC/NFC films, and there are several excellent reviews [33, 47, 56, 158-160] covering various aspects of these films.

2.4.1 Strength Properties

The extent of fibrillation achieved in MFC/NFC production strongly influences the level of hydrogen bonding during film forming [47]. Cellulose raw material and its composition and the MFC/NFC production process affect the fibrillation process, and as a result, the strength properties of MFC/NFC films [23, 105, 161-166]. In addition, the film preparation technique [156, 167, 168] and drying conditions [169] employed affect the strength properties. Furthermore, the DP of cellulose, and porosity and moisture content of MFC/NFC films have also been reported to influence the mechanical properties of MFC/NFC films [159]. The range of tensile strength index and stiffness of MFC/NFC films, obtained from a recent review [47], is 130–212 kNm/kg and 8–11 GPa, respectively. The wide range is not surprising given the variations in raw material source and MFC/NFC production process between different studies. Overall, NFC films are reported to have higher strength compared to MFC films, attributed to the high surface area

of fibrils in the former. In addition, NFC films tend to be more brittle; however, a use of plasticizers, such as glycerol and sorbitol, has been suggested to reduce the brittleness [170].

2.4.2 Barrier Properties

Barrier properties of polymers, in our case cellulose, are largely determined by the crystallinity and the network structure formed by the constituting units in a dry film because it is difficult for other molecules to penetrate the crystalline parts or the very dense network [22, 155, 156]. High crystallinity and dense packing due to the nanoscale size of MFC/NFC fibrils afford the films a high oxygen barrier [22, 156, 171, 172]. However, they have a poor water vapor barrier due to the hydrophilic nature of the cellulose molecule. The water vapor barrier function of these films is affected by various parameters, such as chemical composition of wood sources [105], addition of plasticizers [172] etc. Certain post treatments, such as acetylation and solvent exchange [173], coating of MFC films with cooked starch, beeswax and paraffin [174], gas phase esterification [175], and treatment with alkyl ketene dimer [23], have been reported to improve the water vapor barrier. It is important to note that plasticizing and swelling of the MFC/NFC fibrils by water molecules can cause a dramatic drop in the oxygen barrier properties at high relative humidity (RH) [22, 172]. NFC films with excellent grease barrier and resistance to solvents, such as methanol, toluene and dimethylacetamide, were also reported recently [176].

2.5 MFC and NFC Coatings

MFC and NFC coatings have been explored by several researchers for different purposes. **Figure 7** shows the different utilization strategies for MFC/NFC coatings and their potential target applications. This section first summarizes different coating methods used for MFC/NFC surface application on paper or other substrates, and then discusses the potential applications of the coatings. It is noted that several researchers have explored also the bulk applications of MFC/NFC in paper as wet end additives, and these are summarized in recent reviews [18, 44, 45, 51]. For example, Xu et al. [99] used a commercial Hydra-Sizer™, a curtain coating equipment developed by GL&V (USA), to apply MNFC as a structuring layer within a TMP sheet during papermaking to improve the mechanical and barrier properties of the TMP sheet. Furthermore, there are recent reports on pilot scale trials on usage of MFC as wet end additive to improve mechanical, barrier and printing properties of paper [177]. In a related context, surface application of mineral pigment and MFC mixture at the wet-end to improve printing and mechanical properties of paperboard was also reported recently [91, 178, 179].

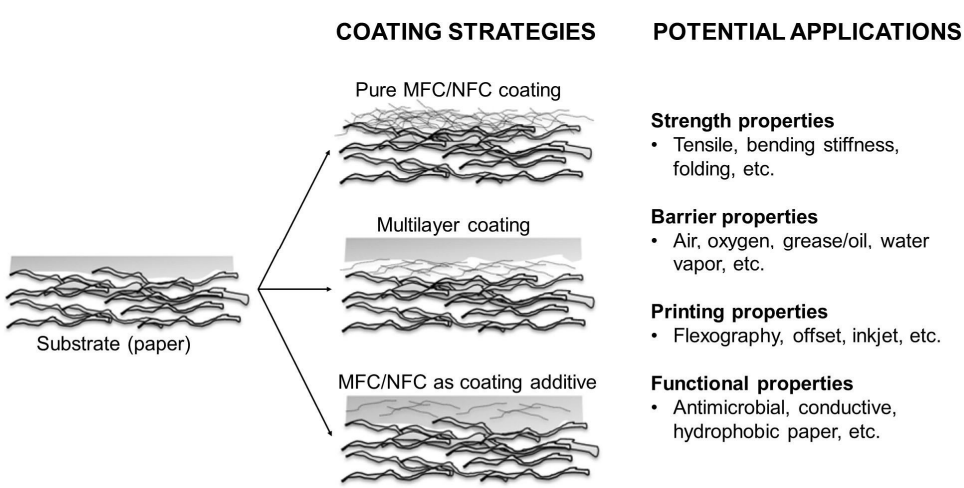

Figure 7. Strategies for utilization of MFC/NFC as coating (modified from [18]).

2.5.1 Coating Methods

There is a multitude of coating processes for paper, but only some of them are applicable when MFC/NFC suspensions are the coating material. The very high viscosity of these suspensions at low solids content limits the suitable techniques. Some of the coating methods utilized for MFC surface application have been rod coating, size press, spray coating, and foam coating. **Table 1** lists the MFC/NFC coating techniques utilized so far and reported in literature. Most of these studies have applied multilayer coatings, the reason of which will become clear in the further discussion.

Bench-scale rod/bar coating has been the most employed technique, as is clear from **Table 1**. Different kinds of MFCs and NFCs at various solids content, typically between 0.5–2%, have been used for coating with this method to obtain coat weights of approx. 1–8 gsm, in single and multilayer applications [22, 180, 185, 186, 189, 190, 200-202]. In addition, two of these studies used higher MFC solids content of 3% as well [189, 201]. Furthermore, Ridgway and Gane [188] applied commercial grade ARBOCEL NFC (ANFC) (4% solids) and Omya MFC (OMFC) (10% solids) coatings in single, double and triple layers, which resulted in 2.1–5.6 gsm and 2.5–11.9 gsm ANFC and OMFC coat weights, respectively. In a separate study [187], the same authors also reported coating of ANFC (10% solids) at a coat weight of 4 gsm. Lavoine et al. [192-199] used this coating process to apply enzymatic MFC (2% solids) on paperboard in many separate studies. The authors reported five- and ten-layer application to obtain coat weights of 6–7 gsm and 14 gsm, respectively. Based on these reports, one can conclude that rod coating technique produces coat weight of a few gsm in a single layer application. Multiple coating layers are required to obtain coat weights sufficient for suitable barrier performance. Besides, the high viscosity of

MFC/NFC suspensions limits the maximum solids content that can be used with this coating method.

Size press is another technique that has been frequently utilized for MFC coating. In one of their studies, Lavoine et al. [198] used a size press for MFC (1.6% solids) coating. However, five- and ten-layer application with size press achieved only low coat weights of 3 gsm and 4 gsm, respectively. Boissard [205] recently used size press (flooded configuration) to apply MFC coating on paper and obtained low coat weights of approx. 1 gsm. Richmond [108] also reported a laboratory type size press device (flooded and metered configuration), and a cylindrical laboratory coater (CLC) for five-layer coating of mechanically produced MFC suspensions (3.5–10% solids) on a bleached wood free paper. He obtained a range of coat weights (2–8 gsm) using these different techniques. Multiple layers in size press coating do not increase the coat weight significantly, as observed in all these studies. This could be due to the impregnation of the MFC into the substrate due to the pressure applied by the rolls, and once the paper structure is filled with MFC, it hinders further accumulation of MFC on the surface.

Other less commonly used techniques are foam and spray coating. Pilot-scale foam coating of enzymatic MFC (2% solids) and TEMPO-NFC (2.9% solids) using a narrow slot-type applicator was recently reported by Kinnunen-Raudaskoski et al. [53]. The authors applied single and multilayer coating at 100 m/min to obtain coat weights of 0.1–2.6 gsm. Beneventi et al. [203] applied enzymatic MFC (2% solids) using a bench-scale spray coating onto wet substrates moving on a conveyer at speeds of 0.5–12 m/min to get MFC coat weights from 3–40 gsm. Amini et al. [204] used filtration and deposition technique to apply mechanically produced MFC/silver nanoparticle coating on paper and obtained coat weights 0.5–2.5 gsm. Syverud and Stenius [156] reported coating of MFC (0.06% headbox consistency) on paper using a dynamic sheet former (FiberTech, Sweden). The MFC top layer and the base paper were combined wet in wet, and the final MFC coat weight varied between 2–8 gsm.

Table 1. Coating techniques utilized for MFC/NFC surface application

Coating process	No. of applied layers	Reference
Bench-scale rod/bar coating	Single/multilayer	[22, 57, 180-202]
Foam coating using narrow slot-type applicator	Single/double layer	[53]
Bench-scale spray coating onto wet substrates	Single layer	[203]
Filtration and deposition	Single layer	[204]
Size press	Single/multilayer	[108, 198, 205]
Dynamic sheet former (wet on wet application)	single layer	[156]
Cylindrical laboratory coater	Single/multilayer	[108]

Drying is another important factor in MFC coating application. The water sensitivity of substrates and the large water content of MFC suspensions make the drying process energy-intensive. In addition, this might influence the final properties of the coated substrates. A variety of drying methods were used in the previous studies. Contact drying [108, 185, 191-199, 205], infra-red (IR) drying [53, 57, 108, 181-184, 198, 205] and hot air drying [53, 186-188, 190] have been the most commonly used techniques. In addition, oven drying [180, 189], vacuum drying [203] and room temperature drying [204] have been employed in some studies. In most cases, the coated substrates were dried under tension to avoid curling problems.

It should be noted that these coating methods do work for MFC/NFC coating application, but they are limited in some ways. For example, the maximum coat weight obtained in single layer application is low due to possibility to coat at only low solids content, limited by the high viscosity of MFC/NFC suspensions. Furthermore, drying is a challenge due to the large amounts of water that need to be evaporated, and therefore most of these coatings are batch processed, except the foam coating reported by Kinnunen-Raudaskoski et al. [53]. However, the coat weights obtained with the foam coating method used by the authors were too low to provide an efficient barrier performance. It is also interesting to note that most of these studies report a multilayer coating to achieve high enough coat weight for a considerable barrier performance. A key issue that prevents the immediate use of MFC/NFC as a coating is the complex rheology and the large water content of these suspensions. Even at a solids content below 2%, the flow behavior is non-Newtonian with significantly high viscosities. This creates the need for a coating method that can overcome the challenges associated with these conventional coating techniques.

2.5.2 End-use Applications

Typical end-use applications of MFC/NFC coatings on paper can be classified into two broad categories: (i) barrier and strength applications, (ii) printing and functional applications. Literature reports addressing each of these application categories are summarized in the following sub-sections. For the first category, only reports using pure MFC/NFC or MFC/NFC as main component in a coating layer are included in the discussion to remain within the scope of this work. However, in the second category, usage of MFC/NFC as a secondary component in functional coatings is also included in the discussion.

Barrier and Strength Applications

This has been the most commonly targeted category for applications of MFC/NFC coatings. This is due to the excellent barrier properties of MFC/NFC, when used as a film or as a paper coating material. Air, water vapor, oil/grease and oxygen

barrier properties of MFC/NFC coatings are the most reported in literature. Improvement in strength properties of substrate is expected with MFC/NFC coating due to the inherent strength of MFC/NFC films, as discussed earlier. Tensile strength, stiffness, bending stiffness and surface strength improvements with MFC/NFC coating have been reported in literature.

Syverud and Stenius [156] were the first ones to report significant improvements in air barrier of paper with MFC coating application. They found the air permeance of base paper to drop from 65 μm/Pa·s to 0.33–0.0036 μm/Pa·s, with increasing coat weight of MFC from 2 to 8 gsm. Aulin et al [22] were next to confirm these findings. They found the NFC coating to significantly decrease the air permeance of wrapping paper and greaseproof paper. The air permeance dropped from 69 μm/Pa·s to 0.0048 μm/Pa·s for wrapping paper just with a single coating layer application (coat weight, 1.3 gsm), and further to 0.003 μm/Pa·s with the application of a second coating layer (total coat weight, 1.8 gsm). For the greaseproof paper, the air permeance was reduced from 0.66 μm/Pa·s to 0.0002 μm/Pa·s upon application of a single coating layer (coat weight, 1.3 gsm). In addition, Nygårds et al. [206] from the same group showed that NFC coating as air barrier performs better compared to MFC coating, owing to a closer packed structure obtained in the former due to smaller fibrils. Bardet et al. [207] also found that thin MFC coatings exert a positive impact on CO_2 and air barrier properties. Furthermore, there have been many recent studies [53, 189, 198, 201, 203] confirming the air barrier improvement with MFC/NFC coatings.

Aulin et al [22] were the first to investigate the oil barrier properties of NFC coatings and found the nanoporous network formed by entangled microfibrils to be responsible for improved oil resistance of the coated paper. Amini et al. [204] reported improvements in water vapor barrier and oil resistance of NFC/Ag coated papers. Mousavi et al. [189] recently reported coating of MFC on paperboard to improve water, moisture, and grease barrier performance and found that CMC used as an additive improved coatability and final coating quality. In addition, a higher degree of fibrillation of MFC material led to more uniform coating and thus superior barrier performance.

Use of MFC/NFC as a layer in a multilayer coating structure containing other materials has been reported to be beneficial for barrier performance. For example, Hult et al. [208] found a multilayer structure comprising a MFC pre-coat layer and a shellac topcoat layer to drop the oxygen and water vapor permeability significantly. Aulin and Ström [200] found the NFC coating layer to notably affect the homogeneity and barrier performance of the alkyd resin layers in a multilayer coating structure. On the same principle, Axrup et al. [209] have patented a paper substrate covered with a MFC pre-coat layer (coat weight,

1.2 gsm) in combination with a polymer topcoat layer deposited by lamination or extrusion coating. These different studies seem to point that MFC/NFC performs better in combination with other barrier layers because the moisture sensitivity issues of MFC/NFC can largely be avoided in such situation.

In terms of strength properties, Syverud and Stenius [156] were again the first to report an improvement in strength and surface smoothness of paper sheets with MFC coating, credited to the filling of large surface pores by MFC. Charani et al. [202] reported MFC coatings leading to a significant improvement in the strength properties of coated hand sheets. Lavoine et al. [197] reported improvement in strength properties of cardboard with MFC coating. In another study [198], they also observed considerable improvement in bending stiffness of paper coated with MFC. Afra et al. [201] showed that MFC coating improves surface smoothness, surface strength, tensile strength, and stiffness of paper. At the same coat weights, a double coating layer applied at low solids (1.5%) concentration performed better than a single coating layer applied at high solids (3%) concentration, as reported by the authors. Amini et al. [204] reported improvements in tensile strength of MFC/Ag coated papers. Recently, Ridgway and Gane [188] found the paper stiffness and surface properties to improve when MFC was applied on a porous pre-coating layer on paper, credited to an excellent MFC holdout on such surface. These findings indicate a great potential for MFC/NFC coatings, for they can provide strength improvements along with the excellent barrier performance.

Printing and Functional Applications

Use of pure MFC/NFC coating to enhance printing properties of substrates is relatively less reported compared to the first category applications. Song et al. [186] were the first to report a slight reduction in linting and dusting propensity of newspaper during offset printing, when a thin NFC coating was applied on the newsprint substrate. Moreover, adding anionic starch to NFC resulted in superior coating performance in terms of reduction in the mentioned properties. During the same year, another group [181] reported improvement in inkjet print quality of synthetic fiber sheets with NFC coating. The improvement was suggested to be due to capturing of ink pigments on the surface by the entangled NFC network. Subsequently, the same group [184] found NFC coating on AKD pre-coated paper to improve the print density and reduce print-through. For screen-printing applications, NFC coating has been utilized to control the excessive vehicle penetration rates which otherwise lead to problems of strike-through and pigment-peeling [183]. Furthermore, Hamada et al. [190] recently reported improvement in color density during inkjet printing of NFC coated woven and nonwoven fabrics. According to the authors, the NFC coating could trap even very small pigments of the inkjet ink that contributed to increase of the

color density on the printed samples. For printing applications, another important benefit of NFC coating is that the coated areas do not differ visually or optically from the uncoated areas on paper-based substrates because of the characteristic fiber structure of the coating [190].

The functional applications of MFC/NFC coatings are starting to receive attention. These applications mainly include conductive coatings and antimicrobial coatings among others.

Conductive coatings have potential uses in various energy generation and storage applications, e.g. in batteries, supercapacitors, and photovoltaics. Compared to MFC/NFC, there are more reports on use of CNCs in these applications [210, 211]. In conductive coating applications, MFC/NFC can find use as a pre-coating before the conductive layer is applied or as a binder in the conductive coating layer itself [157, 212, 213]. For example, the nanoporous network provided by the MFC/NFC coating layer may help retain the functional components of the conductive coating on surface. Furthermore, the excellent solvent barrier properties reported for NFC films [176] could be utilized for production of NFC coated substrates for printed electronics applications, which require these barrier properties during printing of functional inks. Hoeng et al. [35] and Zhu et al. [214] recently provided comprehensive reviews on the use of nanocellulose in printed electronics applications. In addition, Andres et al. [215] recently showed benefits of using NFC as a binder in nanographite electrodes for supercapacitors. NFC binder improved mechanical performance of electrodes while not harming the electrical performance. On the other hand, Osong et al. [216] have reported addition of nanographite to NFC to produce conductive composite films.

The antimicrobial coatings comprising NFC and silver nanoparticles (Ag) have been recently reported [204, 217]. The results of Amini et al. [204] demonstrated that the NFC/Ag coating exhibited good antibacterial activity against Escherichia coli (Gram-negative) and Staphylococcus aureus (Gram-positive) bacteria. Martins et al. [217] investigated antibacterial properties of NFC/Ag embedded starch coatings towards S. aureus and K. pneumoniae microorganisms and found the coatings to perform well even at low Ag contents. Furthermore, Lavoine et al. [195] recently reported coating of a chlorhexidine digluconate (CHX) solution mixed with MFC onto paperboard samples for developing antibacterial bio-packaging. MFC coating was found to help control the release of CHX providing antibacterial function against Bacillus subtilis. The same group has reported many such controlled release studies [192-194, 196, 199] for active packaging applications. These studies have truly revealed the significance of using MFC in functional active packaging applications.

In conclusion, the applications in this category are promising for MFC/NFC because they bring opportunities for the large-scale production of low-cost value-added paper-based materials utilizing MFC/NFC.

2.6 Summary of Challenges in MFC Rheology and Coating

Based on the literature review in this chapter, many challenges have been identified, which are obstacles for commercial MFC/NFC coated products.

It is difficult to compare the findings in literature on MFC/NFC due to variety of sources and production methods used by different researchers. Development of standard protocols for characterization of these materials is still in its nascent stage, considering that the standard terms and their definitions for cellulose nanomaterial have just been finalized recently (TAPPI: WI 3021 & ISO/TS 20477:2017).

For MFC fibrils, the high aspect ratio, strong interfibrillar forces, wide size distribution, and their flocculating and phase-separating tendencies challenge a reliable determination of their rheology using conventional rheometers. The issue is further complicated by the physical entanglement of fibrils and the growth or break down of flocs with shear. Additionally, high shear rheology, which is industrially relevant, has not been explored.

MFC/NFC coatings improve the barrier performance, yet the low coat weights of pure MFC/NFC are not sufficient to achieve desired levels. Moreover, it is challenging to increase the deposited coat weights using conventional coating techniques due to the low solids content of MFC suspensions. A coating technique that can allow depositing high coat weights while allowing drying of the MFC coating in a continuous process is desired to proliferate the industrial use. Furthermore, it should be able to overcome the challenges associated with the high viscosity of MFC/NFC suspensions at rather low solids content.

At the same time, it is also important to demonstrate the utility of such method for functional coatings containing MFC/NFC. The functional coating suspensions may have similar challenges in coating either due to their own constituting units or due to the presence of MFC/NFC.

3. Materials and Methods

3.1 Materials

MFC used in this work (**Publication I-IV**) was produced by the Process Development Center of the University of Maine (Orono, USA), as described by others [57, 108]. It was prepared mechanically from a bleached softwood Kraft pulp without using any pre-treatments. A double disk refiner (GL&V, USA) equipped with specialized plates operating at carefully controlled low clearance was used for the mechanical treatment. The pulp was first dispersed using a beater and subsequently circulated through the refiner until the fines content reached over 90%, as measured with a standard fiber size analyzer MorFi (Techpap, France). The MFC suspension was obtained at ca. 3.5% solids content and stored refrigerated. For experiments, the solids content was adjusted by adding distilled water.

CMC (FINNFIX® 4000G) in dry powder form was provided by CP Kelco Oy (Äänekoski, Finland). CMC solution (1 wt%, 2 wt% and 3 wt%) was prepared by dispersing an appropriate amount of CMC powder in distilled water by stirring at 500 rpm for 5 h at room temperature. The solution was stored overnight before use to ensure complete dissolution. The degree of polymerization, degree of substitution (DS) and molecular weight of CMC were 2 000, 0.8 and 450 000 g/mol, respectively.

In **Publication IV**, six different pre-coatings, listed in **Table 2**, were used before applying the MFC coating.

Water based coating formulation (**Publication V**) at ca. 3% solids was provided by the Mid Sweden University (Sundsvall, Sweden). It consisted of nanographite as pigment and a nanofibrillated cellulose (NFC) as binder at 10 wt% of the total pigment. Based on the previous experience from Andres et al. [215], this binder amount was suitable for a stable dispersion and optimal mechanical and electrical performance of the electrodes prepared with the suspension.

Nanographite was produced according to the method described by Blomquist et al. [218]. First, a thermally expanded graphite (SO# 5-44-04) (Superior Graphite, Sweden) was dispersed into water at a concentration of 20 g/L using a polyacrylic acid dispersant at 2 wt% of the graphite amount. Subsequently, the dispersion was passed through a hydrodynamic tube-shearing device for ten cycles to mechanically exfoliate the graphite. The freshly prepared nanographite

dispersion was a mixture of graphene, multi-layer graphene and larger graphite particles.

NFC (**Publication V**) was produced using TEMPO-mediated oxidation, as described by Saito et al. [16]. Briefly, an amount of 100 g of a never dried fully bleached softwood Kraft pulp was diluted to 2.5% solids in 4 L deionized water. Sodium bromide (NaBr) (Merck Millipore, Sweden) and TEMPO (Sigma-Aldrich, Sweden) were added to the pulp suspension at 2 mmol and 0.2 mmol per g oven-dry pulp, respectively. Thereafter, the suspension was stirred to disintegrate any agglomerated wood fibers. During stirring, 9 mmol sodium hypochlorite (NaClO) (VWR, Sweden) per g oven-dry pulp was titrated into the suspension, while maintaining the pH at 10–11. When the reaction was finished, the pulp was dewatered and washed thoroughly. Finally, the washed pulp was diluted to 1% consistency with deionized water and disintegrated with an IKA T25 digital Ultra-Turrax disperser (rotor S25N-25F) for 30 min to obtain the NFC suspension.

Table 2. Pre-coating formulations (**Publication IV**)

Coating	Formulation description
HC-60	Pigment: HYDROCARB®-60 (Omya Development AG, Switzerland) with median particle size by weight (d_{50}): 1.4 µm Binder: Styrene acrylate latex DL 1066 (Trinseo Suomi Oy, Finland) added at 10 pph of the pigment Coating suspension solids: 60%
HC-90	Pigment: HYDROCARB®-90 (Omya Development AG, Switzerland) with median particle size by weight (d_{50}): 0.7 µm Binder: Styrene acrylate latex DL 1066 (Trinseo Suomi Oy, Finland) added at 10 pph of the pigment Coating suspension solids: 60%
CMC	FINNFIX® 10 (CP Kelco Oy, Finland) with DS: 0.8, and Molecular weight: 60 kg/mol Coating suspension solids: 5%
NFC	Nanocellulose (PFI, Norway) produced using TEMPO oxidation pre-treatment with charge content*:* approx. 900 µmol/g Coating suspension solids: 1%
Latex	Acrylate latex CHP 585 (CH-Polymers Oy, Finland) with T_g: 0 °C and particle size: 50 nm Coating suspension solids: 5%
PVOH	Polyvinyl alcohol POVAL® 6-98 (Kuraray Europe GmbH, Germany) with Degree of hydrolysis: 98.0–98.8 mol% Coating suspension solids: 3%

3.2 Fibril Characterization

3.2.1 Morphology

Optical Microscopy (OM)
MFC fibrils were imaged on a cover slip at room temperature using a BX60 microscope (Olympus Optical, Japan) with BX-FLA reflective light fluorescence attachment without fluorescent filters, a Nikon DS-FI2 camera, and an NIS Elements software. Two Olympus UPlanFI objective lenses were used: 10× magnification with 0.30 NA and 20× magnification with 0.50 NA.

Scanning Electron Microscopy (SEM)
SEM images of freeze-dried MFC were acquired using a Leo (Zeiss) 1530 Gemini Microscope. Before imaging, the samples were sputter coated with gold for 2 min. The microscope was operating in secondary electron mode, and the images were acquired from a working distance of 7 mm, using 2.7 kV acceleration voltage.

Transmission Electron Microscopy (TEM)
The MFC fibrils were also imaged using a JEOL JEM-1400 Plus (JEOL, Japan) (TEM) operated at 80 kV acceleration voltage. Before imaging, 0.05% (w/v) MFC suspension was drop cast on Formvar/carbon-coated 400 MESH copper grids and negatively stained with 1% (w/v) uranyl acetate in water for 40 s.

3.2.2 Carboxylate Content
Carboxylate content of MFC was determined by conductometric titration, as described by Araki et al. [219]. An amount of 50 mg of MFC was diluted to 0.1% (w/v) and mixed with 2.0 ml of 0.1 M HCl followed by addition of 1.0 ml of 1.0 mM NaCl. The slurry was stirred for 90 min and subsequently titrated with 0.1 M NaOH at a rate of 0.1 ml/min. The carboxylate content was estimated from the resultant conductivity and pH curves, assuming that the strong acid and weak acid correspond to the added HCl and the carboxyl groups, respectively.

3.3 Suspension Characterization

3.3.1 Suspension Stability and Zeta Potential
The MFC suspensions used in this work were prone to phase separation and settling. The settling tendency of the suspensions was qualitatively determined by imaging them in glass test tubes over a one-week period. For imaging, suspensions at varying solids contents, i.e. 0.1%, 0.5%, 1%, 2% and 3%, were poured into vertical glass test tubes and covered with lids to avoid evaporation. Thereafter, images were acquired at regular intervals ranging from few minutes to several days.

The zeta potential of the suspensions (pH~6) was determined using a Malvern Zeta-sizer 3000 (Malvern Instruments Ltd., UK). Prior to measurement, the samples were diluted with deionized water to a solids content of 0.01%. The results are reported as an average of five measurements.

3.3.2 Water Retention

Coating suspensions were characterized for their dewatering properties at different concentrations. Static gravimetric dewatering of the MFC suspensions was measured following the Åbo Akademi Gravimetric Water Retention (ÅA-GWR) method, originally developed by Sandås et al. [220] for coating colors. **Figure 8** shows a schematic of the ÅA-GWR device. For measurement, 10 ml of the suspension was inserted into the sample cylinder placed above a 5 µm polycarbonate membrane (GE Water & Process Technologies, USA) backed by absorbent blotter papers. Eight, instead of the usual two, blotter papers were used in each measurement to avoid saturation due to a large amount of water in the suspensions. After sealing the measuring cylinder, air pressure of 50 kPa was applied for 90 s. GWR value represents the amount of water released by the suspension per unit area, and it is obtained using the equation:

$$\frac{W_f - W_i}{A}.$$

Here, W_f and W_i are the final and initial weights, respectively, of the blotter paper, and A is the cross-sectional area of the measuring cylinder. The results are an average of three parallel determinations. Time durations of 15, 30, 60, 90, 180 and 360 s were also used to determine the time dependency of water retention. The MFC suspension at 2% solids was used for these studies. The impact of the CMC addition level (1 pph, 3 pph and 5 pph of dry MFC) on water retention of the MFC suspensions was also explored. To understand the impact of hydrophobic base on the dewatering rate during coating, a water retention study was conducted with the top absorbent blotter paper replaced by the sized paperboard (used as one of the substrates in this work).

Pressure filtration (schematic of the setup in **Figure 9**) was used as an additional tool to measure the water retention of the suspensions. First, 20 ml of a suspension was injected into the cylindrical filtration chamber containing a 5 µm polycarbonate membrane (GE Water & Process Technologies, USA) kept over a sturdy wire mesh at bottom. The water (filtrate) from the suspension released under applied pressure of 10 bars was constantly collected and measured over time. The result is reported as the filtrate amount per unit area (g/m^2) as a function of time. Three parallel measurements were performed to ensure repeatability.

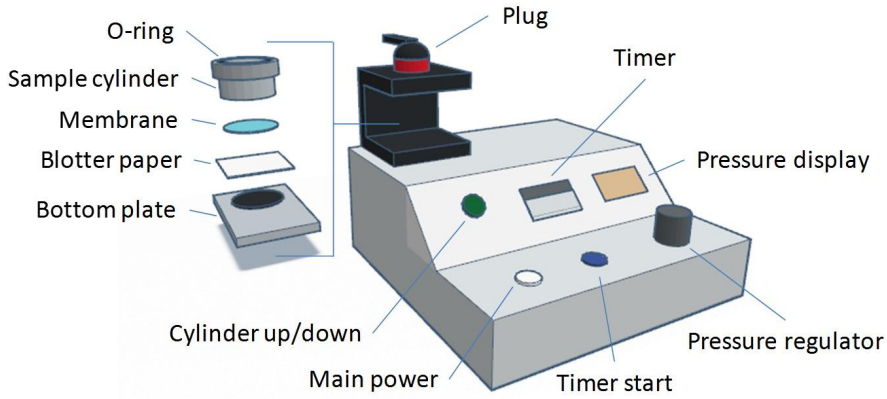

Figure 8. Schematic diagram of the ÅA-GWR device.

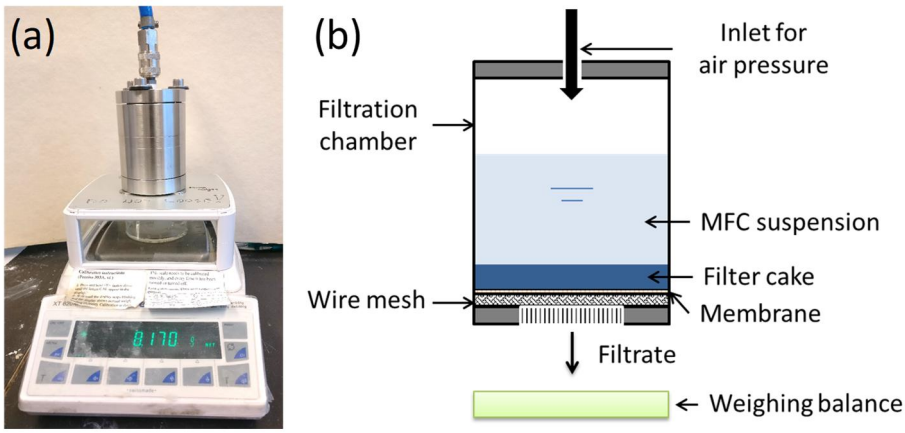

Figure 9. (a) Pressure filtration setup. (b) Schematic diagram of the setup.

3.3.3 Rheology in Boundary-driven Flow

Rheology measurements with parallel-plate geometry (plate diameter: 50 mm, measurement gap: 1 mm) and Couette geometry (coaxial cylinder: CC27, measurement gap: 1.128 mm) were carried out using a Paar Physica Modular Compact Rheometer (MCR) 300 (Anton Paar GmbH, Austria). In addition, a serrated bob (vertical serrations with 2.3 mm gap and 0.5 mm depth) and a sand-blasted cup were also used in Couette geometry, though the measurement gap was similar to the smooth geometry. Measurements with cone-plate geometry were not successful due to ejection of the MFC material from the measurement gap, even at low solids content.

For viscoelastic and shear flow measurements, the protocol suggested by Naderi et al. [120, 221] was employed. Briefly, the samples were pre-sheared at 100 s^{-1} for one minute in the measuring chamber to ensure homogeneity and were then left to equilibrate for two minutes before conducting the measurement. The

shear flow tests were conducted in a shear rate range of 0.1–1 000 s^{-1}, with 30 s integration time per measurement point. To identify the linear viscoelastic region, oscillatory strain sweep tests were conducted in a strain range of 0.01–100% at a frequency of 1.592 Hz. Subsequently, frequency sweep measurements were performed in a frequency range of 0.1–100 Hz, while keeping the strain at 0.5% (within the linear viscoelastic region). Integration time per measurement point was 10 s in both types of viscoelastic measurements, and ten points were collected per decade change in strain (%) or frequency (Hz). A working gap of 9.15 mm was employed in all measurements with the Couette geometry. Furthermore, the serrated geometry was employed for the viscoelastic tests.

The protocol of Naderi et al. [120, 221] was followed again for studying the thixotropic behavior of the suspensions. Briefly, the samples were pre-sheared at 100 s^{-1} for one minute to ensure homogeneity. Subsequently, the viscosity was recorded at a shear rate of 0.1 s^{-1} for 20 min. Thereafter, a shear rate of 1 000 s^{-1} was applied for 30 s. Finally, the viscosity was measured again at the shear rate of 0.1 s^{-1} for 10 min. The viscosity data were collected every second during the measurements.

All the samples were equilibrated overnight at room temperature before conducting the rheology tests at 25 °C, and a protective cover was used during the studies to minimize the sample evaporation. In addition, each measurement was repeated three times to ensure repeatability.

3.3.4 Rheology in Pressure-driven Flow

Pressure-driven flow, at room temperature, was characterized using the slot-die geometry shown in **Figure 10**. It consists of a distribution channel with a radius of 16 mm, and a slot of the length and width of 34 mm and 74 mm, respectively. The slot gap can be altered to 500, 750, and 1 000 μm. An air-pressurized container feeds the MFC suspension to the slot-die. The steady state flow rate at an applied pressure is measured gravimetrically by collecting the outflow during a known time interval. The slot walls were kept smooth in order to predict the high shear rheological behavior of the MFC suspensions under usual industrial conditions.

The slot geometry was used to measure viscosity of two Newtonian fluids (silicone oil and honey) of known viscosities. The viscosities of these liquids obtained from slot geometry were reproducible within ±8% and found to agree with parallel plate geometry measurements. The slot geometry was further verified with rheology measurements of a 2% CMC solution, a known shear thinning suspension.

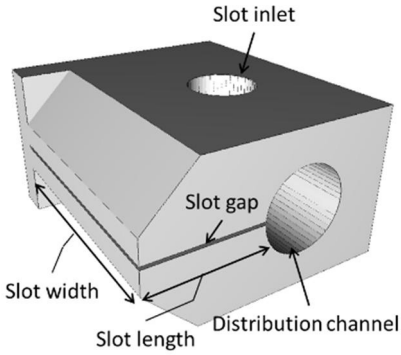

Figure 10. Schematic of the slot-die.

The theory of flow in a slot-die is well known [60, 222], and the flow rate and pressure drop data can be utilized to calculate the rheological parameters. However, pressure-driven high shear rheometry often requires kinetic energy and Bagley corrections for the obtained data. For example, the kinetic energy correction represents the viscous pressure drop needed to accelerate a fluid from rest to the fully developed flow, and shear stress can easily be overestimated if this correction is not considered. Therefore, the pressure drop due to change in the kinetic energy [223] was included in the analysis of the slot-die rheology data and calculated using the equation:

$$P_{KE} = \frac{27 f \rho Q^2}{35 h^2 W^2}.$$

Here, ρ is the density of the suspension and f is a correction factor for non-Newtonian liquids. In these studies, f was ~ 0.78, calculated using the method presented by Krieger and Huang [223]. The kinetic energy corrections at the highest flow rates reached as high as 15 and 45% for 3 and 1% MFC suspensions, respectively, but they were negligible at low flow rates. It should be noted that this equation might overcorrect for the pressure losses because the velocity profile in the slot is not parabolic for shear thinning fluids. The pressured drop correction related to entrance effects of the flow into a slot can be implemented using Bagley plots, which are obtained based on the assumption that one can represent the extra entrance pressure drop by an equivalent length of a slot-die [60, 222]. In the current work, Bagley corrections produced negative intercepts for the pressure losses and, therefore, were not used.

3.4 MFC Film Preparation

MFC films, at two different grammages of approximately 15 and 25 gsm, were prepared by casting and evaporation in polystyrene petri dishes (diameter: 8.5 cm) in conditioned environment (23 °C and 50% RH). The petri dishes were placed on a flat surface to ensure a uniform dry film thickness. Before casting, the suspension was diluted to 0.5% solids and mixed well using a magnetic stirrer

RCT Basic (IKA, Germany) at 700 rpm for 30 min. MFC films with 5 pph CMC were also prepared following the same procedure, for comparison with the coatings.

3.5 Coating

3.5.1 Substrates

The main substrate used for coatings in this work was a recycled fiber linerboard (Dong Il Paper, South Korea) with grammage and thickness 180 ± 5 gsm and 190 ± 5 µm, respectively. The second substrate (**Publication IV**) was a sized packaging paperboard Trayforma™ Natura (Stora Enso, Finland) with grammage and thickness 190 ± 3 gsm and 250 ± 5 µm, respectively. The terms Linerboard and Paperboard are used to distinguish the two substrates, where needed.

3.5.2 Coating Methods

A custom-built slot-die, as shown in **Figure 10**, was used to apply the MFC coatings (**Publication III & IV**) and the nanographite-nanocellulose coatings (**Publication V**). The slot-die was installed on a modified mini pilot-scale Rotary Koater (RK PrintCoat Instruments, United Kingdom), as shown in **Figure 11**. Horizontal movement of the adjustable rail closer to or away from the backing roll was used to control the distance between the slot lips and the substrate, referred to as slot-web gap (SWG). Fine adjustment of the SWG controls the thickness of the wet-coating layer applied to the substrate and, thus, the final coat weight. Coating suspensions in this work were applied at different SWGs to obtain different dry coat weights. The width of coating applied with slot-die was approx. 7 cm on a 10–15 cm wide substrate. Coating speed was 1–20 m/min. The coating suspension was fed to the slot-die from an air-pressurized container.

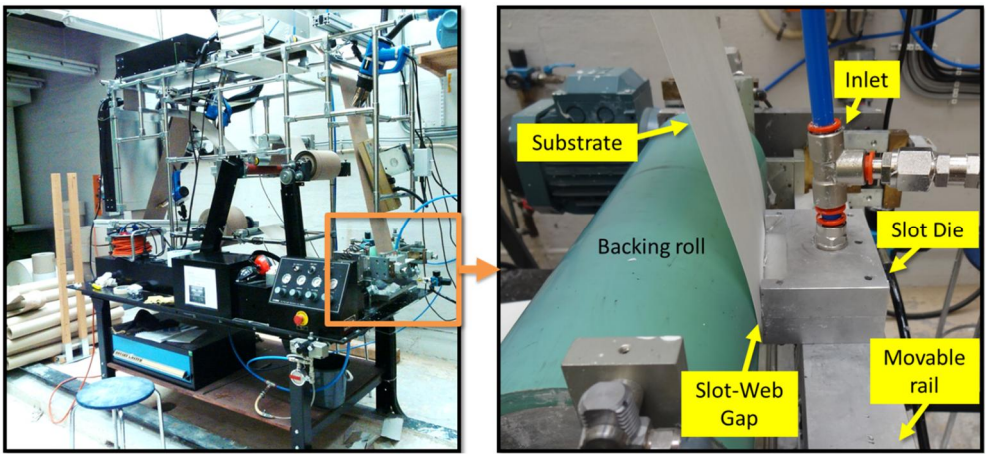

Figure 11. Slot-die setup on the coating machine.

The low solids content (≤ 3%) of the suspensions coated using the slot-die required a high drying capacity. In addition to the pre-fitted dryers on the machine (two 10 kW air dryers and one 5 kW IR), four IR heaters (1 kW each) and four air dryers (2 kW each) were installed on the machine to aid the drying process.

The MFC suspensions have large amounts of water, which makes it important to understand the impact of water itself on the paper-based substrate properties. Therefore, water treatments were also performed by applying water on the paper substrate using the same coating and drying techniques, as described above. The properties of water-treated substrates can show the sensitivity of the substrate to water.

All the pre-coatings (**Publication IV**) were applied on Paperboard using a desktop reverse gravure coater MiniLabo (Yasui Seiki, Japan) at a web speed of 1.5 m/min. The pre-coated samples were conditioned at 23 °C and 50% RH for 24 h before applying the MFC coating.

3.5.3 Calendering

In this work, all the samples coated using the slot-die were subsequently calendered with a laboratory soft nip calender (DT Paper Science, Finland), keeping the backside towards the soft roll. Line load, line speed and temperature used for calendering were 100 kN/m, 5 m/min and 60 °C, respectively. In addition, a line load of 200 kN/m was used for the nanographite-nanocellulose coatings (**Publication V**) to study the impact of the calendering line load on electrical sheet resistance. All samples were conditioned (23 °C, 50% RH) for at least 24 h before further characterization.

3.6 Substrate, Film and Coating Characterization

3.6.1 Coat Weight and Thickness

Thickness of the MFC films and the coated samples was determined using a Micrometer SE-250 (Lorentzen & Wettre, Sweden). The thickness of the films was also obtained from SEM cross-section images. Grammage of the samples was determined by weighing a known sample size, and coat weight was obtained as a difference of grammages of the substrate and its coated counterpart. A precise determination of the low MFC coat weights was difficult due to variation in the grammage of the substrates. However, approx. coat weights for the thick MFC coatings (**Publication III**) were up to 16 gsm. TAPPI standard (T550) was followed for moisture content determination of the samples.

3.6.2 Surface Roughness and Wettability

Surface roughness of the substrates and the pre-coatings (**Publication IV**) was measured with a Parker Print-Surf (PPS ME-90, Version 1.8c) smoothness tester (Messmer Büchel BV, The Netherlands).

Water contact angles of the substrates and the pre-coatings (**Publication IV**) were measured to determine their hydrophilicity. A 4 µL water droplet was placed on the sample surface, and the dynamic wetting of the surface was subsequently recorded using a high-speed camera on a CAM 200 contact angle goniometer (KSV Instruments Ltd., Finland) for a duration of 60 s. Thereafter, the contact angle values were obtained with OneAttension software. TAPPI T-441 standard method was used to determine the Cobb-60 values (**Publication IV**).

3.6.3 MFC Coating Coverage

Coating coverage can be determined qualitatively using various techniques, e.g. SEM surface imaging. However, an optical similarity between the MFC coating and pulp fibers in the paper-based substrates challenges the coating coverage determination. To avoid the issue in this work, a pigment-coated linerboard (**Publication III**), in addition to the main substrate, was also coated with MFC using the same process parameters.

Surface images of the MFC coated samples (**Publication III & IV**) were acquired using a Leo (Zeiss) 1530 Gemini SEM. Before imaging, the specimen was sputtered with a thin layer of gold. SEM images were acquired in secondary electron mode from a working distance of 11 mm, using an acceleration voltage of 10 kV. Alternatively, a qualitative idea of the MFC coating coverage and surface porosity was also obtained from print penetration tests (**Publication III & IV**). An IGT AIC2-5 tester by IGT Testing Systems (Amsterdam, The Netherlands) was used, following the standard method IGT-W24.

3.6.4 Strength Properties

Strength properties of the MFC films and the coated samples were determined using a tensile strength tester SE-060 (Lorentzen & Wettre, Sweden) with a 200 N load cell (**Publication III**). Tensile strength index (TS), stretch, and tensile energy absorption index (TEA) were obtained. A pulling rate of 12 mm/min was used on a 15 mm wide sample strip. The span length was 100 mm. An average is reported from ten parallel measurements.

Surface strength of the samples (**Publication IV**) was determined using an L&W ZD-tensile tester (Lorentzen & Wettre, Sweden), following the ISO-15754 standard method. In addition, a qualitative measure of the coating adhesion was obtained using a tape test, following the standard IPC-TM-650.

3.6.5 Barrier Properties

Air permeance of the substrates, MFC films and the coated samples (**Publication III & IV**) was determined using an L&W Air permeability tester SE-166 (Kista, Sweden) with a measurement range of 0.003–100 µm/(Pa·s). Five parallel measurements were performed on different areas of each sample. The measrements were done at 50% RH and 23 °C.

ASTM Standard (E96/E96M-05) method was followed for water vapor transmission rate (WVTR) determination (**Publication III**). The test sample was placed and sealed using molten wax over the mouth of a cup containing anhydrous calcium chloride ($CaCl_2$). Thereafter, the cup was left in a conditioned environment (23 °C, 50% RH), and the increase in weight of the cup in 24 h due to water vapor permeation through the test sample was used to determine the WVTR. Heptane vapor transmission rate (HVTR) was determined following a similar procedure (**Publication III**), as described by Miettinen et al. [224]. A volume of 20 mL of heptane, instead of $CaCl_2$, was used in the cup, and the decrease in weight of the cup in 24 h due to evaporation of heptane through the test sample was used to determine the HVTR. For both WVTR and HVTR, an average of three parallel measurements is reported.

Grease resistance (**Publication III**) of the MFC coated samples was determined using the KIT Test, following the TAPPI standard (T 559). Attenuated total reflectance Fourier transform infrared spectroscopy (ATR-FTIR) was utilized to qualitatively determine the mineral oil barrier of the MFC coatings (**Publication III**). The procedure of O'Neill et al. [225] was followed, and a PerkinElmer Spectrum One FTIR Spectrometer (Norwalk, CT, USA) with measuring head diameter of 5 mm was used. First, reference measurements were made by obtaining the transmittance spectra, in the wavenumber range 600–4 000 cm^{-1}, of the offset printing ink [226] mineral oil PKWF 4/7 (Haltermann, Germany) and the coated side of the samples. Each measurement consisted of four wavelength sweeps. For the barrier tests, a 20 µL drop of the mineral oil was placed on the back (uncoated) side of the coated sample, and the transmittance spectra from the coated side were obtained at the following times: 0 (reference), 1, 3, 25, and 50 h, after placing the drop on the surface. Three parallel measurements were performed for all the samples. The measured spectra will not show any peaks originating from the mineral oil, if the coating functions as an effective barrier. In addition, barrier properties of MFC coatings and films were also studied with Oil Red O, as reported by Vähä-Nissi [227]. Briefly, 200 µL of a dyed oil, Oil Red O solution (Sigma Aldrich, USA), was placed on the coated side of the samples. A 50-g weight was put on top, and the backside was scanned at pre-selected intervals to detect any oil penetration through the sample.

Oxygen barrier measurements for the MFC films (**Publication I**) were conducted at Tampere University of Technology, Finland. A standard oxygen transmission rate testing system (MOCON OX-TRAN 2/21 MH) was used, following the ASTM D3985-05 test standard. The result is reported as a mean of two measurements. Oxygen barrier tests were also conducted for the MFC coated samples, but they had to be aborted due to poor performance of the coatings. All oxygen barrier tests were conducted at 23 °C and 50% RH.

3.6.6 Electrical Properties

A Hewlett Packard 3457A Multimeter was used in four-point probe mode to measure electrical sheet resistance of the nanographite-coated samples (**Publication V**), and the mean value of five measurements is reported. To determine the impact of humidity on sheet resistance, measurements were also performed at 20% RH and 85% RH, besides at the standard conditions (50% RH and 23 °C).

The impact of creasing and bending on sheet resistance was also explored. Samples were creased using a custom-built creasing equipment, as shown in **Figure 12**. The creasing rule pushes the paperboard into the gap between the rolls, creating a permanent crease. Bending was performed by attaching the coated sample (coated side out) around a rod with 24.5 mm diameter.

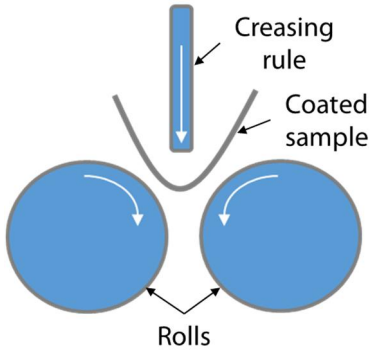

Figure 12. Schematic of the creasing equipment.

4. Results and Discussion

4.1 Properties of MFCs and Suspensions

4.1.1 Morphology and Charge Content

The morphology and size of MFC affect the packing of fibrils during film formation and, consequently, contribute to the final film/coating properties. Micrographs of MFC (**Figure 13**) obtained using different techniques show a broad size distribution. Some fiber fragments and flocs are also visible. The diameter of fibrils estimated using TEM images varies between 20 and 500 nm, and their length reaches several microns. Moreover, these fibrils appear flexible and irregular in shape with high aspect ratio.

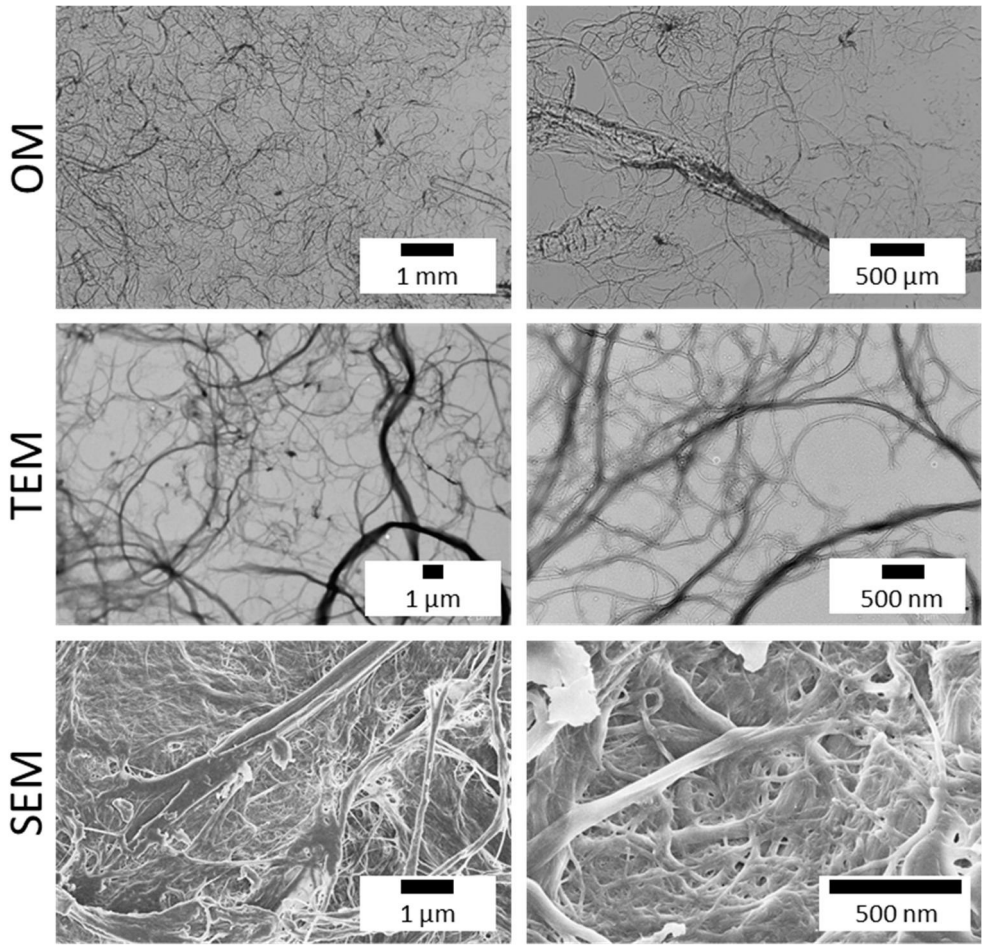

Figure 13. Micrographs of MFC at different resolutions.

The physical characteristics of MFC agree with previous reports where a pure mechanical treatment was employed to produce nanocellulose [95, 96]. However, MFC herein differs from NFC in terms of morphology and size distribution. The chemical pre-treatments used in the production of NFC lead to a very fine-scale nanocellulose with narrow size distribution. The diameter of NFC fibrils has been reported to vary between 3 and 100 nm [20].

Interestingly, a post-treatment of MFC to introduce surface charge on fibrils may be helpful in determining the actual diameter of fibrils, as observed in a recent work [228]. The TEM images (**Figure 14**) of MFC at different post TEMPO-mediated oxidation levels show that the electrostatic repulsion between fibrils due to additional surface charge helps in highlighting the nanoscale fibrils. The approx. charge content of MFC after the post oxidation were 1340, 1430 and 1870 μmol/g for low, medium and high levels, respectively. The MFC fibrils tend to stay as bundles in absence of these charges, leading to a larger average fibril diameter. Based on the TEM images in **Figure 14**, the estimated diameter of the MFC fibrils reaches below 5 nm. Thus, the mechanical treatment alone can achieve a high level of fibrillation, but it is not visible due to agglomeration of the MFC fibrils caused by the absence of sufficient surface charges. Charge content of MFC herein was found in the range 310–340 μmol/g, which is much lower, compared to that reported for NFC in literature [47, 66]. This is due to the absence of chemical pre-treatments, which introduce additional charge on the fibril surface.

Charge content of MFC suspensions affects their stability, water retention and rheology. Hence, the low charge content of MFC causes phase separation, resulting in an unstable suspension, especially at low solids, as shown in **Figure 15**. In addition, the structure of MFC seems flocculated in water suspensions. Although the MFC fibrils have significantly smaller dimensions and a higher aspect ratio than pulp fibers, yet their floc structure is somewhat similar to pulp suspensions [95, 96, 229].

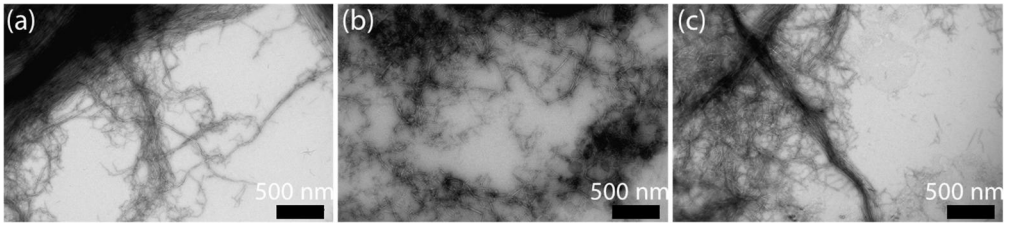

Figure 14. TEM images of MFC at different post TEMPO-mediated oxidation levels: (a) low, (b) medium, and (c) high.

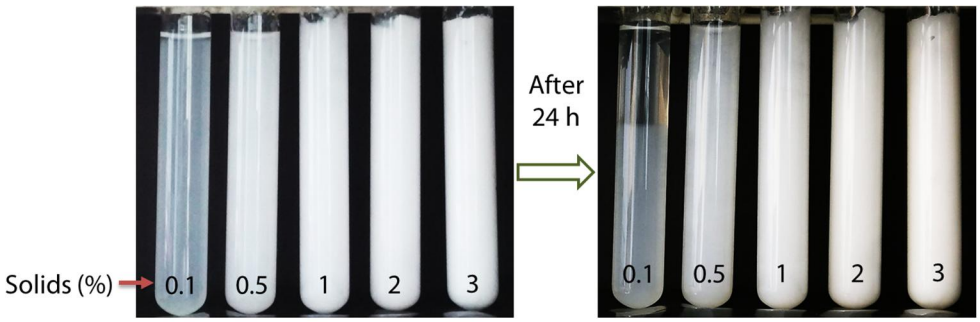

Figure 15. Settling tendency of the MFC suspensions at different solids content.

It has been shown previously that the morphology of cellulose fibers can be modified by adding water soluble polymers such as CMC [230, 231]. Addition of CMC to the MFC suspensions herein resulted in increased stability of the suspensions. Moreover, the suspensions seemed visibly better dispersed with CMC addition. This is likely due to the interaction between the negatively charged MFC fibril surface and the CMC chains dissolved in water. The negatively charged CMC may surround the MFC fibrils diminishing their flocculating tendency. The charge content of the MFC suspensions increased to approx. 450 µmol/g upon 5 pph CMC addition (**Figure 16**). The charge content of pure CMC solution was approx. 2.3 mmol/g. The magnitude of zeta potential (negative) also increased with increasing CMC addition levels, as shown in **Figure 16**. Zeta potential is one of the key parameters affecting the stability of suspensions. The low value of zeta potential for the pure MFC suspensions is an indicator of their poor stability and tendency to flocculate. However, addition of CMC retards this flocculating tendency via increased anionic charge and magnitude of zeta potential.

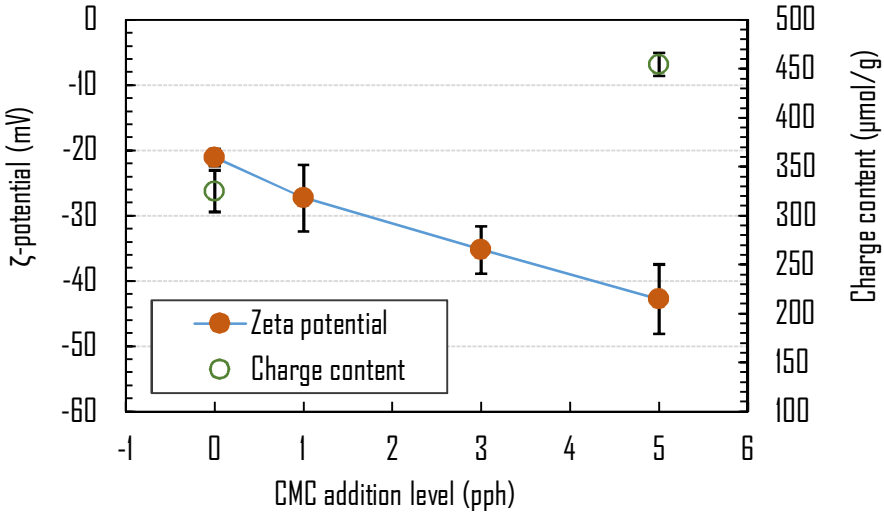

Figure 16. Zeta potential (pH~6) and charge content of the MFC suspensions.

4.1.2 Water Retention

Water retention, i.e., the ability of a coating suspension to resist dewatering into the substrate, is an important coating process parameter. The rate of water released into the substrate affects both the wet film formation and process runnability. Therefore, it is important to control the water retention for successful processing. The dewatering tendency of the MFC suspensions at different solids content is shown in **Figure 17**. The large water content of the MFC suspensions herein leads to high dewatering rates. However, the dewatering rate drops significantly as the solids content increases. The decreasing dewatering rate with increased solids content is likely due to the increased mechanical entanglement of the MFC fibrils and lowered permeability, which improve the water holding capacity of the structure. In addition, a larger number of fibrils per unit volume leads to an increased amount of bound water. **Figure 18** shows the comparison of ÅA-GWR for 2% MFC suspension at varying times to the dewatering rate obtained through pressure filtration. There is a reasonable agreement between the dewatering values obtained from the two techniques. However, these methods are static ones, and the dewatering values obtained may differ from the actual dewatering happening under dynamic coating conditions. The substrate used for coating may also influence the dewatering rate. For example, the dewatering rate for 2% MFC dropped slightly, ca. 10%, when the top absorbent paper was replaced with the sized paperboard in ÅA-GWR tests.

The dewatering tendency of the MFC suspensions is much lower compared to pulp suspensions [232]. However, from a coating perspective, the dewatering values of the MFC suspensions are approximately an order of magnitude higher compared with the conventional pigment coating suspensions (100–300 g/m^2). Such poor water-retaining ability may lead to poor coatability of these suspensions, but this could likely be addressed with appropriate water-retention chemicals, e.g. CMC, generally used for pigment coating suspensions [233]. For example, addition of CMC increases the water holding capacity of 2% MFC suspension significantly, as illustrated in **Figure 17.** This could be due to the improved dispersion of the MFC fibrils upon CMC addition, which has been reported earlier as well [57, 99, 189]. A well-dispersed system should have more fibril surface area available to bind water compared to an aggregated system. Furthermore, the reduced flocculating tendency of the MFC suspension with CMC addition should improve the water retention.

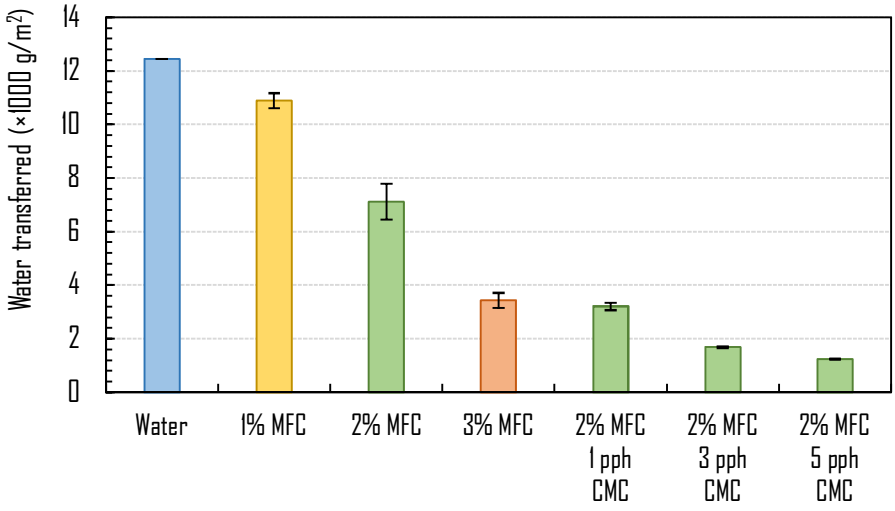

Figure 17. ÅA-GWR of the MFC suspensions at different solids content and CMC addition levels.

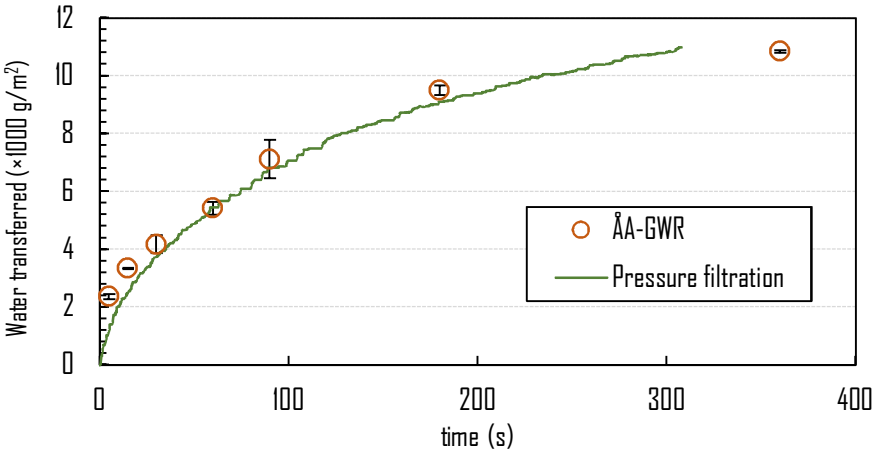

Figure 18. ÅA-GWR and pressure filtration results for 2% MFC suspension.

4.1.3 Rheology

The nanoscale size and high aspect ratio of MFC fibrils (see **Figure 13**) causes their water suspensions to have a complex microstructure and gel-like appearance already at low solids content. As mentioned earlier, MFCs form entangled, three-dimensional networks, and their structure is flocculated in water suspensions. The rheology results from oscillatory and shear flow (boundary and pressure-driven) measurements are discussed in this section. First, the impact of geometry (boundary-driven flow) on shear flow properties is presented, followed by demonstration of the impact of rough/serrated Couette geometry surface on these properties. Subsequently, viscoelastic properties obtained using serrated Couette geometry and smooth parallel-plate geometry

are discussed. In addition, the impact of CMC addition on the rheology of MFC suspensions is clarified. Thereafter, high shear rheology results obtained using the slot-die geometry and their potential implications for a coating process are discussed in detail.

Impact of Geometry Type

There has been much discussion [54-56, 133] about selecting the right type of geometry for rheology determinations of MFC suspensions. The results on the impact of geometry type are shown in **Figure 19**. Clearly, there is a significant difference in the shear viscosity results from the two geometries. The measured flow resistance in the parallel-plate setup is higher compared to that in the Couette geometry. This could be due to the squeezing out of water from the gap in parallel-plate, resulting in overall solids content increase in the measurement gap. This does not happen in the Couette geometry, because any squeezed out water re-enters the measurement gap. Furthermore, the Couette geometry can measure the true response in terms of the "kink" observed in the viscosity curve, which is typical of MFC suspensions, as reported earlier [14, 111, 120]. The difference in shear rate profiles in two geometries may also be responsible for the differences observed in flow curves.

Impact of Geometry Surface

Figure 20 shows the impact of using a serrated geometry, instead of a smooth one. Similar to the previous parallel-plate results, there is an increase in viscosity with the serrated geometry. Reduced wall slip has been suggested as a reason for this [120, 129]. However, the mechanism behind this is not entirely clear. The difference could also be due to a breakdown of the fiber-depleted water-rich boundary layer, as will be discussed in the coming sections. In this context, it is noted that it may be good to use serrated geometry to determine true rheological behavior of MFC suspensions, but the behavior for process design etc. should be determined using smooth geometries. In most industrial processes, the material more often deals with smooth surfaces. Furthermore, the fiber-depletion near solid boundaries during flow can be beneficial for the flow of viscous suspensions such as MFC.

Figure 21 shows the impact of CMC addition on shear rheology of MFC suspensions. There is no significant impact of CMC addition on the flow properties. The "kink" in the viscosity curve seems to disappear, though, suggesting increased dispersion of MFC. CMC may reduce the friction between fibrils helping them flow past each other relatively easily. In addition, CMC diminishes the flocculating tendency that is likely responsible for the "kink" observed in the viscosity curve of pure MFC suspensions because the appearance

of "kink" has been previously associated with the presence of fibril aggregates [56].

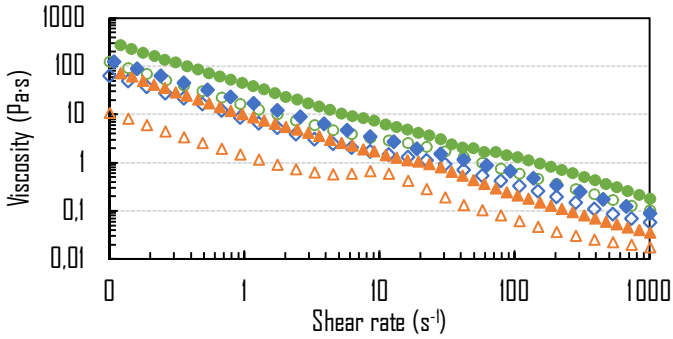

Figure 19. Shear viscosity of MFC suspensions in parallel-plate (filled markers) and Couette (empty markers) geometries. 1% MFC (triangle), 2% MFC (diamond), 3% MFC (circle).

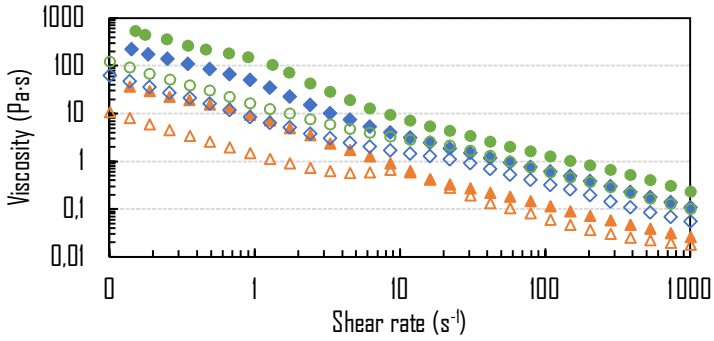

Figure 20. Shear viscosity of MFC suspensions in smooth (empty markers) and serrated (filled markers) Couette geometries. 1% MFC (triangle), 2% MFC (diamond), 3% MFC (circle).

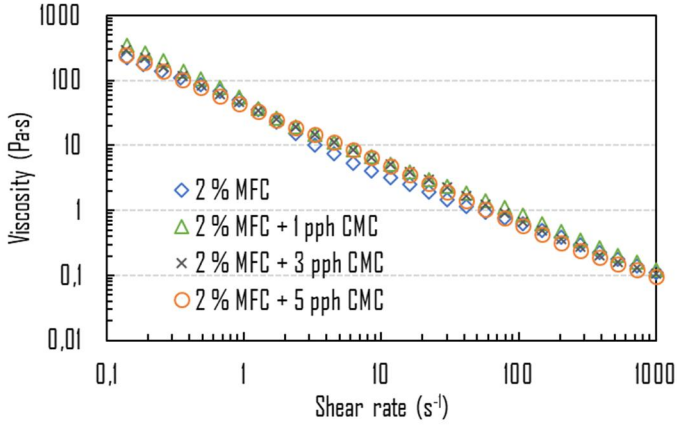

Figure 21. Influence of CMC addition on shear viscosity of 2% MFC suspension. Serrated Couette geometry was used.

Linear Viscoelastic Behavior

The rheology of MFC suspensions can also be investigated using linear oscillatory tests without breaking down the microstructure in the system. A higher value of elastic modulus (G´) than the viscous modulus (G´´) for MFC suspensions herein (see **Figure 22a** and **Figure 23a**) indicates that they exhibit solid-like behavior due to fibril flocs or networks. As solids content increases, the number of connections between fibrils increases giving rise to an increase in both the moduli [229]. The strain domains where the elastic structure of MFC suspensions remains stable are below 1%, which indicates the linear viscoelastic region. The frequency sweep tests carried out in the linear viscoelastic region show the elastic behavior to be the dominant one (**Figure 24a**). G´ and G´´ are largely frequency independent (up to 10 Hz) and almost parallel to each other. Herein, the elastic modulus exhibits a power law behavior in the linear viscoelastic region, $G' \propto c^n$, where c is solids content of the suspension. The exponent value comes out to be ~2.4, which is within the range reported in literature.

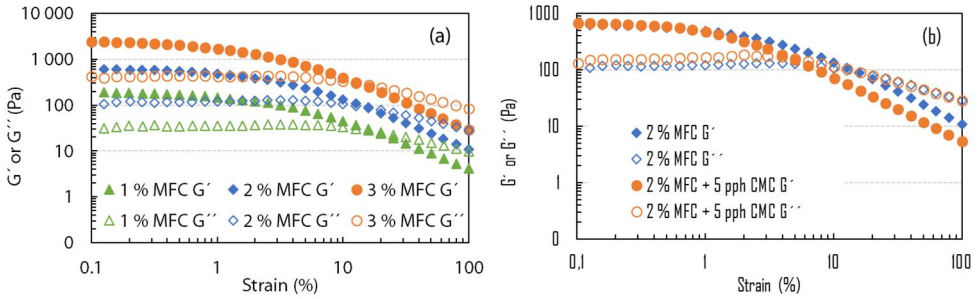

Figure 22. Strain sweep results for MFC suspensions using parallel-plate geometry. (a) Impact of solids content. (b) Impact of CMC addition on 2% MFC suspension.

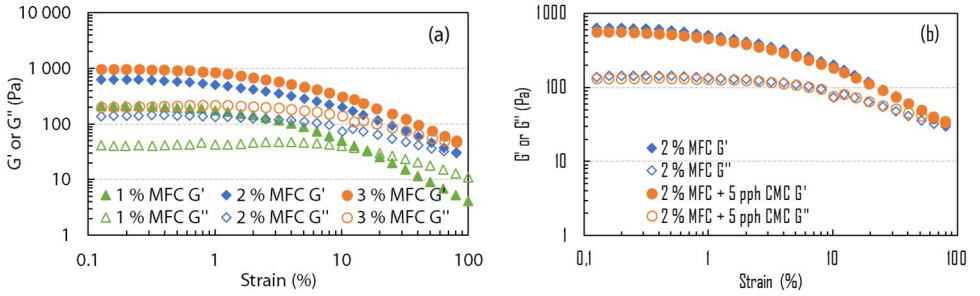

Figure 23. Strain sweep results for MFC suspensions using serrated Couette geometry. (a) Impact of solids content. (b) Impact of CMC addition on 2% MFC suspension.

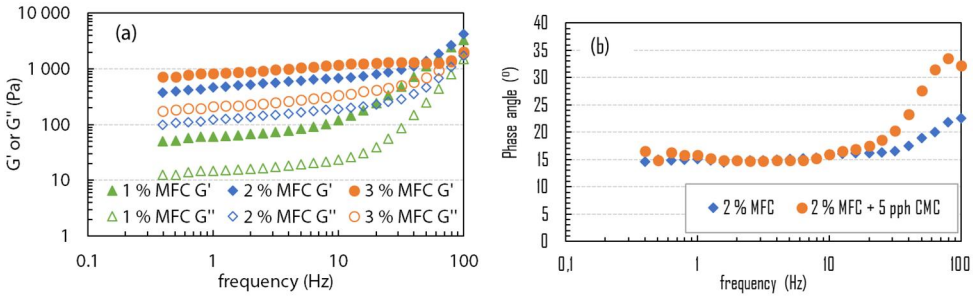

Figure 24. Frequency sweep results for MFC suspensions using serrated Couette geometry. (a) Impact of solids content. (b) Impact of CMC addition.

Addition of CMC leads to an increase in G´´, as shown in **Figure 22b**. This results in a decrease in the gel stiffness (G´/G´´) of the system, which indicates a reduced network strength [120]. Consequently, the presence of CMC in the suspension may improve the film forming properties of MFC by minimizing the flocculation under shear. Interestingly, the parallel-plate geometry shows the impact of CMC addition on the viscoelastic behavior better, compared to the Couette geometry (**Figure 23b**). Addition of CMC also leads to a slight increase in the phase angle at higher frequencies (**Figure 24b**), indicating increased viscous behavior.

Thixotropic Behavior

The thixotropic behavior of 2% MFC suspension is demonstrated in **Figure 25**. It is interesting that pure MFC suspension quickly recovers its initial viscosity values (at 10 s^{-1}) when going from high to low shear rate (1 000–10 s^{-1}), whereas presence of CMC delays this quick response. This behavior may be associated with the decreased entanglement of MFC fibrils with CMC addition, which delays the elastic response. This can be very useful for the coating application process discussed in coming sections.

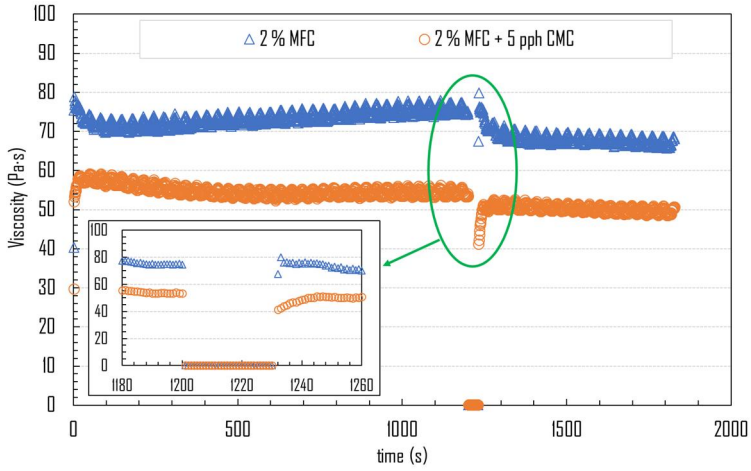

Figure 25. Thixotropic behaviors of 2% MFC suspension with and without CMC.

Yield Stress

MFC suspensions possess a considerable yield stress. **Figure 26** shows the volumetric flow rate of MFC suspensions at different solids content with increasing pressure drop in three different slot gaps. The pressure required for achieving the same flow rate increases with the increasing concentration and/or decreasing slot gap. Furthermore, there is a minimum pressure required to start the flow in the slot, and it increases multifold with increasing concentration, indicating a yield-stress behavior. The apparent yield stress can be estimated from this minimum pressure because no flow was observed for lower pressures. The growing yield stress with increasing suspension solids content can be attributed to the increased fiber-fiber interactions elevating the strength of the fiber network. The yield-stress behavior is also apparent from **Figure 27**, which demonstrates the behavior of 3% MFC suspension at rest and with increasing shear rates in narrow gap flow.

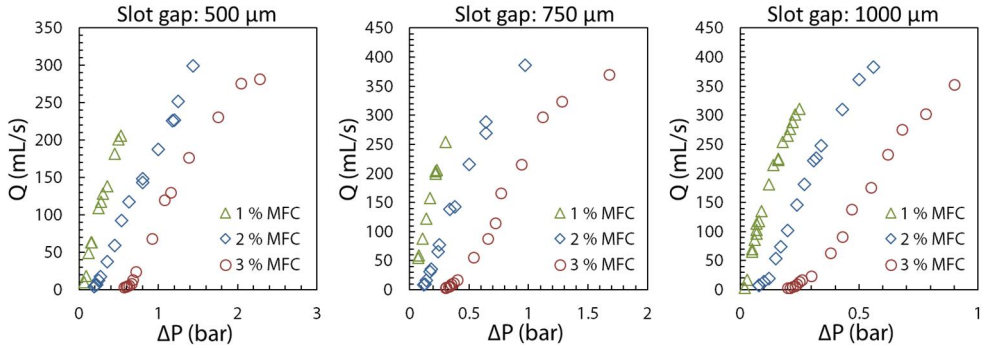

Figure 26. Flow rate against pressure drop for MFC suspensions in different slots.

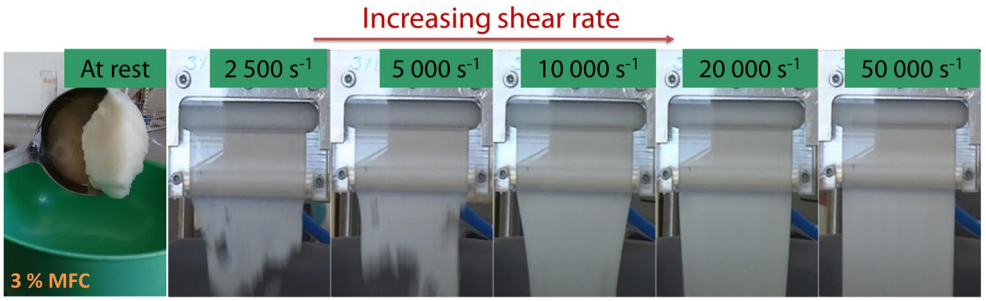

Figure 27. Flow of 3% MFC suspension in slot-die with increasing shear rates.

Shear Flow Properties in Slot-die

Figure 28 shows apparent viscosity vs shear rate for MFC suspensions at three solids content (1, 2, and 3%) in different slot gaps. The viscosity grows almost ten-fold with increasing solids content from 1% to 3%, indicating a strong dependence of the viscosity on the solids content. This suggests development of a more rigid fiber network with the increasing solids content [234]. The suspensions are also shear thinning, with the effective power law indices in the range 0.22–0.43 for 3–1% solids content. However, they are in the range 0.1–0.15, if only the results at shear rates less than 1 000 s^{-1} are included for calculation. These values and the decreasing power law index with increasing solids agree with what has been reported in literature (ca. 0.1–0.44) [117, 235].

The apparent shear thinning appears to transform into a Newtonian plateau at high shear rates (**Figure 28**). For MFC suspensions, this Newtonian plateau has been observed earlier [14, 111, 120] in the form of a "kink" between shear rates of 10–100 s^{-1}, and in this work at low shear rates, as shown in **Figure 19**. However, the reasons for the reappearance of this plateau at high shear rates are unclear. Nikbakht et al. [236] have explained the appearance of a Newtonian plateau in the flow of fiber suspensions due to transition from laminar plug flow to turbulent flow regime, which increases the flow resistance. Interestingly, the Reynolds numbers calculated using the apparent suspension viscosity for the full slot gap for the slot data herein reach the critical value ($Re > 2300$) at the point where the Newtonian plateau appears. Entrance flow instabilities at very high shear rates can also possibly increase the flow resistance. The apparent viscosity for shear rates up to ca. 20 000 s^{-1} seems independent of the slot gap, but the Newtonian plateau appears earlier for the larger slot gaps. This suggests that the apparent shear thinning behavior can be maintained using a narrower slot gap. However, the fibrous material may clog the slot entrance if the slot gap is too narrow. Therefore, it is necessary to optimize the gap size vs the apparent viscosity needed for a successful MFC coating application with the slot-die.

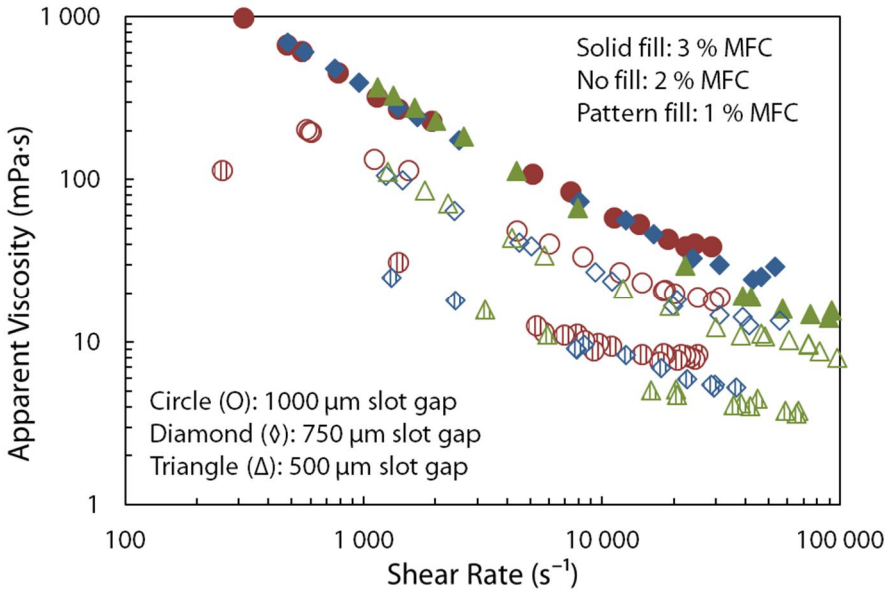

Figure 28. Viscosity against shear rate for MFC suspensions in different slot gaps.

Fiber-depleted Water-rich Boundary Layers

Two possible mechanisms (see **Figure 29**) for the apparent high shear thinning observed for MFC suspensions are proposed here. The first one is based on dynamic yielding, in which a yielding layer surrounds a non-yielded center region (plug). Considering this mechanism, one can fit the shear thinning rheology of MFC suspensions with two material models (Casson and Herschel-Bulkley) that include yield stress as a parameter. The second mechanism is based on the presence of fiber-depleted water-rich boundary layers lubricating the flow. In this work, the second mechanism is assumed to be the dominant one, based on the phase-separating tendencies of MFC suspensions. There is also some support in literature for the existence of this phenomenon in MFC suspensions [96, 131, 132, 151, 235]. The existence of a "plug" with the development of a clear water annulus in pulp suspension flow in a pipe has also been reported [140, 153, 237, 238]. The presence of water-rich boundary layers may look like wall slip, but the traditional wall slip definition that implies a non-zero velocity boundary condition is not applicable here because the water constantly adheres to the boundaries. The true wall-slippage and formation of the water-rich boundary layer are different mechanisms, because the latter can transfer stresses to the center non-yielding region. Furthermore, the concentration of the disperse phase (MFC) in the water layer gradually increases when moving away from the boundary. The tendency of a material to form water-rich boundary layers should be utilized as such in determining its process viscosity, because it is the rheological nature of the material.

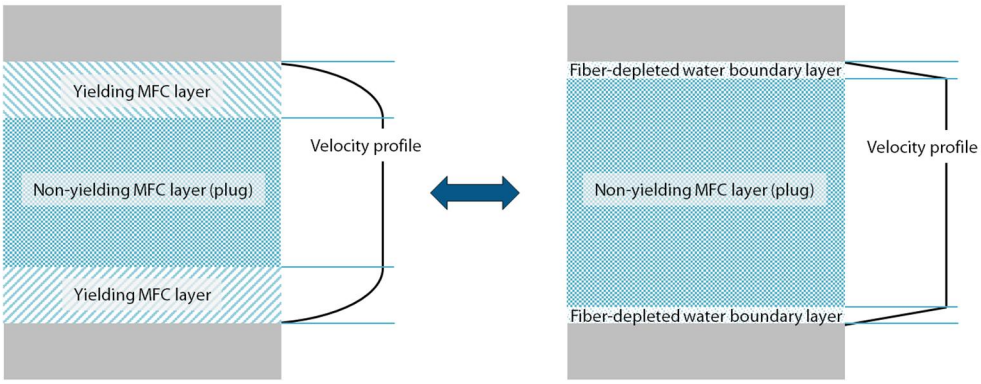

Figure 29. Suggested mechanisms for apparent high shear thinning behavior.

Different mechanisms have been suggested for the wall depletion. Babkin [237] suggested the boundary layers to form due to the deformation of the fiber network and bending of the boundary fibers protruding from the flow core (the so-called "blown grass" effect). Jäsberg [238] described that the lift force acting on the fibers is the main parameter that contributes to the formation of the water layer. The fibers do not easily move out from the plug into the water layer due to entanglements (the "blown grass" effect). "Pole vaulting" has also been suggested as a potential mechanism, where fibers near a boundary push themselves away from it due to the flow. The thickness of the fiber-depleted water-rich boundary layer can be predicted assuming that a non-deforming plug of material is separated from the boundary by a water layer in which all the shear happens (meaning no yielded interlayer). The shear rate in the water layer separating the plug from the boundary is given by the equation:

$$\dot{\gamma} = U/\delta.$$

Here, δ is the water layer thickness (WLT), and U is the velocity of the plug. Neglecting the edge effects, a force balance on the plug of thickness H, width W and length L would give:

$$\Delta P_{slot} HW = 2\tau WL.$$

Above, ΔP_{slot} is pressure drop in the slot and τ is the shear stress from the water layer calculated as the product of the shear rate $\dot{\gamma}$ from earlier equation and the water viscosity η_w. If the average flow-velocity v is the velocity of the plug in the slot with gap h, the plug thickness is then given by the equation:

$$v = \frac{\Delta P_{slot} h^2}{12\eta L}.$$

Here, η is the Newtonian viscosity of the suspension. Now, if

$$H = h - 2\delta,$$

and the water layer thickness δ is small comparable to h, then $H = h$, and the WLT (δ) is given by the equation:

$$\delta = \frac{\eta_w h}{6\eta}.$$

Using this equation, the calculated water layer thickness (**Figure 30**) for MFC suspension flow in different slots is between 5 and 20 µm, which is in the same order of magnitude as recently reported for MFC suspensions [131, 132]. Similar water layer thickness values have been observed for flow of pulp suspensions [152, 239]. The slot gap does not influence the water layer thickness, but a thicker water layer is formed with increasing flow velocity and/or decreasing solids content. Nikbakht et al. [236] also reported a decreasing plug size, meaning a thicker water layer, with increasing flow velocities. Interestingly, the lubrication effect provided by the material-depleted boundary layer can actually be exploited for processing purposes, as has been demonstrated in work by Smay et al. [240].

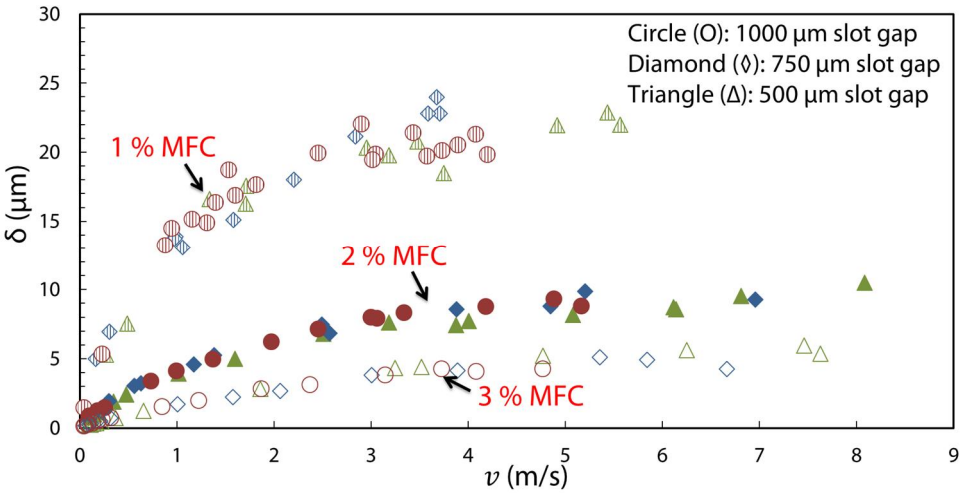

Figure 30. Calculated water layer thickness for MFC suspensions in slot flow.

4.2 MFC Coatability and Coating Properties

4.2.1 The Coating Concept

It is clear from the water retention and rheological behavior of MFC suspensions that the conventional techniques may not work efficiently for their coating application. For example, phase separation of fibrils may become a challenge in reverse gravure coating and film coating (during transfer). Blade coating may face problems, such as clogging of blade heel region, high blade pressures from the high viscosity etc. Furthermore, the insufficient extension due to yield stress and fast structure recovery may cause challenges in curtain coating. From **Figure 27**, one can see that these suspensions appear to exhibit uniform flow when pushed through a narrow gap at high shear rates, which should allow forming a uniform wet film essential for a coating process. Although the shear rates in conventional coating techniques such as blade coating are sufficient for this purpose, the high coating speeds needed to obtain such high shear rates lead to drying challenges. During coating, the large amounts of water in MFC suspensions require either additional drying capacity or reduced coating speeds in order to obtain a dry coating with existing drying capacity. However, reducing the coating speed results in reduced shear rates, which are not sufficient to form a wet MFC film. Therefore, a coating technique that can impose high shear rates irrespective of coating speed is required to coat MFC suspensions. It should be noted that nanocellulose materials with small enough particle size, e.g. CNC or NFC, might be suitable for some traditional coating techniques.

The concept developed in this work tries to eliminate the challenges (discussed above) in MFC suspension coating using conventional techniques. It combines a shearing and a metering element into one construction. The slot-die is used as a coating applicator in an unconventional mode, where it is placed at approx. three o`clock position against a backing roll, as shown in **Figure 31**.

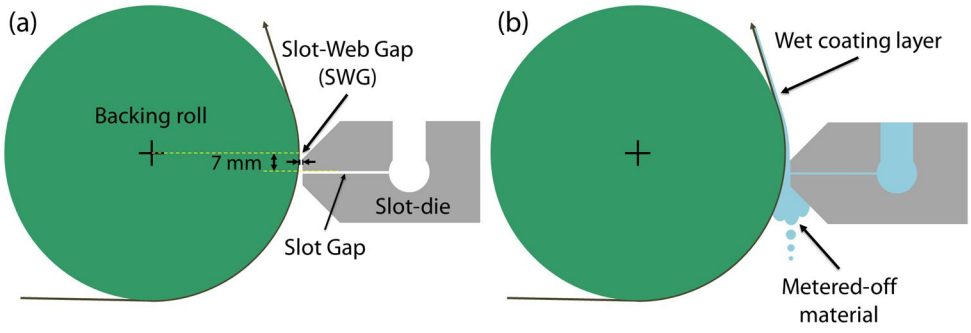

Figure 31. (a) Schematic of the slot-die and backing roll positions. (b) Schematic of the slot-die in operation.

The position of the slot-die is offset 6–7 mm below the horizontal centerline of the backing roll. This creates a converging geometry between the substrate and the slot-die lips, which enables controlling the wet film thickness applied by changing the gap between the slot lips and the substrate web, referred to as slot-web gap (SWG). MFC suspension is fed from an air-pressurized container through a narrow slot gap at high shear rates to impose shear thinning. The resulting fluidized (shear thinned) suspension allows easy metering with the top slot lip. The balance between the pressure-driven extrusion flow forcing the suspension out and the shear-drag of the moving substrate web pulling the coating along upwards determines the split, i.e. the ratio of amount of MFC suspension forming the wet film to that being metered off. In the converging narrow gap geometry, the pressure-driven flow scales to the third power of the SWG, whereas the shear drag upward is inversely proportional to the SWG. Therefore, the split can be controlled by adjusting the SWG, the feeding pressure and/or the web speed. This setup allows film formation even at low coating speeds, and the resulting MFC coating can be dried in a roll-to-roll process. Several suspension characteristics and process parameters affect this coating process and properties of the resulting MFC coatings. These are discussed in the subsequent sub-sections.

4.2.2 Impact of Suspension Properties

Solids Content

The solids content of MFC suspensions plays a critical role in their coatability with the slot-die. MFC suspension at low solids content, i.e., ≤ 1%, is easy to feed into the narrow slot gap, but the final coat weights achieved are too low to impart any benefits as a coating. In addition, the low solids require high drying capacity. Therefore, MFC suspensions with solids content 2% or higher were used for coating purposes in this work. Although maximum possible solids content of MFC is desired to minimize the required drying capacity and increase the obtained coat weights, yet the maximum solids content is limited by the increasing feeding pressure required for feeding the slot. In terms of coating performance, 3% MFC suspension resulted in similar coating properties as 2% MFC suspension at same coat weights of approx. 10 gsm (see **Table 3**). However, it is difficult to comment on the trend of coating properties with further increase in solids content of MFC. Higher solids content of MFC could not be tried due to pressure limitations of the feeding equipment used in this work. The feeding problem can probably be solved with a piston, gear or double screw pump, which create forced flow.

As expected, the water-treated sample under same coating conditions shows a reduction in the strength properties of the substrate, but the MFC coating makes

up for the lost strength by increasing the stretchability. Water destroys the existing hydrogen bonding between fibers in the substrate in addition to causing swelling of fibers, which leads to the reduction observed in strength. However, a slight decrease in air permeance is observed with water treatment, which is likely due to a reduction in pore size caused by the fiber swelling. These observations are in line with the findings of Lavoine et al. [197].

CMC Addition

The wet film formation achieved with pure MFC suspensions was of poor quality due to the aggregation of fibrils, as shown in **Figure 32**. The suspension without CMC comes out of the gap between the slot lips and the substrate with flocs and chunks settled onto the paper. However, the suspension containing CMC leaves the gap as a homogenous suspension without any obvious separation between the fibrils and water. CMC addition thus improves the MFC dispersion leading to overall improvement in the film formation. Furthermore, increasing the CMC addition levels from 1 pph to 5 pph resulted in coating performance improvements in terms of strength and barrier properties. A 3 pph or higher CMC addition level seems to achieve optimal improvements. Therefore, all the results in subsequent sections are for MFC coatings with 5 pph CMC addition.

The improvements with CMC addition can be ascribed to the change in dispersion, water retention and rheological behavior of MFC suspensions. For example, CMC provides a dispersing effect in the MFC suspension, which avoids the unwanted aggregation of fibrils during wet film formation. Moreover, the improved water retention of MFC suspensions with CMC addition (**Figure 17**) leads to a slow dewatering into the substrate, which minimizes web breaks and improves drying efficiency. In a rheological perspective, CMC delays the elastic response of the MFC suspension (see **Figure 25**) coming out of the slot-die, which allows efficient metering and wet film formation. The above suggests that if MFC suspensions are to be used for coating, CMC is needed to boost film forming and to lower the flocculation of the suspension.

Table 3. Impact of MFC solids content on coating performance

Property / Sample	TS (*kNm/kg*)	Stretch (*%*)	TEA (*J/kg*)	Air permeance (*μm/Pa·s*)
Substrate (linerboard)	49.01 ± 1.52	1.87 ± 0.12	603.7 ± 59.7	1.7200 ± 0.0321
Water treated substrate	48.52 ± 1.08	1.79 ± 0.11	563.3 ± 58.4	0.8140 ± 0.0800
2% MFC coating	48.97 ± 1.09	2.01 ± 0.11	643.6 ± 48.6	0.0741 ± 0.0027
3% MFC coating	43.96 ± 1.13	2.3 ± 0.15	672.6 ± 64.3	0.0548 ± 0.0037

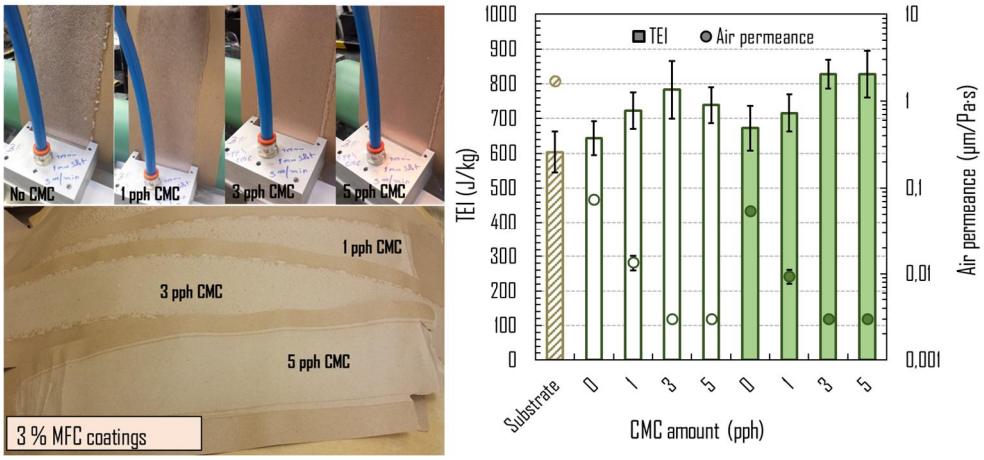

Figure 32. Impact of CMC addition on MFC coating quality. Blank bars/circles (2% MFC), and filled bars/circles (3% MFC).

4.2.3 Impact of Coating Process Parameters

Slot Gap

Slot gap does not influence the final coating quality obtained as long as it is not clogged due to occasional large aggregates in the MFC suspensions. Large slot gaps are beneficial to avoid clogging of the slot entrance. In this work, a slot gap of 1 000 µm was found optimal, especially for 2% MFC, as it allowed using low feeding pressures with minimal to no clogging of the slot.

SWG

SWG is the most important coating process parameter, as it controls the wet coating thickness and hence the final coat weight. The minimum value of SWG used in these studies was 50 µm. The maximum value of SWG is dependent on the drying capacity required at a particular coating speed. For example, SWGs up to 700 µm were used in this work at a speed of 3 m/min. **Table 4** shows the approximate coat weights obtained using different SWGs. It should be noted that the variation in grammage of substrate used here makes it difficult to precisely determine the MFC coat weight, especially at low SWGs. Coating coverage is an important parameter that affects the coating quality and thereby the barrier performance. MFC coating coverage on the linerboard and pigment-coated linerboard with increasing SWG is shown in **Figure 33**. The coverage improves with increasing SWG, and full surface coverage is obtained already at 300 µm SWG. Furthermore, the MFC coating seems to close the surface structure of the substrate, which is evident from the print penetration test results in **Figure 34**, which quantify the surface porosity in terms of stain length. A longer stain indicates a more closed surface. For 300 µm SWG, the stain length is already outside the measurement limit. The strength properties also improve with

increasing SWG (see **Table 4**). The improvement in TS and Stretch at highest SWG is around 10% and 20%, respectively, and TEA increases by 30%. Furthermore, air permeance is below the measurement limits at SWG-300, when full surface coverage is obtained.

Table 4. Impact of SWG on strength and air barrier properties of MFC coatings

Property / Sample	Coat weight (*gsm*)	TS (*kNm/kg*)	Stretch (*%*)	TEA (*J/kg*)	Air permeance (*μm/Pa·s*)
Substrate	0	49.01 ± 1.52	1.87 ± 0.12	603.7 ± 59.7	1.72 ± 0.0321
SWG-50	1	47.73 ± 0.96	2.11 ± 0.08	650.6 ± 36.0	0.3680 ± 0.0304
SWG-100	3-4	50.85 ± 1.15	2.18 ± 0.04	722.2 ± 24.3	0.0567 ± 0.0129
SWG-200	5	50.12 ± 1.76	2.18 ± 0.12	708.8 ± 62.1	0.0159 ± 0.0029
SWG-300	6	50.12 ± 1.13	2.07 ± 0.08	677.2 ± 38.8	0.0030*
SWG-400	9	51.97 ± 1.45	2.11 ± 0.11	721.5 ± 53.4	0.0030
SWG-500	11	52.60 ± 1.25	2.13 ± 0.09	739.1 ± 51.4	0.0030
SWG-600	13	51.72 ± 1.72	2.14 ± 0.16	731.6 ± 85.0	0.0030
SWG-700	16	53.61 ± 1.03	2.25 ± 0.10	798.2 ± 50.6	0.0030

*Detection limit of the instrument

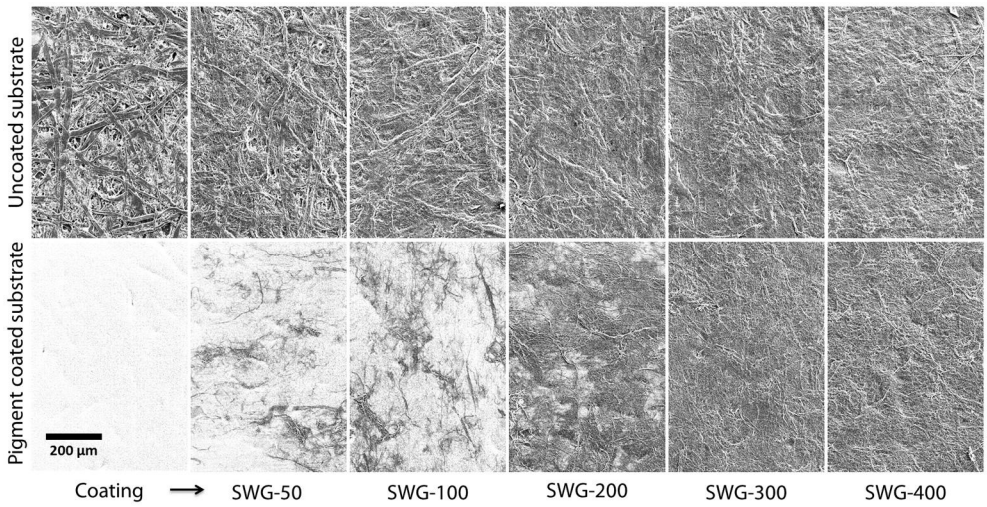

Figure 33. SEM images showing the impact of SWG on surface coverage of MFC coatings on recycled fiber linerboard (top) and pigment coated linerboard (bottom).

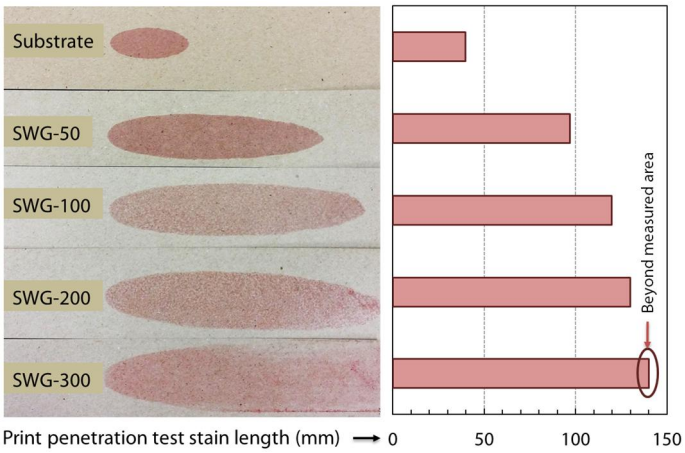

Figure 34. Print penetration test results for MFC coatings.

Drying

Drying is one parameter that can affect the MFC coating performance significantly. **Figure 35a** shows the mechanical performance of MFC coatings dried to different moisture levels on the coating machine, and subsequently dried in conditioned environment (23 °C and 50% RH). It is noted that all the MFC coatings in drying studies had an air permeance below the detection limit. Although the air barrier of MFC coatings is not affected by the different drying conditions, there is a clear impact on the mechanical performance. Coatings dried at room temperature perform better mechanically compared to those dried fully on the machine. This suggests that improved MFC film formation is obtained with slow drying. Slow drying might allow for a more optimal reorganization of fibrils and improved hydrogen bonding between them. In addition, the constraint-drying happening on the machine may result in a different microstructure of the MFC coating layer. Drying of MFC/NFC films has also been found to influence their strength properties, as material distortions occur during drying due to development of moisture gradients within the fibril network [169].

Coating Speed

Different coating speeds of 3, 6, 10 and 20 m/min were used at different SWGs, which did not seem to significantly affect the coating quality obtained (see **Figure 35**b). A slight improvement in the air barrier of MFC coating applied at increasing speed could be due to relatively more uniform coating achieved at higher speed. This is a positive finding considering the industrial scale processes. Coating speeds can be optimized for MFC suspensions with different solids content and drying capacity available. No impact was observed on the strength properties.

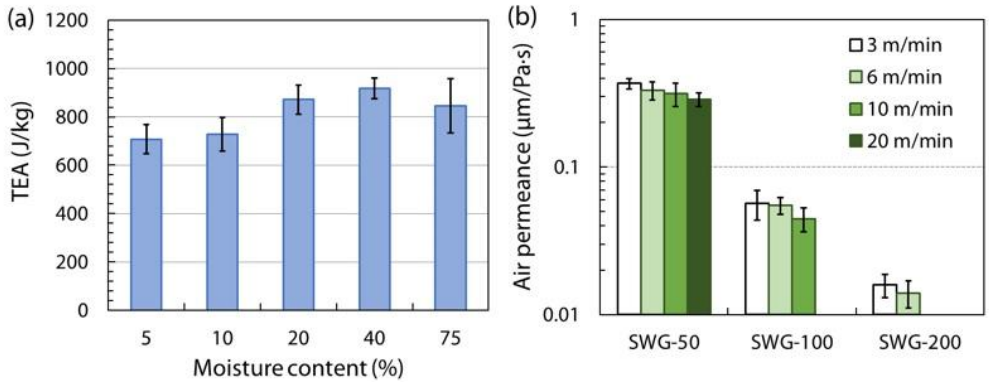

Figure 35. Impact of (a) drying and (b) coating speed on MFC coating quality. SWG-500 was used for drying studies.

4.2.4 Impact of Substrate Parameters

Substrate properties

Paper-based substrates can vary considerably in terms of surface/bulk physical and chemical features affecting the coatability of MFC suspensions. For example, coating of MFC on sized paperboards can be challenging due to poor wetting, spreading and adhesion of the wet film to the substrate. Therefore, it is essential to understand and quantify the impact of substrate properties on MFC coatability. In **Publication IV**, a sized paperboard was pre-coated with different materials to obtain substrates with varying physical and chemical surface properties. **Table 5** lists these different pre-coatings, their coat weights, and Cobb-60 values.

Figure 36 shows various properties of the substrates/pre-coatings listed earlier. Surface roughness, surface porosity and wettability are some of the key substrate parameters that affect the coatability of MFC. Due to the low coat weights attainable with MFC coatings in general, these properties are critical for the final coating uniformity, coverage and mechanical anchoring to the surface. Uniform MFC coating coverage is desired for an effective barrier performance. From print penetration test results in **Figure 36**a, it is clear that Paperboard and Linerboard have quite high surface porosity, which is lowered significantly by the pigment pre-coatings (HC-60 and HC-90) and the CMC pre-coating. Other pre-coatings also reduce the surface porosity to some extent. Low surface porosity, in principle, should lead to an improved holdout of the MFC coating layer. Air permeance (**Figure 36**b) shows a trend similar to the surface porosity. An effective closure of the surface by the CMC pre-coating is reflected in a significantly lowered air permeance. Paperboard and Linerboard have quite high surface roughness (**Figure 36**c). As expected, the pigment pre-coatings reduce the surface roughness of Paperboard, and HC-90 being finer in size leads to a

greater reduction. Contrarily, the Latex, NFC, PVOH, and CMC pre-coatings increase the surface roughness likely due to the swelling of Paperboard caused by the application of these pre-coatings at low solids content. Overall, there is a good correlation between the surface porosity, air permeance, and surface roughness.

Table 5. Pre-coating coat weights and Cobb-60 values for different substrates

Substrate/ Pre-coating	Paperboard	HC-60	HC-90	NFC	CMC	Latex	PVOH	Linerboard
Coat weight approx. (*gsm*)	0	30	30	1	2-3	1	1	0
Cobb-60 (*gsm*)	24 ± 1	25 ± 1	32 ± 1	27 ± 1	24 ± 2	27 ± 2	25 ± 1	255 ± 9

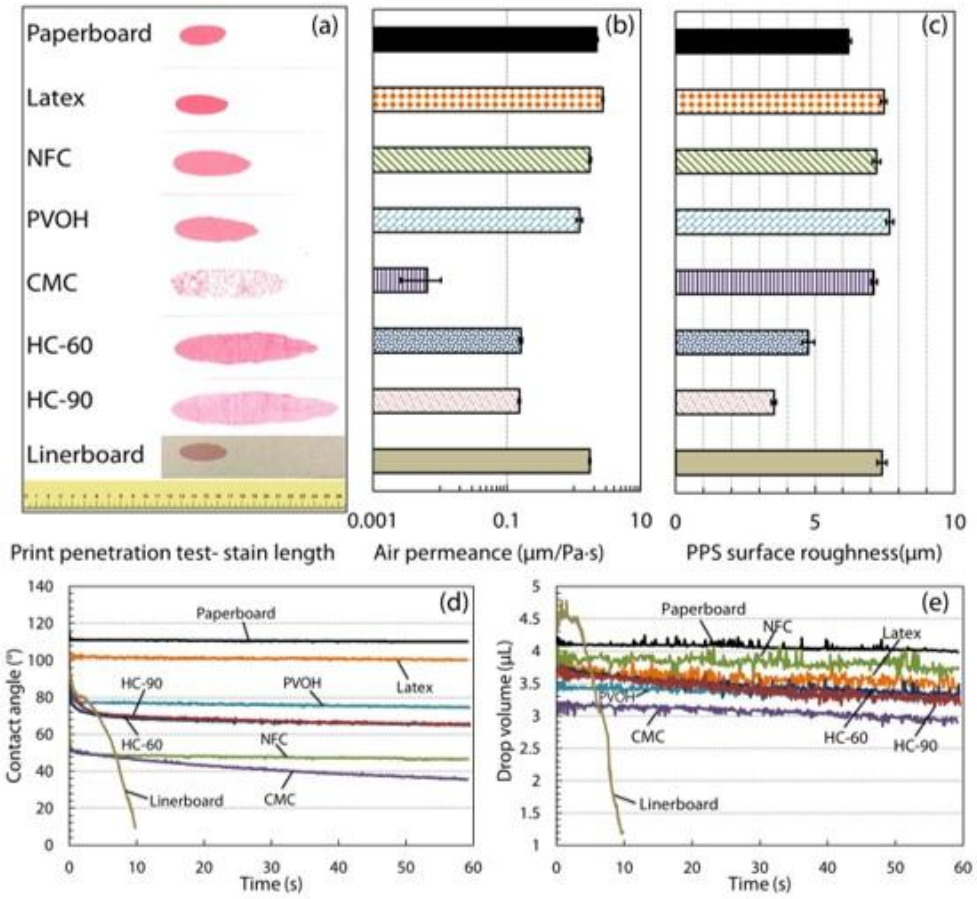

Figure 36. Substrate properties. (a) Stain length from print penetration tests. (b) Air permeance. (c) PPS surface roughness. (d) Water contact angle. (e) Change in volume of the water drop over time.

Figure 36d shows the water contact angle for the substrates and the pre-coatings. It plays a critical role in the wet film spreading on the surface during coating application. Linerboard is quite hydrophilic, but Paperboard is quite hydrophobic due to sizing. The nature of Paperboard surface changes towards the hydrophilic side upon the pre-coating application. The largest change is observed with the NFC and CMC pre-coatings, followed by the pigment and PVOH pre-coatings. The Latex pre-coating inflicts the smallest change. The results imply that even low coat weights of hydrophilic materials, e.g. NFC and CMC, are sufficient to lower the hydrophobicity of Paperboard. Figure 36e shows the water absorption behavior. The water droplet volume stays nearly constant for Paperboard indicating its poor water absorbing capacity. Linerboard, on the other hand, absorbs water rapidly, as indicated by the quick reduction in the droplet volume. This agrees with the water absorption rates indicated by the Cobb-60 values in Table 5. Furthermore, the pre-coatings on Paperboard show negligible impact on the water absorbance. This could be due to the hydrophobic nature of Paperboard preventing water absorption once pre-coating is filled with water. This variation in wettability and water absorption can significantly affect the coating substrate interactions.

As discussed earlier, the MFC suspensions have a propensity to form fiber-depleted water-rich boundary layers under shear. This solids depletion effect may also occur near the substrate surface due to the shearing happening in the gap between the slot lips and the substrate during coating. An adequate water absorbance capacity of the substrate ensures quick absorption of this water-rich boundary layer. This is essential for proper adhesion of the wet MFC coating film to the substrate and prevention of the film contraction. Furthermore, it may also allow backside drying, which is important for efficient evaporation of the large amount of water. However, a non-absorbent substrate may lead to a non-uniform and defective coating because the non-absorbed water-rich film might act as lubricant between the MFC and the substrate, thus, allowing the MFC gel to re-agglomerate as patches.

Coating performance

To evaluate the impact of substrate properties on MFC coatability, coatings were applied using the slot-die process at two different SWGs, 150 and 300 µm, resulting in MFC coat weights of approx. 2–3 and 5–6 gsm, respectively. Afterwards, the different MFC coated samples were characterized for their air permeance and coating adhesion to the substrate.

Figure 37 shows air permeance of the different MFC coated substrates. The air permeance decreases with MFC coating, and the high coat weight results in a greater reduction. Air barrier performance of MFC coatings (5–6 gsm) on Linerboard and the CMC, HC-60 and HC-90 pre-coated boards is significantly

superior to the others. This indicates that a uniform MFC coating is obtained on these substrates. For pigment pre-coatings, these results are attributable to their smooth and closed surface, which results in a uniform MFC coating layer. The CMC pre-coating itself reduces the air permeance more than other pre-coatings, which is then reflected in a significant reduction with the MFC coatings. The hydrophilic nature of the PVOH and NFC pre-coatings seems to promote more uniform MFC coating at high coat weights, as opposed to the hydrophobic Paperboard and the Latex pre-coating. At low coat weights, however, the surface roughness seems to play a major role in MFC coating coverage and uniformity obtained. At low coat weights, MFC ends up filling the high surface roughness of the substrate, as is the case, e.g. with Linerboard. At high coat weights, Linerboard performs better than Paperboard due to its highly hydrophilic and water absorbent nature. The high adhesive forces of wet MFC layer with Linerboard and quick absorption of water by Linerboard may prevent the retracting tendency of MFC material due to cohesive forces, thus, ensuring a uniform film formation. Furthermore, MFC coating on the hydrophobic Paperboard substrate may develop pinholes during drying, resulting in a poor air barrier.

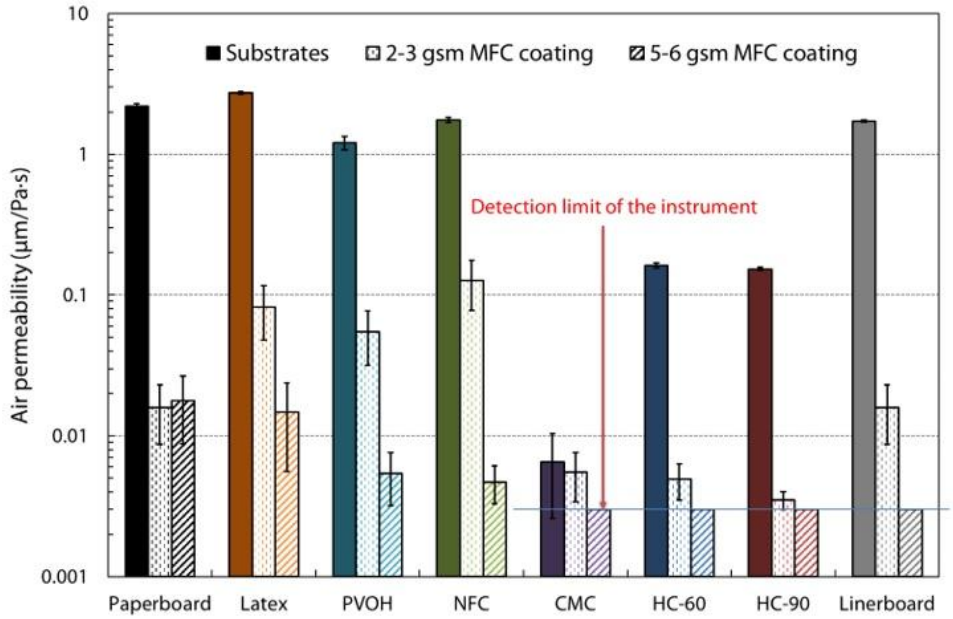

Figure 37. Air permeance of different MFC coated substrates.

Adequate adhesion of MFC coating to the substrate is important for converting processes and end-use applications. **Figure 38** shows z-strength and tape test results of the substrates and MFC coatings. Paperboard shows the poorest adhesion to the MFC coating, which improves slightly with the pre-coatings. However, there are no differences among the different pre-coated substrates. After the MFC coating, z-strength is significantly improved for Linerboard in contrast to the pre-coated substrates, which show no improvement or deterioration in surface strength. From tape test results, it is clear that the MFC coating is adhering well only to Linerboard and the CMC pre-coating where the fracture happens in the substrate structure, when the tape is pulled off. In all other cases, the MFC coating is delaminated from the substrate.

Cellulose fiber bonding in paper and related products occurs over a practical length scale ranging from the nanoscale to millimeters [241]. Mechanical interlocking, hydrogen bonding, adsorption or wetting theory, diffusion theory, and the theory of weak boundary layers are some of the adhesion concepts that have been examined in the bonding of cellulose fibers in paper and related materials [241]. The surface roughness of the substrates here does not seem to influence the adhesion of the MFC coating, e.g. Paperboard and HC-90 pre-coating (see **Figure 38**). This indicates that the mechanical interlocking may be a secondary factor in the adhesion of the MFC coatings to the substrate. Slightly improved adhesion with the pre-coatings indicates that the chemical bonding could be playing a major role here. For example, the hydrophilic nature of the CMC pre-coated board and Linerboard promotes hydrogen bonding and, thus, provides the best adhesion to the MFC coating. In addition, Linerboard allows some MFC to migrate inside the pores due to its high surface porosity and hydrophilic nature, resulting in the improvement observed in the z-strength of Linerboard with the MFC coating. Although Paperboard is equally porous, as indicated by the air permeance results (see **Figure 37**), its hydrophobic nature prevents such reinforcement with the MFC coating. It is worth mentioning that some later tests (unpublished results) have shown that a pre-coating with cationic polymers, e.g. cationic starch, improves the adhesion of the MFC coating to the substrate.

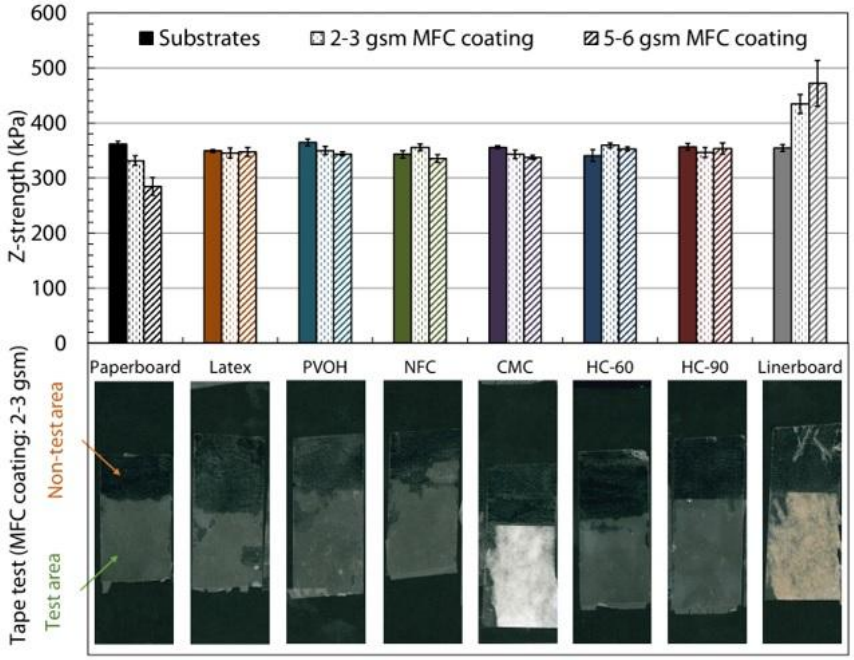

Figure 38. Z-strength and tape test results for MFC coatings on different substrates.

4.2.5 MFC Films vs Coatings

Mechanical performance

Table 6 lists strength properties of the MFC films at two different grammages (15 and 25 gsm), with and without CMC addition. Comparison of the strength properties of the substrate with the thickest MFC coating and the same grammage MFC film (**Figure 39**) shows that there is a large difference between the coated sample and the pure MFC film. It seems that the strength increasing potential of the MFC layer is not fully utilized in the coating. An explanation for this may be a presence of microscale pinholes in the MFC coating, resulting in a discontinuous film on the surface. In addition, the difference in drying process of the MFC films and coatings may cause a microstructure difference in their structure. Furthermore, the MFC films prepared at low solids content (0.5%) may have improved fibril arrangement and optimal bonding as opposed to the MFC coating applied at 2% or 3% solids. The overall strength for the coated sample here is largely controlled by the substrate and, therefore, the improvement in strength is only minor with the MFC coating. By optimizing the coating process parameters, it may be possible to obtain a larger strength increase with the MFC coating. However, it is probably better to mix the MFC in the papermaking furnish than to apply it as a coating if the strength increase is the main objective.

Table 6. Mechanical properties of MFC films

Property / Sample	Grammage (*gsm*)	TS (*kNm/kg*)	Stretch (*%*)	TEA (*J/kg*)
MFC-15	15 ± 1	95.91 ± 14.07	2.41 ± 1.11	1958 ± 1069
MFC-25	25 ± 2	98.64 ± 5.99	3.44 ± 0.69	2375 ± 585.5
MFC-15C	15 ± 1	100.8 ± 19.38	2.84 ± 0.97	2056 ± 950
MFC-25C	25 ± 1	106.4 ± 10.00	3.67 ± 0.86	2700 ± 861

Table 7. Barrier properties of MFC films

Property / Sample	Grammage (*gsm*)	HVTR ($g/m^2/day$)	WVTR ($g/m^2/day$)	OTR ($cm^3/m^2/day$)	KIT (-)	Air permeance ($\mu m/Pa{\cdot}s$)
MFC-15	15 ± 1	0	148 ± 19	fail	12	0.0030*
MFC-25	25 ± 2	0	110 ± 16	1.7 ± 0.4	12	0.0030
MFC-15C	15 ± 1	0	160 ± 22	fail	12	0.0030
MFC-25C	25 ± 1	0	147 ± 17	-	12	0.0030

*Detection limit of the instrument. - Sample not measured.

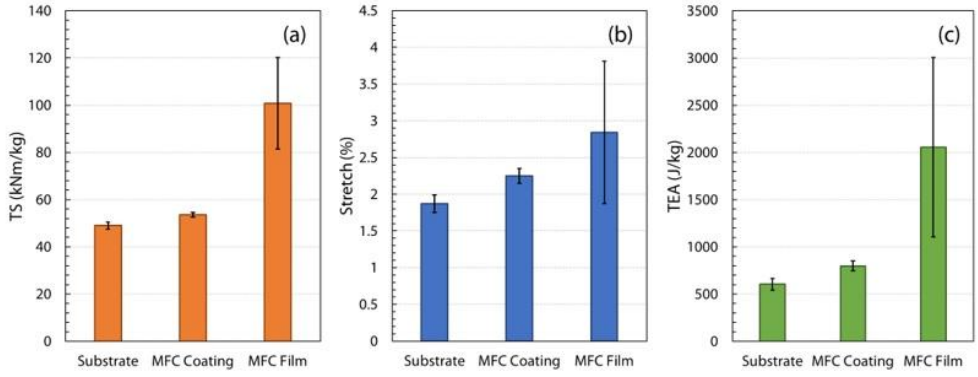

Figure 39. Comparison of strength properties of MFC coating (16 gsm) and film (MFC-15C).

Barrier Performance

Figure 40a shows air permeance and WVTR results for the MFC coatings with increasing coat weight and the MFC film (~15 gsm). There is a drastic reduction in the air permeance with the MFC coating, ascribed to a closed coating structure provided by the MFC layer, as reported previously in literature [22, 156, 189, 201, 204]. For 6 gsm and higher coat weights, the values are below the detection limit of the instrument, indicating a full and uniform coating coverage, as also evident from the SEM images and print penetration test results (see **Figure 33**

and **Figure 34**). Moreover, the coatings perform at par with the film for air barrier properties. Interestingly, a drop (~85%) in WVTR (**Figure 40a**) can be observed with the MFC coatings at high coat weights. Again, the coating performs at par with the film. However, this reduction is still not enough for these coated boards to be suitable for moisture barrier applications. The hydrophilic nature of the MFC films and coatings is not able to reduce the WVTR so significantly. This is because the moisture transport happens through a combination of adsorption and diffusion, and the natural sensitivity of cellulosic materials to moisture promotes both of these phenomena.

Migration of mineral oil from packaging material to food is a major concern to the food packaging industry [224, 242, 243]. Heptane is one of the components in various mineral oils used in printing inks and, therefore, HVTR can be used as an indicator of the mineral oil barrier [224]. A substantial reduction in HVTR with the increasing MFC coat weights was observed, as shown in **Figure 40b**. There was no heptane vapor transmission detected at the MFC coat weights of 9 gsm and higher. Furthermore, this reduction in HVTR is greater than the reduction achieved using other water-based barrier coatings reported earlier [224]. FTIR spectra of mineral oil barrier measurements (**Figure 41**) for the MFC coating (9 gsm) further confirms the mineral oil barrier. No mineral oil peak is seen even after 50 h, indicating that the MFC coating is impermeable to the mineral oil, provided the coat weight is high enough. This agrees with the improvement in mineral oil and castor oil barriers with NFC coating observed by Amini et al. [204].

MFC coatings can also be a potential candidate for grease barrier in various packaging applications, such as bakery products, fast foods, and pet foods [22, 204]. The KIT test method, a standard method in the paper industry, is used to characterize the grease resistance of barrier-coated materials. A clear improvement in KIT number with the increasing MFC coat weight can be observed in **Figure 40b**. In fact, the thickest coating almost reaches the KIT value (12) of the MFC film. However, oil Red O test results, shown in **Figure 42**, do not support the KIT results. This may be due to the different time scales of these measurement techniques. The MFC coatings do not seem to provide as effective oil Red O barrier as the MFC films. Furthermore, the thickest MFC coating did not show any oxygen barrier, whereas the MFC (25 gsm) film showed a significant oxygen barrier (see **Table 7**). This indicates that the MFC coatings may have pinholes. A defect-free coating is required to achieve an optimal barrier performance.

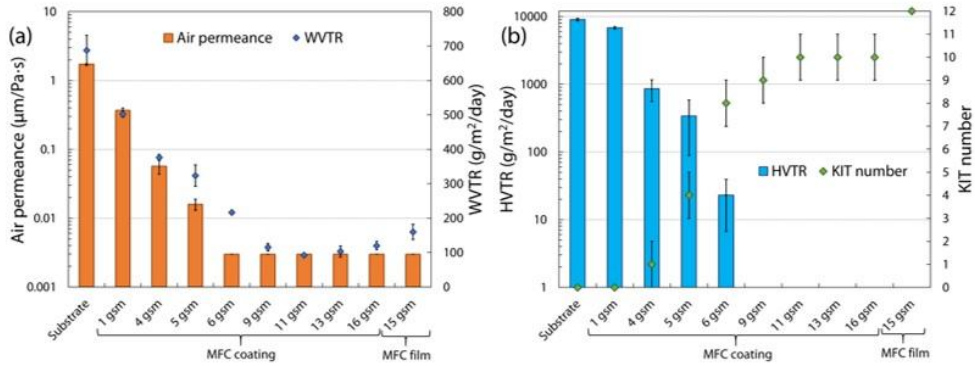

Figure 40. Comparison of barrier properties of MFC coatings and film (MFC-15C).

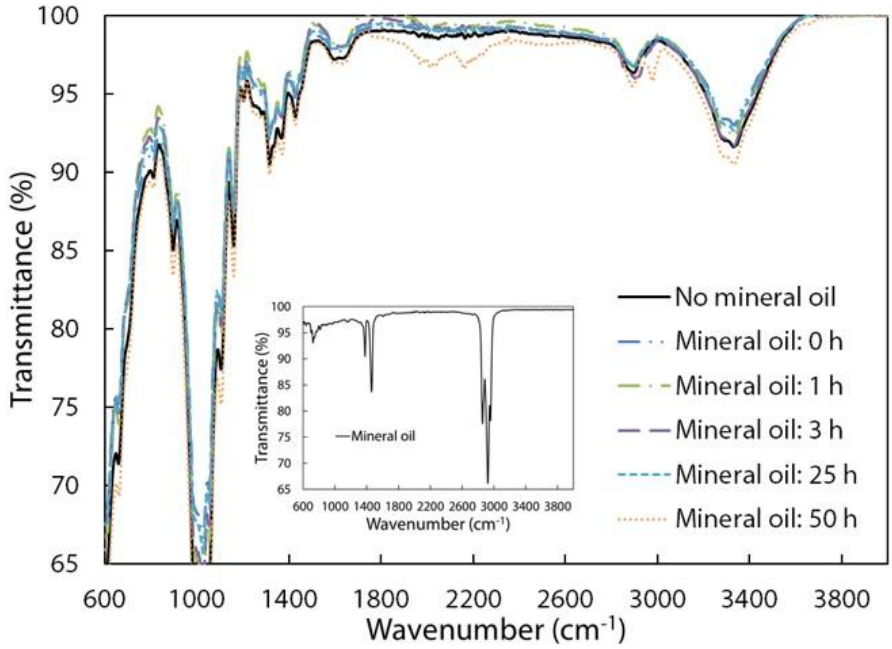

Figure 41. Mineral oil barrier of MFC coating (9 gsm) on the linerboard.

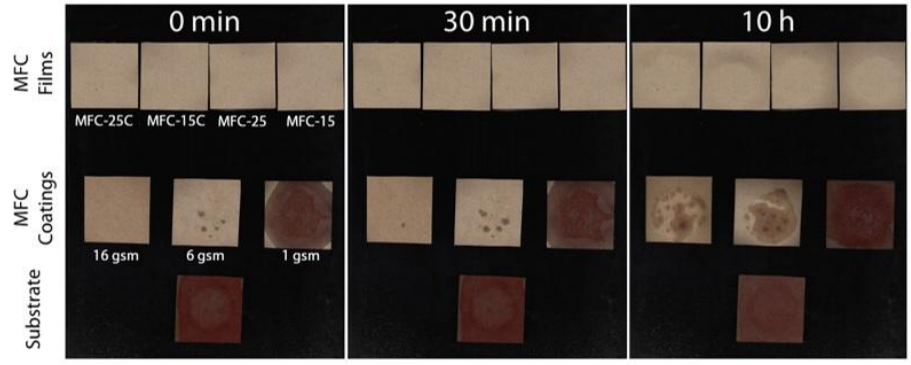

Figure 42. Oil red O test results for MFC coatings and films.

4.3 Functional Coating Containing Nanocellulose

4.3.1 Coatability

The coating suspensions used in **Publication V** are a complex system consisting of nanographite and NFC (see **Figure 43**). There are also large flaky graphene and graphite particles present in these suspensions. Similar to MFC suspensions, these are difficult to coat using conventional coating techniques. Therefore, they were first characterized for their water retention and rheological behavior and subsequently coated with the slot-die process, as a proof of concept.

Water Retention, Rheology, and Coating

ÅA-GWR values for nanographite suspensions were 6330 ± 150 gsm, which is comparable to 2% MFC suspensions used in this work (see **Figure 17**). This high dewatering value is a result of low solids content, i.e. 3%. As mentioned earlier, such high dewatering rates may cause runnability problems during coating on paper-based substrates.

Rheology determination of pure MFC suspensions is already challenging and the complexity of rheological behavior increases further in nanographite suspensions, as they contain a mixture of particles with varying morphology along with NFC. Rheology of such complex systems has been reported to be rather challenging to assess [58, 123, 244]. The high aspect ratio of constituents in these suspensions results in a similar rheological behavior as MFC suspensions. They display excessively high viscosity even at low solids content of 3% and highly shear thinning behavior, as shown in **Figure 44**. Addition of NFC as binder also partially contributes to the high viscosity observed. The shear thinning can be due to either dynamic yielding (breakdown of aggregated structures and alignment of high aspect ratio constituents along the flow) or apparent boundary slip due to material-depleted water-rich boundary layers, as discussed earlier for MFC suspensions. It is interesting to note that the shear thinning behavior observed at low shear rates in boundary-driven flow continues to high shear rates in pressure-driven slot flow. In addition, there is a reasonable agreement between the rheology data obtained from the two techniques. Furthermore, the apparent viscosity reaches almost that of water at shear rates beyond 10 000 s^{-1}. The rheological similarity of nanographite suspensions to MFC suspensions allows successful use of the slot-die coating process developed for the latter to coat them on paper-based substrates, as demonstrated in **Figure 45**. The coating was applied on the linerboard using two different SWGs of 400 and 800 µm, which resulted in approximate dry coat weights of 7–8 and 14–16 gsm, respectively.

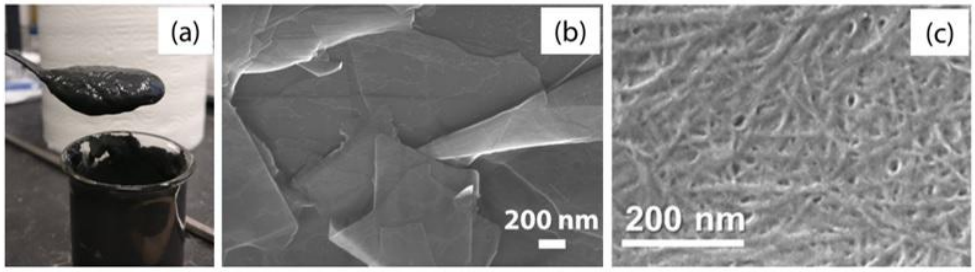

Figure 43. (a) Nanographite suspension at 3% solids, (b) SEM image of nanographite particles, and (c) SEM image of NFC binder.

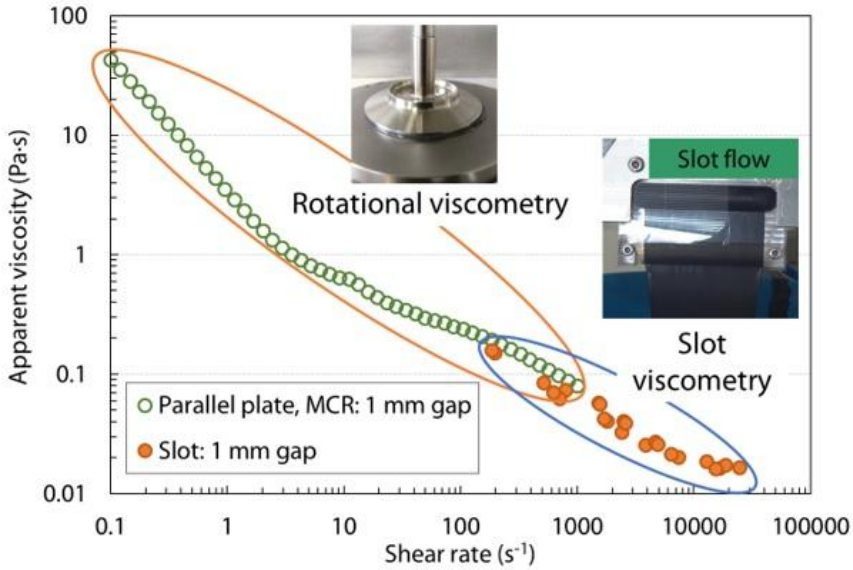

Figure 44. Shear rheology of nanographite NFC suspensions.

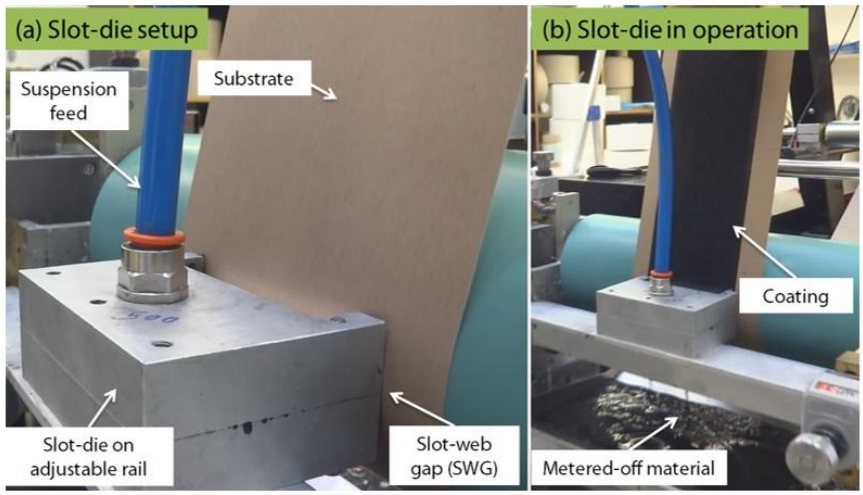

Figure 45. Coating process: (a) slot-die setup, (b) slot-die in operation.

4.3.2 Electrical Properties

This work reports electrical sheet resistance of coated samples, instead of conductivity. For conductivity determinations, precise coating thickness must be known, which was difficult to determine here due to the substrate being very rough and porous. Additionally, coating application at low solids resulted in large amounts of water going into the paper structure leading to further increased roughness. Sheet resistance reported here is assumed to be anisotropic.

Impact of Coat weight and Calendering

Figure 46 shows that higher coat weight results in lower sheet resistance, as expected. This is simply due to an increased amount of conductive material at high coat weights. Doubling the coat weight causes almost 70% reduction in sheet resistance. Sheet resistance of calendered samples is as low as 1.6 Ω/□. Calendering compresses the coating structure, as illustrated in the SEM images in **Figure 46**. Calendering at 200 kN/m reduced cumulative pore volume of the coated sample from 677 mm^3/g to 312 mm^3/g (pore size range: 3 nm to 10 µm) and 136 mm^3/g to 101 mm^3/g (pore size range: 3 nm to 1 µm), as measured using Mercury Porosimetry. This results in an improved connectivity in the structure, which reduces sheet resistance. The highest reduction was observed in going from uncalendered coating to the calendered coating at 100 kN/m line load, but increasing the calendering line load from 100 to 200 kN/m delivered a rather low reduction, especially at high coat weight. However, it is clear that a maximum densification of the coating structure is important for performance of the conductive coatings.

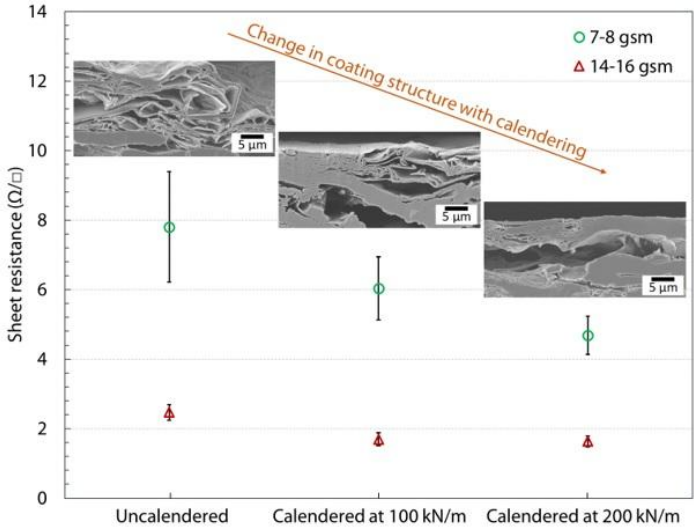

Figure 46. Sheet resistance against calendering nip load for nanographite coatings. SEM images of cross-sections of the same coatings show the coating structure. (Calendering was done at 60 °C. Measurement conditions: RH 50%).

Impact of RH

Humidity can affect the performance of paper-based electrodes negatively by influencing the conductive coating properties either directly or indirectly. The direct influence can come from presence of moisture in the pore structure of the coating, which disrupts the conductive network connectivity. The indirect influence can come from fiber swelling and de-bonding in the base paper at high humidity, which can disrupt the coating structure. Here, RH seems to have a minor impact on the electrical performance of the coated samples (see **Figure 47**). Low coat weight samples show higher variation in sheet resistance with changing RH, which could be due to a higher influence of the base paper at low coat weights. At high coat weights, RH has a negligible impact on sheet resistance. Calendering seems to reduce further the impact of RH, which could be due to the low porosity of the calendered samples that hinders the entrance of moisture into the structure. This is an important result for practical applications of these coatings in various humidity conditions.

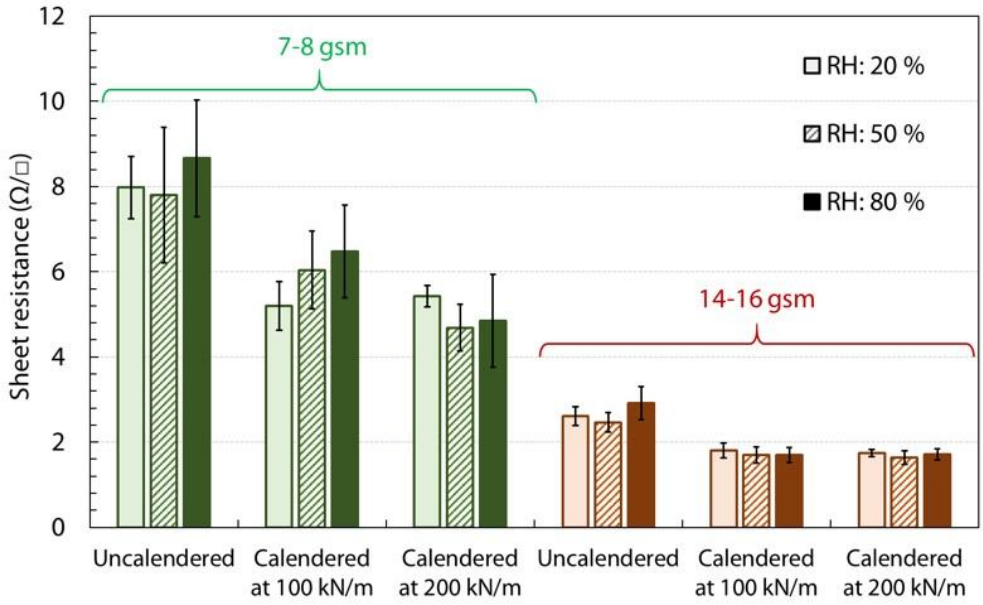

Figure 47. Impact of RH on sheet resistance. (Calendering was done at 60 °C).

Impact of Creasing and Bending

Paper-based coatings may be exposed to various mechanical forces, e.g. folding and bending, during production and/or end-use applications. It is important to understand and quantify the impact of such actions on the electrical performance. Most samples showed some increase in sheet resistance after creasing, as shown in **Figure 48**. Although this was expected, the change was surprisingly small (~10–20%). SEM images of creased samples in **Figure 49** show a minimal damage to the coating structure upon subjecting to creasing. Furthermore, bending of the samples did not influence their sheet resistance. This suggests that these coatings are rather flexible and fit for various end-use applications.

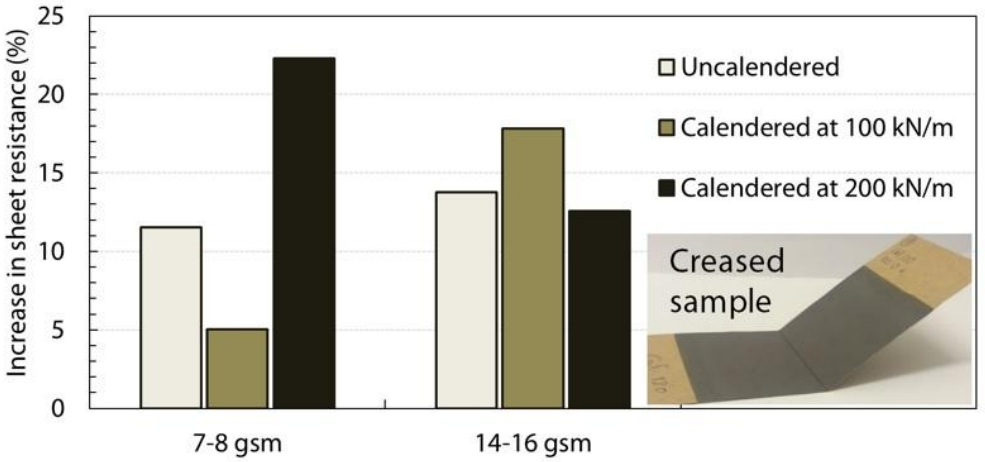

Figure 48. Impact of creasing on sheet resistance.

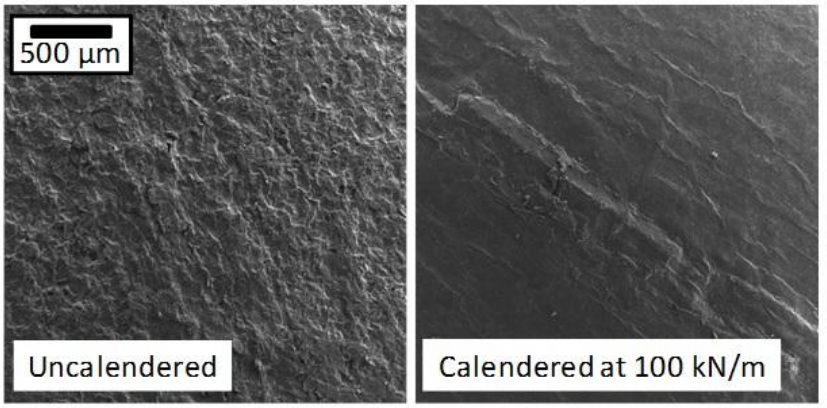

Figure 49. SEM images of the creased sample (14-16 gsm).

5. Concluding Remarks

MFC fibrils showed a wide size distribution. Some unrefined fiber chunks were also visible. Refining can produce highly fibrillated nanoscale MFC, but the smallest fibrils are usually in aggregated forms, resulting in overestimation of their diameter. This is attributable to the inherently low charge content of MFC. However, a post TEMPO-mediated oxidation was found to help reveal the true fibril size obtained with the refining process.

MFC suspensions showed flocculating and phase-separating tendencies. Zeta potential measurements suggest that the suspensions were quite unstable and not well dispersed. The improved magnitude of zeta potential with CMC addition further suggests an improved dispersion. CMC addition might have improved the fibril dispersion through slightly increased charge content. MFC suspensions also showed high dewatering rate for coating purposes on paper based substrates, but it was possible to reduce it multifold with the CMC addition.

MFC suspensions demonstrated complex rheological properties. The viscosities obtained from employing different geometries differed significantly. The use of a rough geometry caused further differences in results. The suspensions typically showed a gel-like behavior. From viscoelastic measurements, it was found that the solid-like behavior is dominant even at low solids content, i.e. 1%. Addition of CMC changed the rheological behavior in terms of gel strength and thixotropic properties. It reduced the gel strength and delayed the elastic recovery after shear, thus modifying the rheology positively for the coating process.

Pressure-driven flow in the slot-die enabled measuring of MFC suspension rheology up to shear rates of 100 000 s^{-1}, while boundary-driven flow measurements are usually limited to shear rates lower than 1 000 s^{-1}, due to sample ejection issues. MFC suspensions exhibited high shear thinning (pseudo-plasticity) and the solids content of the suspensions significantly affected the apparent viscosity. The high shear thinning can be attributed to the likely presence of a partially yielding plug center region surrounded by fiber-depleted water-rich boundary layers. A Newtonian plateau was also observed at very high shear rates arising potentially due to the turbulence created by strong wall friction at very high flow rates that might disrupt the fiber plug, resulting in an increased flow resistance. The calculated thickness of the water-rich boundary layers (assuming a non-yielding plug) extended to tens of microns at high flow rates and low solids content. One of the limitations of using slot-die geometry for rheology determination was clogging, especially at high suspension

concentrations, probably due to the presence of some unrefined fiber chunks. For instance, using a 250 μm slot was not successful due to excessive clogging.

A novel method for roll-to-roll coating of MFC suspensions on paperboard was developed and demonstrated successfully. The highly shear thinning behavior of MFC suspensions was exploited to help process them into uniform coating layers. The coating apparatus, i.e. the slot-die, was used in an unconventional manner, where shearing and metering were combined into one setup, thereby enabling application of thick and uniform MFC coatings in a continuous manner. The low process viscosity of MFC suspension resulting from slot flow was utilized to make the suspension coatable. Offset slot-die placement enabled easy metering with slot-to-paper gap control. Various parameters affecting the coating quality and runnability were identified and optimized. Addition of CMC was found to improve the coatability of MFC suspensions.

MFC coating improved the strength and barrier properties. There was a substantial improvement in barrier properties of coated paperboards with increasing MFC coat weights. MFC-coated paperboards demonstrated excellent barrier properties against air, grease, heptane and mineral oil, provided there was a full coverage of the paper by the MFC material. Even WVTR improved significantly with the MFC coating. The barrier properties of MFC coatings were comparable to the freestanding MFC films of grammage similar to MFC coat weight. Furthermore, a smooth, but porous, and highly hydrophilic substrate seemed to be an optimal choice for MFC coating application.

The slot-die coating method worked well for roll-to-roll coating of low-solids nanographite suspensions with rheological and water retention behavior similar to nanocellulose suspensions. Coat weights up to 15–16 gsm could be achieved in single layer application. High coat weight resulted in low sheet resistance, with the lowest values being approx. 2 Ω/□. Calendering decreased the sheet resistance, and a higher line load resulted in a greater reduction. RH and bending or creasing did not largely deteriorate the electrical performance of nanographite-coated samples. This could be important for the commercialization potential of these coatings in demanding applications, if the sheet resistance can be lowered further.

Although this work demonstrates a successful use of slot-die for coating of nanocellulose suspensions, yet there are process challenges that need to be addressed. For example, higher concentrations of nanocellulose suspensions may lead to air entrainment and difficulties in their pumping to the slot-die. An even distribution of these highly viscous and high yield-stress suspensions in wide slot-dies at industrial scale may become challenging. Another important issue is the high drying energy requirement caused by the low solids content of

MFC suspensions. Furthermore, the findings of the current work may comply well with the slot-die coating, but do not necessarily apply to other high-speed coating techniques.

Future work should focus on slot-die coating of nanocellulose at higher solids contents. A substrate with lower surface roughness and/or a finer nanocellulosic material may help solve the issue of insufficient MFC coating coverage at low coat weights. Potential solutions for eliminating the problem of pinholes include the use of multilayer coatings and/or finer grade nanocellulose. The moisture sensitivity of the MFC coatings should also be addressed, because it is well known that the swelling of MFC at high humidity deteriorates the barrier properties. Future work should also focus on developing a better understanding of flow dynamics in the slot-paper gap. Flow modeling, e.g. through CFD, may be helpful. There is also a need to better understand the mechanism of CMC interaction with nanocellulose.

For conductive coatings, increasing the solids content of suspensions through optimizing the dispersion and particle size distribution would be useful for both the coating process and the electrical performance of the resulting coatings. In terms of calendering, higher line loads, number and nature (hard or soft) of nips, moisture and temperature used, etc. are worth exploring. Furthermore, laser annealing of the coating or doping of graphene and graphitic material can potentially improve the electrical performance. One future direction of research could be applying the conductive coating either as patterned coating or through printing on paper.

References

[1] Pöyry (2015). "Paper and paperboard market: Demand is forecast to grow by nearly a fifth by 2030." <http://www.poyry.com/news/paper-and-paperboard-market-demand-forecast-grow-nearly-fifth-2030> (accessed: September 21, 2017).

[2] Holik, H. (2013). *Handbook of Paper and Board: Volume 1&2,* Second Ed., Wiley-VCH, Weinheim, Germany.

[3] Rager, J. (2016). "Global industry outlook: A platform for innovation?" *in: Annual Executive Conference: Renewable Bioproducts Institute,* April 5-6, Georgia, Atlanta, USA.

[4] CEPI Statistics (2016). *Key Statistics: European Pulp & Paper Industry,* Confederation of European Paper Industries (CEPI), Brussels, Belgium.

[5] Klemm, D., Kramer, F., Moritz, S., Lindström, T., Ankerfors, M., Gray, D., and Dorris, A. (2011). "Nanocelluloses: A New Family of Nature-Based Materials," *Angewandte Chemie International Edition* 50(24), 5438-5466.

[6] Klemm, D., Schumann, D., Kramer, F., Heßler, N., Koth, D., and Sultanova, B. (2009). "Nanocellulose materials–different cellulose, different functionality," *Macromolecular Symposia* 280(1), 60-71.

[7] Abitbol, T., Rivkin, A., Cao, Y., Nevo, Y., Abraham, E., Ben-Shalom, T., Lapidot, S., and Shoseyov, O. (2016). "Nanocellulose, a tiny fiber with huge applications," *Curr. Opin. Biotechnol.* 39, 76-88.

[8] Vinogradova, Y. S., and Chen, J. Y. (2016). "Micron-and nano-cellulose fiber regenerated from ionic liquids," *The Journal of the Textile Institute* 107(4), 472-476.

[9] Lindström, T., Naderi, A., and Wiberg, A. (2015). "Large scale applications of nanocellulosic materials: a comprehensive review," *Journal of Korea Technical Association of the Pulp and Paper Industry* 47(6), 5-21.

[10] Nickerson, R. F., and Habrle, J. A. (1947). "Cellulose intercrystalline structure," *Industrial and Engineering Chemistry* 39(11), 1507-1512.

[11] Rånby, B. G. (1949). "Aqueous colloidal solutions of cellulose micelles," *Acta Chemica Scandinavica* 3, 649-650.

[12] Turbak, A. F., Snyder, F. W., and Sandberg, K. R. (1983). "Microfibrillated cellulose, a new cellulose product: properties, uses, and commercial potential," *J. Appl. Polym. Sci.: Appl. Polym. Symp.* 37, 815-823.

[13] Herrick, F. W., Casebier, R. L., Hamilton, J. K., and Sandberg, K. R. (1983). "Microfibrillated cellulose: morphology and accessibility," *Journal of Applied Polymer Science: Applied Polymer Symposium* 37, 797-813.

[14] Pääkkö, M., Ankerfors, M., Kosonen, H., Nykänen, A., Ahola, S., Österberg, M., Ruokolainen, J., Laine, J., Larsson, P. T., Ikkala, O*., et al*. (2007). "Enzymatic Hydrolysis Combined with Mechanical Shearing and High-Pressure Homogenization for Nanoscale Cellulose Fibrils and Strong Gels," *Biomacromolecules* 8(6), 1934-1941.

[15] Saito, T., and Isogai, A. (2004). "TEMPO-Mediated Oxidation of Native Cellulose. The Effect of Oxidation Conditions on Chemical and Crystal Structures of the Water-Insoluble Fractions," *Biomacromolecules* 5(5), 1983-1989.

[16] Saito, T., Nishiyama, Y., Putaux, J., Vignon, M., and Isogai, A. (2006). "Homogeneous suspensions of individualized microfibrils from TEMPO-catalyzed oxidation of native cellulose," *Biomacromolecules* 7(6), 1687-1691.

[17] Wågberg, L., Decher, G., Norgren, M., Lindström, T., Ankerfors, M., and Axnäs, K. (2008). "The build-up of polyelectrolyte multilayers of microfibrillated cellulose and cationic polyelectrolytes," *Langmuir* 24(3), 784-795.

[18] Bardet, R., and Bras, J. (2014). "Cellulose Nanofibers and their use in Paper Industry," in: *Handbook of Green Materials: Processing Technologies, Properties and Applications*, K. Oksman, A. P. Mathew, A. Bismarck, O. Rojas, and M. Sain (eds.), World Scientific, New Jersey, USA, pp. 207-232.

[19] Gama, M., Gatenholm, P., Klemm, D. (2012). *Bacterial NanoCellulose: A Sophisticated Multifunctional Material,* 1st Ed., CRC Press, New York, USA.

[20] Isogai, A. (2013). "Wood nanocelluloses: fundamentals and applications as new bio-based nanomaterials," *Journal of Wood Science* 59(6), 449-459.

[21] Moon, R. J., Schueneman, G. T., and Simonsen, J. (2016). "Overview of cellulose nanomaterials, their capabilities and applications," *The Journal of the Minerals, Metals & Materials Society* 68(9), 2383-2394.

[22] Aulin, C., Gällstedt, M., and Lindström, T. (2010). "Oxygen and oil barrier properties of microfibrillated cellulose films and coatings," *Cellulose* 17(3), 559-574.

[23] Fukuzumi, H., Saito, T., Iwata, T., Kumamoto, Y., and Isogai, A. (2009). "Transparent and High Gas Barrier Films of Cellulose Nanofibers Prepared by TEMPO-Mediated Oxidation," *Biomacromolecules* 10(1), 162-165.

[24] Nakagaito, A. N., Nogi, M., and Yano, H. (2010). "Displays from Transparent Films of Natural Nanofibers," *MRS Bull* 35(03), 214-218.

[25] Nogi, M., Iwamoto, S., Nakagaito, A. N., and Yano, H. (2009). "Optically Transparent Nanofiber Paper," *Adv Mater* 21(16), 1595-1598.

[26] Yagyu, H., Saito, T., Isogai, A., Koga, H., and Nogi, M. (2015). "Chemical modification of cellulose nanofibers for the production of highly thermal resistant and optically transparent nanopaper for paper devices," *ACS Applied Materials & Interfaces* 7(39), 22012-22017.

[27] Eichhorn, S. J., Dufresne, A., Aranguren, M., Marcovich, N. E., Capadona, J. R., Rowan, S. J., Weder, C., Thielemans, W., Roman, M., Renneckar, S.*, et al.* (2010). "Review: current international research into cellulose nanofibres and nanocomposites," *J. Mater. Sci.* 45(1), 1-33.

[28] Jawaid, M., Boufi, S., Khalil H.P.S., A. (2017). *Cellulose-Reinforced Nanofibre Composites Production, Properties and Applications,* 1st Ed., Woodhead Publishing, Kidlington, UK.

[29] Khalil, H. A., Bhat, A., and Yusra, A. I. (2012). "Green composites from sustainable cellulose nanofibrils: A review," *Carbohydr. Polym.* 87(2), 963-979.

[30] Lee, K., Aitomäki, Y., Berglund, L. A., Oksman, K., and Bismarck, A. (2014). "On the use of nanocellulose as reinforcement in polymer matrix composites," *Composites Sci. Technol.* 105, 15-27.

[31] Lindström, T., and Aulin, C. (2014). "Market and technical challenges and opportunities in the area of innovative new materials and composites based on nanocellulosics," *Scand. J. for. Res.* 29(4), 345-351.

[32] Siqueira, G., Bras, J., and Dufresne, A. (2010). "Cellulosic bionanocomposites: a review of preparation, properties and applications," *Polymers* 2(4), 728-765.

[33] Hubbe, M., Ferrer, A., Tyagi, P., Yin, Y., Salas, C., Pal, L., and Rojas, O. (2017). "Nanocellulose in thin films, coatings, and plies for packaging applications: a review," *BioResources* 12(1), 2143-2233.

[34] France, K. J. D., Hoare, T., and Cranston, E. D. (2017). "Review of Hydrogels and Aerogels Containing Nanocellulose," *Chemistry of Materials* 29(11), 4609-4631.

[35] Hoeng, F., Denneulin, A., and Bras, J. (2016). "Use of nanocellulose in printed electronics: a review," *Nanoscale* 8, 13131-13154.

[36] Jorfi, M., and Foster, E. J. (2015). "Recent advances in nanocellulose for biomedical applications," *J Appl Polym Sci* 132(14), 41719.

[37] Lin, N., and Dufresne, A. (2014). "Nanocellulose in biomedicine: Current status and future prospect," *European Polymer Journal* 59, 302-325.

[38] Lu, Y., Tekinalp, H. L., Peter, W. H., Eberle, C., Naskar, A. K., and Ozcan, S. (2014). "Nanocellulose in Polymer Composites and Biomedical: Research and Applications," *Tappi J.* 13(6), 47-54.

[39] Hoeng, F., Denneulin, A., Reverdy-Bruas, N., Krosnicki, G., and Bras, J. (2017). "Rheology of cellulose nanofibrils/silver nanowires suspension for the production of transparent and conductive electrodes by screen printing," *Appl. Surf. Sci.* 394, 160-168.

[40] Phipps, J., Bourgoin, S., Legrix, A. H. R., and Vinnicombe, G. (2013). "Compositions for paint," Patent number: WO2011124759A1.

[41] Johansson, C., Bras, J., Mondragon, I., Nechita, P., Plackett, D., Simon, P., Svetec, D. G., Virtanen, S., Baschetti, M. G., and Breen, C. (2012). "Renewable fibers and bio-based materials for packaging applications: a review of recent developments," *BioResources* 7(2), 2506-2552.

[42] Khan, A., Huq, T., Khan, R. A., Riedl, B., and Lacroix, M. (2014). "Nanocellulose-based composites and bioactive agents for food packaging," *Crit. Rev. Food Sci. Nutr.* 54(2), 163-174.

[43] Li, F., Mascheroni, E., and Piergiovanni, L. (2015). "The Potential of NanoCellulose in the Packaging Field: A Review," *Packaging Technology and Science* 28(6), 475-508.

[44] Osong, S. H., Norgren, S., and Engstrand, P. (2016). "Processing of wood-based microfibrillated cellulose and nanofibrillated cellulose, and applications relating to papermaking: a review," *Cellulose* 23(1), 93-123.

[45] Samyn, P., Barhoum, A., Öhlund, T., and Dufresne, A. (2017). "Review: nanoparticles and nanostructured materials in papermaking," *Journal of Materials Science* Online, 1-39.

[46] Rastogi, V. K., and Samyn, P. (2015). "Bio-Based Coatings for Paper Applications," *Coatings* 5(4), 887-930.

[47] Lindström, T. (2017). "Aspects on nanofibrillated cellulose (NFC) processing, rheology and NFC-film properties," *Current Opinion in Colloid & Interface Science* 29, 68-75.

[48] Cowie, J., Bilek, E. M., Wegner, T. H., and Shatkin, J. A. (2014). "Market projections of cellulose nanomaterial-enabled products - Part 2: Volume estimates," *TAPPI Journal* 13(6), 57-69.

[49] Shatkin, J. A., Wegner, T. H., Bilek, E. M., and Cowie, J. (2014). "Market projections of cellulose nanomaterial-enabled products — Part 1: Applications," *TAPPI Journal* 13(5), 9-16.

[50] Bajpai, P. (2017). *Pulp and Paper Industry: Nanotechnology in Forest Industry,* First Ed., Elsevier, Amsterdam, Netherlands.

[51] Brodin, F. W., Gregersen, O. W., and Syverud, K. (2014). "Cellulose nanofibrils: Challenges and possibilities as a paper additive or coating material–A review," *Nord Pulp Pap Res J* 29(1), 156-166.

[52] Boufi, S., González, I., Delgado-Aguilar, M., Tarrès, Q., Pèlach, M. À, and Mutjé, P. (2016). "Nanofibrillated cellulose as an additive in papermaking process: A review," *Carbohydr. Polym.* 154, 151-166.

[53] Kinnunen-Raudaskoski, K., Hjelt, T., Kenttä, E., and Forsström, U. (2014). "Thin coatings for paper by foam coating," *TAPPI Journal* 13(7), 9-19.

[54] Naderi, A., and Lindström, T. (2015). "Rheological Measurements on Nanofibrillated Cellulose Systems: A Science in Progress," in: *Cellulose and Cellulose Derivatives: Synthesis, Modification and Applications*, M. I. H. Mondal (eds.), Nova Science, New York, USA, pp. 187-202.

[55] Nechyporchuk, O., Belgacem, M. N., and Pignon, F. (2016). "Current progress in rheology of cellulose nanofibril suspensions," *Biomacromolecules* 17(7), 2311-2320.

[56] Naderi, A. (2017). "Nanofibrillated cellulose: properties reinvestigated," *Cellulose* 24(5), 1933-1945.

[57] Nazari, B. (2015). *New Applications for Cellulose Nanofibers: Rheological Challenges,* PhD thesis, The University of Maine, Orono, USA.

[58] Dimic-Misic, K. (2014). *Micro and Nanofibrillated Cellulose (MNFC) as Additive in Complex Suspensions: Influence on Rheology and Dewatering,* PhD thesis, Aalto University, Helsinki, Finland.

[59] Iotti, M., Gregersen, Ø W., Størker, M., and Lenes, M. (2011). "Rheological Studies of Microfibrillar Cellulose Water Dispersions," *Journal of Polymers and the Environment* 19(1), 137-145.

[60] Barnes, H. A. (2000). *A Handbook of Elementary Rheology,* University of Wales, Institute of Non-Newtonian Fluid Mechanics, Wales, UK.

[61] Klemm, D., Heublein, B., Fink, H., and Bohn, A. (2005). "Cellulose: fascinating biopolymer and sustainable raw material," *Angewandte Chemie International Edition* 44(22), 3358-3393.

[62] Heinze, T. (2015). "Cellulose: Structure and Properties," in: *Cellulose Chemistry and Properties: Fibers, Nanocelluloses and Advanced Materials*, Anonymous (eds.), Springer, pp. 1-52.

[63] An, X., Cheng, D., Shen, J., Jia, Q., He, Z., Zheng, L., Khan, A., Sun, B., Ni, Y., and Xiong, B. (2017). "Nanocellulosic materials: research/production activities and applications," *Journal of Bioresources and Bioproducts* 2(2), 45-49.

[64] Stelte, W., and Sanadi, A. R. (2009). "Preparation and characterization of cellulose nanofibers from two commercial hardwood and softwood pulps," *Industrial & Engineering Chemistry Research* 48(24), 11211-11219.

[65] Chen, Y., Geng, B., Ru, J., Tong, C., Liu, H., and Chen, J. (2017). "Comparative characteristics of TEMPO-oxidized cellulose nanofibers and resulting nanopapers from bamboo, softwood, and hardwood pulps," *Cellulose* 24(11), 4831-4844.

[66] Lindström, T., Aulin, C., Naderi, A., and Ankerfors, M. (2014). "Microfibrillated Cellulose," in: *Encyclopedia of Polymer Science and Technology*, Anonymous (eds.), John Wiley & Sons, Published Online, pp. 1-34.

[67] Moon, R. J., Martini, A., Nairn, J., Simonsen, J., and Youngblood, J. (2011). "Cellulose nanomaterials review: structure, properties and nanocomposites," *Chem. Soc. Rev.* 40(7), 3941-3994.

[68] Aspler, J., Bouchard, J., Hamad, W., Berry, R., Beck, S., Drolet, F., and Zou, X. (2013). "Review of Nanocellulosic Products and their Applications," in: *Biopolymer Nanocomposites: Processing, Properties, and Applications*, A. Dufresne, S. Thomas, and L. A. Pothen (eds.), John Wiley & Sons, Hoboken, NJ, USA, pp. 461-508.

[69] Nechyporchuk, O., Belgacem, M. N., and Bras, J. (2016). "Production of cellulose nanofibrils: A review of recent advances," *Industrial Crops and Products* 93, 2-25.

[70] Siró, I., and Plackett, D. (2010). "Microfibrillated cellulose and new nanocomposite materials: a review," *Cellulose* 17(3), 459-494.

[71] Tejado, A., Alam, M. N., Antal, M., Yang, H., and van de Ven, Theo GM. (2012). "Energy requirements for the disintegration of cellulose fibers into cellulose nanofibers," *Cellulose* 19(3), 831-842.

[72] Liimatainen, H., Visanko, M., Sirviö, J., Hormi, O., and Niinimäki, J. (2013). "Sulfonated cellulose nanofibrils obtained from wood pulp through regioselective oxidative bisulfite pre-treatment," *Cellulose* 20(2), 741-749.

[73] Sirviö, J. A., Kolehmainen, A., Visanko, M., Liimatainen, H., Niinimäki, J., and Hormi, O. E. (2014). "Strong, self-standing oxygen barrier films from nanocelluloses modified with regioselective oxidative treatments," *ACS Applied Materials & Interfaces* 6(16), 14384-14390.

[74] Pei, A., Butchosa, N., Berglund, L. A., and Zhou, Q. (2013). "Surface quaternized cellulose nanofibrils with high water absorbency and adsorption capacity for anionic dyes," *Soft Matter* 9(6), 2047-2055.

[75] Isogai, A., Saito, T., and Fukuzumi, H. (2011). "TEMPO-oxidized cellulose nanofibers," *Nanoscale* 3(1), 71-85.

[76] Bragd, P., Van Bekkum, H., and Besemer, A. (2004). "TEMPO-mediated oxidation of polysaccharides: survey of methods and applications," *Topics in Catalysis* 27(1), 49-66.

[77] Pierre, G., Punta, C., Delattre, C., Melone, L., Dubessay, P., Fiorati, A., Pastori, N., Galante, Y. M., and Michaud, P. (2017). "TEMPO-mediated oxidation of polysaccharides: An ongoing story," *Carbohydr. Polym.* 165, 71-85.

[78] Saito, T., Kimura, S., Nishiyama, Y., and Isogai, A. (2007). "Cellulose nanofibers prepared by TEMPO-mediated oxidation of native cellulose," *Biomacromolecules* 8(8), 2485-2491.

[79] Saito, T., Hirota, M., Tamura, N., Kimura, S., Fukuzumi, H., Heux, L., and Isogai, A. (2009). "Individualization of nano-sized plant cellulose fibrils by direct surface carboxylation using TEMPO catalyst under neutral conditions," *Biomacromolecules* 10(7), 1992-1996.

[80] Tanaka, R., Saito, T., and Isogai, A. (2012). "Cellulose nanofibrils prepared from softwood cellulose by TEMPO/NaClO/NaClO2 systems in water at pH 4.8 or 6.8," *Int. J. Biol. Macromol.* 51(3), 228-234.

[81] Walecka, J. A. (1956). "An investigation of low degree of substitution carboxymethylcellulose," *TAPPI Journal* 39(7), 458-463.

[82] Lindström, T. (1992). "Chemical factors affecting the behaviour of fibres during papermaking," *Nordic Pulp & Paper Research Journal* 7(4), 181-192.

[83] Heinze, T., and Koschella, A. (2005). "Carboxymethyl ethers of cellulose and starch–a review," *Macromolecular Symposia* 223(1), 13-40.

[84] Horvath, A. E., and Lindström, T. (2007). "The influence of colloidal interactions on fiber network strength," *J. Colloid Interface Sci.* 309(2), 511-517.

[85] Bolaski, W., Gallatin, A., and Gallatin, J. C. (1962). "Enzymatic conversion of cellulosic fibers," Patent number: US3041246A.

[86] Henriksson, M., Henriksson, G., Berglund, L. A., and Lindström, T. (2007). "An environmentally friendly method for enzyme-assisted preparation of microfibrillated cellulose (MFC) nanofibers," *European Polymer Journal* 43(8), 3434-3441.

[87] Kang, T. (2007). *Role of External Fibrillation in Pulp and Paper Properties,* PhD thesis, Helsinki University of Technology, Espoo, Finland.

[88] Carrasco, F., Mutje, P., and Pelach, M. (1996). "Refining of bleached cellulosic pulps: characterization by application of the colloidal titration technique," *Wood Sci. Technol.* 30(4), 227-236.

[89] Gane, P. A. C., Schoelkopf, J., Gantenbein, D., Schenker, M., Pohl, M., and Kuebler, B. (2010). "Process for the Production of Nano-Fibrillar Cellulose Suspensions," Patent number: WO2010112519 (A1).

[90] Husband, J. C., Svending, P., Skuse, D. R., Motsi, T., Likitalo, M., and Coles, A. (2010). "Paper Filler Composition," Patent number: WO2010131016 (A2).

[91] Svending, P. (2017). "Microfibrillated cellulose as coating binder," *in: 28th PTS Coating Symposium,* September 5-6, Munich, Germany.

[92] Kangas, H., Lahtinen, P., Sneck, A., Saariaho, A., Laitinen, O., and Hellen, E. (2014). "Characterization of fibrillated celluloses. A short review and evaluation of characteristics with a combination of methods," *Nordic Pulp & Paper Research Journal* 29(1), 129-143.

[93] Chirayil, C. J., Mathew, L., and Thomas, S. (2014). "Review of recent research in nano cellulose preparation from different lignocellulosic fibers," *Reviews on Advanced Materials Science* 37(1/2), 20-28.

[94] Karppinen, A., Vesterinen, A., Saarinen, T., Pietikäinen, P., and Seppälä, J. (2011). "Effect of cationic polymethacrylates on the rheology and flocculation of microfibrillated cellulose," *Cellulose* 18(6), 1381-1390.

[95] Karppinen, A., Saarinen, T., Salmela, J., Laukkanen, A., Nuopponen, M., and Seppälä, J. (2012). "Flocculation of microfibrillated cellulose in shear flow," *Cellulose* 19(6), 1807-1819.

[96] Saarikoski, E., Saarinen, T., Salmela, J., and Seppälä, J. (2012). "Flocculated flow of microfibrillated cellulose water suspensions: an imaging approach for characterisation of rheological behaviour," *Cellulose* 19(3), 647-659.

[97] Eronen, P., Laine, J., Ruokolainen, J., and Österberg, M. (2012). "Comparison of multilayer formation between different cellulose nanofibrils and cationic polymers," *J. Colloid Interface Sci.* 373(1), 84-93.

[98] Taipale, T., Österberg, M., Nykänen, A., Ruokolainen, J., and Laine, J. (2010). "Effect of microfibrillated cellulose and fines on the drainage of kraft pulp suspension and paper strength," *Cellulose* 17(5), 1005-1020.

[99] Xu, X. (2014). *Study of the Relationship between the Dispersion of Micro-Nano-Fibrillated Cellulose (MNFC) and their Ability in Curtain Coating,* Master's thesis, University of Quebec, Trois-Rivières, Quebec, Canada.

[100] Okita, Y., Saito, T., and Isogai, A. (2010). "Entire surface oxidation of various cellulose microfibrils by TEMPO-mediated oxidation," *Biomacromolecules* 11(6), 1696-1700.

[101] Syverud, K., Xhanari, K., Chinga-Carrasco, G., Yu, Y., and Stenius, P. (2011). "Films made of cellulose nanofibrils: surface modification by adsorption of a cationic surfactant and characterization by computer-assisted electron microscopy," *Journal of Nanoparticle Research* 13(2), 773-782.

[102] Cheng, Q., Wang, J., McNeel, J., and Jacobson, P. (2010). "Water retention value measurements of cellulosic materials using a centrifuge technique," *BioResources* 5(3), 1945-1954.

[103] Hubbe, M. A., and Heitmann, J. A. (2007). "Review of factors affecting the release of water from cellulosic fibers during paper manufacture," *BioResources* 2(3), 500-533.

[104] Lahtinen, P., Liukkonen, S., Pere, J., Sneck, A., and Kangas, H. (2014). "A Comparative Study of Fibrillated Fibers from Different Mechanical and Chemical Pulps," *BioResources* 9(2), 2115-2127.

[105] Spence, K. L., Venditti, R. A., Rojas, O. J., Habibi, Y., and Pawlak, J. J. (2010). "The effect of chemical composition on microfibrillar cellulose films from wood pulps: water interactions and physical properties for packaging applications," *Cellulose* 17(4), 835-848.

[106] Dimic-Misic, K., Puisto, A., Paltakari, J., Alava, M., and Maloney, T. (2013). "The influence of shear on the dewatering of high consistency nanofibrillated cellulose furnishes," *Cellulose* 20(4), 1853-1864.

[107] Rantanen, J., Dimic-Misic, K., Pirttiniemi, J., Kuosmanen, P., and Maloney, T. (2015). "Forming and Dewatering of a Microfibrillated Cellulose Composite Paper," *BioResources* 10(2), 3492-3506.

[108] Richmond, F. (2014). *Cellulose Nanofibers use in Coated Papers,* PhD thesis, The University of Maine, Orono, USA.

[109] Karppinen, A. (2014). *Rheology and Flocculation of Polymer-Modified Microfibrillated Cellulose Suspensions,* PhD thesis, Aalto University, Helsinki, Finland.

[110] Gong, G. (2014). "Rheological Properties of Nanocellulose Materials," in: *Handbook of Green Materials: Bionanomaterials: Separation Processes, Characterization and Properties*, K. Oksman, A. P. Mathew, A. Bismarck, O. Rojas, and M. Sain (eds.), World Scientific, New Jersey, USA, pp. 139-157.

[111] Agoda-Tandjawa, G., Durand, S., Berot, S., Blassel, C., Gaillard, C., Garnier, C., and Doublier, J. (2010). "Rheological characterization of

microfibrillated cellulose suspensions after freezing," *Carbohydr. Polym.* 80(3), 677-686.

[112] Hill, R. J. (2008). "Elastic modulus of microfibrillar cellulose gels," *Biomacromolecules* 9(10), 2963-2966.

[113] Lowys, M., Desbrieres, J., and Rinaudo, M. (2001). "Rheological characterization of cellulosic microfibril suspensions. Role of polymeric additives," *Food Hydrocoll.* 15(1), 25-32.

[114] Dong, H., Snyder, J. F., Williams, K. S., and Andzelm, J. W. (2013). "Cation-induced hydrogels of cellulose nanofibrils with tunable moduli," *Biomacromolecules* 14(9), 3338-3345.

[115] Fukuzumi, H., Tanaka, R., Saito, T., and Isogai, A. (2014). "Dispersion stability and aggregation behavior of TEMPO-oxidized cellulose nanofibrils in water as a function of salt addition," *Cellulose* 21(3), 1553-1559.

[116] Jowkarderis, L., and van de Ven, Theo GM. (2014). "Intrinsic viscosity of aqueous suspensions of cellulose nanofibrils," *Cellulose* 21(4), 2511-2517.

[117] Moberg, T., Rigdahl, M., Stading, M., and Levenstam Bragd, E. (2014). "Extensional viscosity of microfibrillated cellulose suspensions," *Carbohydr. Polym.* 102(0), 409-412.

[118] Naderi, A., and Lindström, T. (2014). "Carboxymethylated nanofibrillated cellulose: effect of monovalent electrolytes on the rheological properties," *Cellulose* 21(5), 3507-3514.

[119] Jowkarderis, L., and van de Ven, Theo GM. (2015). "Rheology of semi-dilute suspensions of carboxylated cellulose nanofibrils," *Carbohydr. Polym.* 123, 416-423.

[120] Naderi, A., and Lindström, T. (2016). "A comparative study of the rheological properties of three different nanofibrillated cellulose systems," *Nordic Pulp & Paper Research Journal* 31(3), 354-363.

[121] Sorvari, A., Saarinen, T., Haavisto, S., Salmela, J., Vuoriluoto, M., and Seppälä, J. (2014). "Modifying the flocculation of microfibrillated cellulose suspensions by soluble polysaccharides under conditions unfavorable to adsorption," *Carbohydr. Polym.* 106, 283-292.

[122] Vesterinen, A., Myllytie, P., Laine, J., and Seppälä, J. (2010). "The effect of water-soluble polymers on rheology of microfibrillar cellulose

suspension and dynamic mechanical properties of paper sheet," *J Appl Polym Sci* 116(5), 2990-2997.

[123] Schenker, M., Schoelkopf, J., Mangin, P., and Gane, P. (2016). "Rheological investigation of complex micro and nanofibrillated cellulose (MNFC) suspensions: Discussion of flow curves and gel stability," *TAPPI Journal* 15(6), 405-416.

[124] Moberg, T., Sahlin, K., Yao, K., Geng, S., Westman, G., Zhou, Q., Oksman, K., and Rigdahl, M. (2017). "Rheological properties of nanocellulose suspensions: effects of fibril/particle dimensions and surface characteristics," *Cellulose* 24(6), 2499-2510.

[125] Naderi, A., Lindstrom, T., Erlandsson, J., Sundstrom, J., and Flodberg, G. (2016). "A comparative study of the properties of three nanofibrillated cellulose systems that have been produced at about the same energy consumption levels in the mechanical delamination step," *Nordic Pulp & Paper Research Journal* 31(3), 364-371.

[126] Lasseuguette, E., Roux, D., and Nishiyama, Y. (2008). "Rheological properties of microfibrillar suspension of TEMPO-oxidized pulp," *Cellulose* 15(3), 425-433.

[127] Chen, P., Yu, H., Liu, Y., Chen, W., Wang, X., and Ouyang, M. (2013). "Concentration effects on the isolation and dynamic rheological behavior of cellulose nanofibers via ultrasonic processing," *Cellulose* 20(1), 149-157.

[128] Mendoza, L., Batchelor, W., Tabor, R. F., and Garnier, G. (2018). "Gelation mechanism of cellulose nanofibre gels: A colloids and interfacial perspective," *J. Colloid Interface Sci.* 509, 39-46.

[129] Nechyporchuk, O., Belgacem, M. N., and Pignon, F. (2014). "Rheological properties of micro-/nanofibrillated cellulose suspensions: Wall-slip and shear banding phenomena," *Carbohydr. Polym.* 112, 432-439.

[130] Mohtaschemi, M., Dimic-Misic, K., Puisto, A., Korhonen, M., Maloney, T., Paltakari, J., and Alava, M. J. (2014). "Rheological characterization of fibrillated cellulose suspensions via bucket vane viscometer," *Cellulose* 21(3), 1305-1312.

[131] Haavisto, S., Salmela, J., Jäsberg, A., Saarinen, T., Karppinen, A., and Koponen, A. (2015). "Rheological characterization of microfibrillated cellulose suspension using optical coherence tomography," *TAPPI Journal* 14(5), 291-302.

[132] Lauri, J., Koponen, A., Haavisto, S., Czajkowski, J., and Fabritius, T. (2017). "Analysis of rheology and wall depletion of microfibrillated cellulose suspension using optical coherence tomography," *Cellulose* 24(11), 4715-4728.

[133] Saarinen, T., Lille, M., and Seppälä, J. (2009). "Technical aspects on rheological characterization of microfibrillar cellulose water suspensions," *Annu Trans Nord Rheol Soc* 17, 121-128.

[134] Charani, P. R., Dehghani-Firouzabadi, M., Afra, E., and Shakeri, A. (2013). "Rheological characterization of high concentrated MFC gel from kenaf unbleached pulp," *Cellulose* 20(2), 727-740.

[135] Tatsumi, D., Ishioka, S., and Matsumoto, T. (2002). "Effect of Fiber Concentration and Axial Ratio on the Rheological Properties of Cellulose Fiber Suspensions." *Journal of the Society of Rheology, Japan* 30(1), 27-32.

[136] Shogren, R. L., Peterson, S. C., Evans, K. O., and Kenar, J. A. (2011). "Preparation and characterization of cellulose gels from corn cobs," *Carbohydr. Polym.* 86(3), 1351-1357.

[137] Kroy, K., and Frey, E. (1996). "Force-extension relation and plateau modulus for wormlike chains," *Phys. Rev. Lett.* 77(2), 306.

[138] MacKintosh, F., Käs, J., and Janmey, P. (1995). "Elasticity of semiflexible biopolymer networks," *Phys. Rev. Lett.* 75(24), 4425.

[139] Kerekes, R. J. (2006). "Rheology of fibre suspensions in papermaking: An overview of recent research," *Nordic Pulp & Paper Research Journal* 21(5), 598-612.

[140] Derakhshandeh, B., Kerekes, R. J., Hatzikiriakos, S. G., and Bennington, C. P. J. (2011). "Rheology of pulp fibre suspensions: A critical review," *Chemical Engineering Science* 66(15), 3460-3470.

[141] Grüneberger, F., Künniger, T., Zimmermann, T., and Arnold, M. (2014). "Rheology of nanofibrillated cellulose/acrylate systems for coating applications," *Cellulose* 21(3), 1313-1326.

[142] Taheri, H., and Samyn, P. (2016). "Effect of homogenization (microfluidization) process parameters in mechanical production of micro-and nanofibrillated cellulose on its rheological and morphological properties," *Cellulose* 23(2), 1221-1238.

[143] Martoïa, F., Perge, C., Dumont, P. J., Orgéas, L., Fardin, M., Manneville, S., and Belgacem, M. N. (2015). "Heterogeneous flow kinematics of cellulose nanofibril suspensions under shear," *Soft Matter* 11(24), 4742-4755.

[144] Buscall, R. (2010). "Letter to the Editor: Wall slip in dispersion rheometry," *J. Rheol.* 54(6), 1177-1183.

[145] Barnes, H. A. (1995). "A review of the slip (wall depletion) of polymer solutions, emulsions and particle suspensions in viscometers: its cause, character, and cure," *J. Non Newtonian Fluid Mech.* 56(3), 221-251.

[146] Starkey, T., and James, R. (1956). "Instability of uniform concentration conditions in suspensions under shear," *Nature* 178, 207-208.

[147] Blair, G. S. (1958). "The importance of the sigma phenomenon in the study of the flow of blood," *Rheologica Acta* 1(2-3), 123-126.

[148] Phillips, R. J., Armstrong, R. C., Brown, R. A., Graham, A. L., and Abbott, J. R. (1992). "A constitutive equation for concentrated suspensions that accounts for shear-induced particle migration," *Physics of Fluids A: Fluid Dynamics (1989-1993)* 4(1), 30-40.

[149] Joseph, S. (1999). *Phase Segregation in Multi-Component Polymer Systems,* PhD thesis, University of Toronto, Toronto, Canada.

[150] Pan, W., Caswell, B., and Karniadakis, G. E. (2009). "Rheology, microstructure and migration in Brownian colloidal suspensions," *Langmuir* 26(1), 133-142.

[151] Saarinen, T., Haavisto, S., Sorvari, A., Salmela, J., and Seppälä, J. (2014). "The effect of wall depletion on the rheology of microfibrillated cellulose water suspensions by optical coherence tomography," *Cellulose* 21(3), 1261-1275.

[152] Claesson, J., Wikström, T., and Rasmuson, A. (2013). "The development of a near-wall boundary layer over a flat plate in concentrated pulp fiber suspensions," *Nordic Pulp & Paper Research Journal* 28(3), 399-406.

[153] Li, T., Powell, R. L., Ödberg, L., McCarthy, M. J., and McCarthy, K. L. (1994). "Velocity measurements of fiber suspensions in pipe flow by the nuclear magnetic resonance imaging method," *TAPPI Journal* 77(3), 145-149.

[154] Taniguchi, T., and Okamura, K. (1998). "New films produced from microfibrillated natural fibres," *Polym. Int.* 47(3), 291-294.

[155] Lagaron, J., Catalá, R., and Gavara, R. (2004). "Structural characteristics defining high barrier properties in polymeric materials," *Materials Science and Technology* 20(1), 1-7.

[156] Syverud, K., and Stenius, P. (2009). "Strength and barrier properties of MFC films," *Cellulose* 16(1), 75-85.

[157] Hu, L., Zheng, G., Yao, J., Liu, N., Weil, B., Eskilsson, M., Karabulut, E., Ruan, Z., Fan, S., Bloking, J. T., *et al.* (2013). "Transparent and conductive paper from nanocellulose fibers," *Energy & Environmental Science* 6(2), 513-518.

[158] Lavoine, N., Desloges, I., Dufresne, A., and Bras, J. (2012). "Microfibrillated cellulose – Its barrier properties and applications in cellulosic materials: a review," *Carbohydr. Polym.* 90(2), 735-764.

[159] Benítez, A., and Walther, A. (2017). "Cellulose nanofibril nanopapers and bioinspired nanocomposites: a review to understand the mechanical property space," *Journal of Materials Chemistry A* 5(31), 16003-16024.

[160] Ferrer, A., Pal, L., and Hubbe, M. (2017). "Nanocellulose in packaging: Advances in barrier layer technologies," *Industrial Crops and Products* 95, 574-582.

[161] Iwamoto, S., Abe, K., and Yano, H. (2008). "The effect of hemicelluloses on wood pulp nanofibrillation and nanofiber network characteristics," *Biomacromolecules* 9(3), 1022-1026.

[162] Plackett, D., Anturi, H., Hedenqvist, M., Ankerfors, M., Gällstedt, M., Lindström, T., and Siró, I. (2010). "Physical properties and morphology of films prepared from microfibrillated cellulose and microfibrillated cellulose in combination with amylopectin," *J Appl Polym Sci* 117(6), 3601-3609.

[163] Spence, K. L., Venditti, R. A., Rojas, O. J., Habibi, Y., and Pawlak, J. J. (2011). "A comparative study of energy consumption and physical properties of microfibrillated cellulose produced by different processing methods," *Cellulose* 18(4), 1097-1111.

[164] Dufresne, A., Cavaille, J. Y., and Vignon, M. R. (1997). "Mechanical behavior of sheets prepared from sugar beet cellulose microfibrils," *J Appl Polym Sci* 64, 1185-1194.

[165] Qing, Y., Sabo, R., Zhu, J. Y., Agarwal, U., Cai, Z., and Wu, Y. (2013). "A comparative study of cellulose nanofibrils disintegrated via multiple processing approaches," *Carbohydr. Polym.* 97(1), 226-234.

[166] Siró, I., Plackett, D., Hedenqvist, M., Ankerfors, M., and Lindström, T. (2011). "Highly transparent films from carboxymethylated microfibrillated cellulose: the effect of multiple homogenization steps on key properties," *J Appl Polym Sci* 119(5), 2652-2660.

[167] Varanasi, S., and Batchelor, W. J. (2013). "Rapid preparation of cellulose nanofibre sheet," *Cellulose* 20(1), 211-215.

[168] Sehaqui, H., Liu, A., Zhou, Q., and Berglund, L. A. (2010). "Fast preparation procedure for large, flat cellulose and cellulose/inorganic nanopaper structures," *Biomacromolecules* 11(9), 2195-2198.

[169] Baez, C., Considine, J., and Rowlands, R. (2014). "Influence of drying restraint on physical and mechanical properties of nanofibrillated cellulose films," *Cellulose* 21(1), 347-356.

[170] Hansen, N. L., Blomfeldt, T. J., Hedenqvist, M., and Plackett, D. (2012). "Properties of plasticized composite films prepared from nanofibrillated cellulose and birch wood xylan," *Cellulose* 19(6), 2015-2031.

[171] Chinga-Carrasco, G., and Syverud, K. (2012). "On the structure and oxygen transmission rate of biodegradable cellulose nanobarriers," *Nanoscale Research Letters* 7(1), 1-6.

[172] Minelli, M., Baschetti, M. G., Doghieri, F., Ankerfors, M., Lindström, T., Siró, I., and Plackett, D. (2010). "Investigation of mass transport properties of microfibrillated cellulose (MFC) films," *J. Membr. Sci.* 358(1–2), 67-75.

[173] Rodionova, G., Saito, T., Lenes, M., Eriksen, Ø, Gregersen, Ø, Fukuzumi, H., and Isogai, A. (2012). "Mechanical and oxygen barrier properties of films prepared from fibrillated dispersions of TEMPO-oxidized Norway spruce and Eucalyptus pulps," *Cellulose* 19(3), 705-711.

[174] Spence, K. L., Venditti, R. A., Rojas, O. J., Pawlak, J. J., and Hubbe, M. A. (2011). "Water Vapor barrier properties of coated and filled microfibrillated cellulose composite films," *BioResources* 6(4), 4370-4388.

[175] Rodionova, G., Hoff, B., Lenes, M., Eriksen, Ø, and Gregersen, Ø. (2013). "Gas-phase esterification of microfibrillated cellulose (MFC) films," *Cellulose* 20(3), 1167-1174.

[176] Österberg, M., Vartiainen, J., Lucenius, J., Hippi, U., Seppälä, J., Serimaa, R., and Laine, J. (2013). "A Fast Method to Produce Strong NFC Films as a Platform for Barrier and Functional Materials," *ACS Appl. Mater. Interfaces* 5(11), 4640-4647.

[177] Phipps, J., Svending, P., Selina, T., Kritzinger, J., Larson, T., Skuse, D., Ireland, S. (2017). "Applications of co-processed microfibrillated cellulose and mineral in packaging," *in: TAPPI Papercon,* April 24-26, Minneapolis, MN, USA.

[178] Svending, P., Skuse, D., Phipps, J. (2016). "New applications for microfibrillated cellulose in and on paper and board," *in: PTS Paper & Board Symposium,* September 6-7, Munich, Germany.

[179] Svending, P., Kritzinger, J., Selina, T., Phipps, J. (2017). "Microfibrillated cellulose outside of the box," *in: TAPPI International Conference on Nanotechnology for Renewable Materials,* June 5-8, Montreal, Canada.

[180] Matikainen, L. (2017). *Nanocellulose as Barrier Coating Deposited using a Laboratory Rod Coater,* Master's thesis, Aalto University, Helsinki, Finland.

[181] Hamada, H., and Bousfield, D. W. (2010). "Nano-fibrillated cellulose as a coating agent to improve print quality of synthetic fiber sheets," *in: TAPPI 11th Advanced Coating Fundamentals Symposium,* October 11-13, Munich, Germany.

[182] Hamada, H., Beckvermit, J., Bousfield, D. W. (2010). "Nanofibrillated cellulose with fine clay as a coating agent to improve print quality," *in: TAPPI PaperCon Conference,* May 2-5, Atlanta, USA.

[183] Hamada, H., Tahara, K., Bousfield, D. W. (2012). "The effects of nano-fibrillated cellulose as a coating agent for screen printing," *in: TAPPI Advanced Coating Fundamentals Symposium,* September 10-12, Atlanta, USA.

[184] Luu, W. T., Bousfield, D. W., Kettle, J. (2011). "Application of nano-fibrillated cellulose as a paper surface treatment for inkjet printing," *in: TAPPI Paper Conference and Trade Show,* May 1-4, Covington, Kentucky, USA.

[185] Liu, L., Chen, Y. Z., and Zhang, Z. J. (2014). "Preparation of the microfibrillated cellulose and its application in the food packaging paper," *Applied Mechanics and Materials* 469, 87-90.

[186] Song, H., Ankerfors, M., Hoc, M., and Lindström, T. (2010). "Reduction of the linting and dusting propensity of newspaper using starch and microfibrillated cellulose," *Nordic Pulp & Paper Research Journal* 25(4), 495-504.

[187] Ridgway, C. J., and Gane, P. (2014). "The challenge of coating cracking on multicoated substrates designed for digital printing: Developing a novel interlayer construction strategy," *in: 13th TAPPI Advanced Coating Fundamentals Symposium,* October 7-9, Minneapolis, Minnesota, USA.

[188] Ridgway, C. J., and Gane, P. A. (2012). "Constructing NFC-pigment composite surface treatment for enhanced paper stiffness and surface properties," *Cellulose* 19(2), 547-560.

[189] Mousavi, S. M., Afra, E., Tajvidi, M., Bousfield, D., and Dehghani-Firouzabadi, M. (2017). "Cellulose nanofiber/carboxymethyl cellulose blends as an efficient coating to improve the structure and barrier properties of paperboard," *Cellulose* 24(7), 3001-3014.

[190] Hamada, H., and Mitsuhashi, M. (2016). "Effect of cellulose nanofibers as a coating agent for woven and nonwoven fabrics," *Nordic Pulp & Paper Research Journal* 31(2), 255-260.

[191] Balan, T., Guezennec, C., Nicu, R., Ciolacu, F., and Bobu, E. (2015). "Improving barrier and strength properties of paper by multi-layer coating with bio-based additives," *Cellulose Chem.Technol* 49(7-8), 607-615.

[192] Lavoine, N., Desloges, I., Sillard, C., and Bras, J. (2014). "Controlled release and long-term antibacterial activity of chlorhexidine digluconate through the nanoporous network of microfibrillated cellulose," *Cellulose* 21(6), 4429-4442.

[193] Lavoine, N., Tabary, N., Desloges, I., Martel, B., and Bras, J. (2014). "Controlled release of chlorhexidine digluconate using β-cyclodextrin and microfibrillated cellulose," *Colloids and Surfaces B: Biointerfaces* 121, 196-205.

[194] Lavoine, N., Givord, C., Tabary, N., Desloges, I., Martel, B., and Bras, J. (2014). "Elaboration of a new antibacterial bio-nano-material for food-packaging by synergistic action of cyclodextrin and microfibrillated cellulose," *Innovative Food Science & Emerging Technologies* 26, 330-340.

[195] Lavoine, N., Desloges, I., Manship, B., and Bras, J. (2015). "Antibacterial paperboard packaging using microfibrillated cellulose," *Journal of Food Science and Technology* 52(9), 5590-5600.

[196] Lavoine, N., Guillard, V., Desloges, I., Gontard, N., and Bras, J. (2016). "Active bio-based food-packaging: Diffusion and release of active

substances through and from cellulose nanofiber coating toward food-packaging design," *Carbohydr. Polym.* 149, 40-50.

[197] Lavoine, N., Bras, J., and Desloges, I. (2014). "Mechanical and barrier properties of cardboard and 3D packaging coated with microfibrillated cellulose," *J Appl Polym Sci* 131(8), 40106.

[198] Lavoine, N., Desloges, I., Khelifi, B., and Bras, J. (2014). "Impact of different coating processes of microfibrillated cellulose on the mechanical and barrier properties of paper," *J. Mater. Sci.* 49(7), 2879-2893.

[199] Lavoine, N., Desloges, I., and Bras, J. (2014). "Microfibrillated cellulose coatings as new release systems for active packaging," *Carbohydrate Polymers* 103, 528-537.

[200] Aulin, C., and Ström, G. (2013). "Multilayered alkyd resin/nanocellulose coatings for use in renewable packaging solutions with a high level of moisture resistance," *Ind Eng Chem Res* 52(7), 2582-2589.

[201] Afra, E., Mohammadnejad, S., and Saraeyan, A. (2016). "Cellulose nanofibrils as coating material and its effects on paper properties," *Progress in Organic Coatings* 101, 455-460.

[202] Charani, P. R., Dehghani-Firouzabadi, M., Afra, E., Blademo, Å, Naderi, A., and Lindström, T. (2013). "Production of microfibrillated cellulose from unbleached kraft pulp of Kenaf and Scotch Pine and its effect on the properties of hardwood kraft: microfibrillated cellulose paper," *Cellulose* 20(5), 2559-2567.

[203] Beneventi, D., Chaussy, D., Curtil, D., Zolin, L., Gerbaldi, C., and Penazzi, N. (2014). "Highly porous paper loading with microfibrillated cellulose by spray coating on wet substrates," *Ind Eng Chem Res* 53(27), 10982-10989.

[204] Amini, E., Azadfallah, M., Layeghi, M., and Talaei-Hassanloui, R. (2016). "Silver-nanoparticle-impregnated cellulose nanofiber coating for packaging paper," *Cellulose* 23(1), 1-14.

[205] Boissard, Y. (2017). *MFC for Paper Surface Treatment,* Master's thesis, Luleå University of Technology, Luleå, Sweden.

[206] Nygårds, S. (2011). *Nanocellulose in Pigment Coatings- Aspects of Barrier Properties and Printability in Offset,* Master's thesis, Linköping University, Linköping, Sweden.

[207] Bardet, R., Lavoine, N., Belgacem, N., Desloges, I., Bras, J. (2012). "Barrier properties of specialty papers coated with MFC: Influence of base paper and coat weight," *in: TAPPI International Conference on Nanotechnology for Renewable Materials,* June 4-7, Montreal, Canada.

[208] Hult, E., Iotti, M., and Lenes, M. (2010). "Efficient approach to high barrier packaging using microfibrillar cellulose and shellac," *Cellulose* 17(3), 575-586.

[209] Axrup, L., Heiskanen, I., and Backfolk, K. (2011). "A paper or paperboard substrate having barrier properties, a process for production of the substrate and a food or liquid package formed of the substrate," Patent number: WO2011078770A1.

[210] Hoeng, F., Bras, J., Gicquel, E., Krosnicki, G., and Denneulin, A. (2017). "Inkjet printing of nanocellulose–silver ink onto nanocellulose coated cardboard," *RSC Advances* 7(25), 15372-15381.

[211] Meulendijks, N., Burghoorn, M., van Ee, R., Mourad, M., Mann, D., Keul, H., Bex, G., van Veldhoven, E., Verheijen, M., and Buskens, P. (2017). "Electrically conductive coatings consisting of Ag-decorated cellulose nanocrystals," *Cellulose* 24(5), 2191-2204.

[212] Huang, J., Zhu, H., Chen, Y., Preston, C., Rohrbach, K., Cumings, J., and Hu, L. (2013). "Highly transparent and flexible nanopaper transistors," *ACS Nano* 7(3), 2106-2113.

[213] Valtakari, D., Liu, J., Kumar, V., Xu, C., Toivakka, M., and Saarinen, J. J. (2015). "Conductivity of PEDOT: PSS on Spin-Coated and Drop Cast Nanofibrillar Cellulose Thin Films," *Nanoscale Research Letters* 10(1), 1-10.

[214] Zhu, H., Fang, Z., Preston, C., Li, Y., and Hu, L. (2014). "Transparent paper: fabrications, properties, and device applications," *Energy & Environmental Science* 7(1), 269-287.

[215] Andres, B., Forsberg, S., Dahlström, C., Blomquist, N., and Olin, H. (2014). "Enhanced electrical and mechanical properties of nanographite electrodes for supercapacitors by addition of nanofibrillated cellulose," *Physica Status Solidi (B)* 251(12), 2581-2586.

[216] Osong, S. H., Dahlstr, C., Forsberg, S., Andres, B., Engstrand, P., Norgren, S., and Engstr, A. (2016). "Nanofibrillated cellulose/nanographite composite films," *Cellulose* 23(4), 2487-2500.

[217] Martins, N. C., Freire, C. S., Pinto, R. J., Fernandes, S. C., Neto, C. P., Silvestre, A. J., Causio, J., Baldi, G., Sadocco, P., and Trindade, T. (2012). "Electrostatic assembly of Ag nanoparticles onto nanofibrillated cellulose for antibacterial paper products," *Cellulose* 19(4), 1425-1436.

[218] Blomquist, N., Engström, A., Hummelgård, M., Andres, B., Forsberg, S., and Olin, H. (2016). "Large-Scale Production of Nanographite by Tube-Shear Exfoliation in Water," *PloS One* 11(4), e0154686.

[219] Araki, J., Wada, M., and Kuga, S. (2001). "Steric stabilization of a cellulose microcrystal suspension by poly (ethylene glycol) grafting," *Langmuir* 17(1), 21-27.

[220] Sandås, S., Salminen, P. J., and Eklund, D. (1989). "Measuring the water retention of coating colors," *TAPPI Journal* 72(12), 207-210.

[221] Naderi, A., Lindström, T., and Sundström, J. (2014). "Carboxymethylated nanofibrillated cellulose: rheological studies," *Cellulose* 21(3), 1561-1571.

[222] Steffe, J. F. (1996). *Rheological Methods in Food Process Engineering,* 2nd Ed., Freeman Press, MI, USA.

[223] Krieger, I. M., and Huang, T. A. (1994). "Axial flow through a narrow annulus. I. The kinetic energy correction," *J. Rheol.* 38(1), 141-150.

[224] Miettinen, P., Kuusipalo, J., Auvinen, S., Haakana, S. (2015). "Validity of traditional barrier-testing methods to predict the achievable benefits of the new generation water based barrier coatings for packaging materials," *in: 27th PTS Coating Symposium,* September 16-18, Munich, Germany.

[225] O'Neill, G., Preston, J., Phipps, J., Husband, J., Tedstone, A. (2012). "A barrier coating approach to counter oil migration," *in: 8th International Paper and Coating Chemistry Symposium,* June 10-14, Stockholm, Sweden.

[226] Koivula, H., Preston, J., Heard, P., and Toivakka, M. (2008). "Visualisation of the distribution of offset ink components printed onto coated paper," *Colloids Surf. Physicochem. Eng. Aspects* 317(1), 557-567.

[227] Vähä-Nissi, M. (2016). "Test methods for evaluating grease and mineral oil barriers," *in: TAPPI PLACE Conference,* April 11-13, Fort Worth, Texas, USA.

[228] Kummala, R., Xu, W., Xu, C., and Toivakka, M. (2017). "Stiffness and swelling characteristics of nanocellulose films in cell culture media," *Cellulose* Submitted

[229] Swerin, A. (1998). "Rheological properties of cellulosic fibre suspensions flocculated by cationic polyacrylamides," *Colloids Surf. Physicochem. Eng. Aspects* 133(3), 279-294.

[230] Horvath, A. E., and Lindström, T. (2007). "The influence of colloidal interactions on fiber network strength," *J. Colloid Interface Sci.* 309(2), 511-517.

[231] Liimatainen, H., Haavisto, S., Haapala, A., and Niinimäki, J. (2009). "Influence of adsorbed and dissolved carboxymethyl cellulose on fibre suspension dispersing, dewaterability, and fines retention," *BioResources* 4(1), 321-340.

[232] Chen, H., Park, A., Heitmann, J. A., and Hubbe, M. A. (2009). "Importance of cellulosic fines relative to the dewatering rates of fiber suspensions," *Ind Eng Chem Res* 48(20), 9106-9112.

[233] Clarke, J. B. (1997). "Rheology Modifiers and Pigment Dispersants," in: *Surface Application of Paper Chemicals*, J. Brander and I. Thorn (eds.), Springer Netherlands, Netherlands, pp. 109-128.

[234] Li, M., Wu, Q., Song, K., Lee, S., Qing, Y., and Wu, Y. (2015). "Cellulose Nanoparticles: Structure-Morphology-Rheology Relationships," *ACS Sustainable Chem. Eng.* 3(5), 821-832.

[235] Haavisto, S., Liukkonen, A., Jäsberg, A., Lille, M., Salmela, J. (2011). "Laboratory-scale pipe rheometry: A study of microfibrillated cellulose suspensions," *in: TAPPI Papercon Conference,* May 1-4, Covington, KY, USA.

[236] Nikbakht, A., Madani, A., Olson, J. A., and Martinez, D. M. (2014). "Fibre suspensions in Hagen–Poiseuille flow: Transition from laminar plug flow to turbulence," *J. Non Newtonian Fluid Mech.* 212, 28-35.

[237] Babkin, V. A. (2001). "Fibrous-suspension plug flow in an annular pipe," *Fluid Dynamics* 36(1), 104-110.

[238] Jäsberg, A. (2007). *Flow Behavior of Fibre Suspensions in Straight Pipe: New Experimental Techniques and Multiphase Modeling,* PhD Thesis, University of Jyväskylä, Jyväskylä, Finland.

[239] Xu, H. J., and Aidun, C. K. (2005). "Characteristics of fiber suspension flow in a rectangular channel," *Int. J. Multiphase Flow* 31(3), 318-336.

[240] Smay, J. E., Cesarano, J., and Lewis, J. A. (2002). "Colloidal inks for directed assembly of 3-D periodic structures," *Langmuir* 18(14), 5429-5437.

[241] Gardner, D. J., Oporto, G. S., Mills, R., and Samir, A. (2008). "Adhesion and surface issues in cellulose and nanocellulose," *J. Adhes. Sci. Technol.* 22(5-6), 545-567.

[242] Ewender, J., Franz, R., and Welle, F. (2013). "Permeation of mineral oil components from cardboard packaging materials through polymer films," *Packaging Technology and Science* 26(7), 423-434.

[243] Vollmer, A., Biedermann, M., Grundböck, F., Ingenhoff, J., Biedermann-Brem, S., Altkofer, W., and Grob, K. (2011). "Migration of mineral oil from printed paperboard into dry foods: survey of the German market," *European Food Research and Technology* 232(1), 175-182.

[244] Mehrali, M., Sadeghinezhad, E., Latibari, S. T., Kazi, S. N., Mehrali, M., Zubir, Mohd Nashrul Bin Mohd, and Metselaar, H. S. C. (2014). "Investigation of thermal conductivity and rheological properties of nanofluids containing graphene nanoplatelets," *Nanoscale Research Letters* 9(1), 15.

ISBN 978-952-12-3673-0